Influence of Vasopressin on Vascular Smooth Muscle Cell Calcification

Thesis submitted as requirement to fulfill the degree ,,Doctor of Philosophy" (Ph.D)

at the
Faculty of Medicine
Eberhard Karls Universität
Tübingen

by

Zhu, Xuexue

2022

Dean: Professor Dr. B. Pichler

First reviewer: Professor Dr. Dr. B. Nürnberg
Second reviewer: Professor Dr. R. Lukowski

Date of oral examination: 14.09.2022

Table of contents

List of Figures

List of Tables

List of abbreviations

°C	Degree celsius
µM	Micromolar
$[Ca^{2+}]_i$	Cytosolic Ca^{2+} concentrations
ACTH	Adrenocorticotropic hormone
ADH	Antidiuretic hormone
AGC	Protein kinases A, protein kinases G and protein kinases C
AKT	Protein kinase B
ALP	Alkaline phosphatase
ALPL	Tissue-nonspecific alkaline phosphatase
ANOVA	Analysis of variance
APS	Ammonium persulphate
AVP	Arginine vasopressin
BMP	Bone morphogenetic protein
Ca^{2+}	Calcium ion
CAD	CRAC-activating domain
cADPR	Cyclic adenosine 5'-diphosphate-ribose
CAR	Ca^{2+}-accumulating region
CBD	C-terminal binding domain
CBFA1	Core-binding factor α-1
CC	Coiled-coil
cEF	Canonical EF-hand
CKD	Chronic kidney disease
CRAC	Ca^{2+} release-activated Ca^{2+}
DAG	Diacylglycerol
DCFDA	2',7'–dichlorofluorescein diacetate
DMSO	Dimethyl sulfoxide
DNA	Deoxyribonucleic acid
ECL	Enhanced chemiluminescence
EF	EF-hand
EGTA	Ethylene glycol tetraacetic acid
ER	Endoplasmic reticulum
ERK	Extracellular signal-regulated kinase
ETON	Extended transmembrane Orai1 N-terminal
FACS	Fluorescence activated cell sorting
FBS	Fetal bovine serum
GAPDH	Glyceraldehyde 3-phosphate dehydrogenase
GPCR	G protein-coupled receptors
HAoSMCs	Human aortic smooth muscle cells
HCl	Hydrochloric acid
hEF	Hidden EF-hand
HEPES	4-(2-Hydroxyethyl)-piperazine-1-ethanesulfonic acid
HRP	Horseradish peroxidase
IP_3	Inositol 1,4,5-triphosphate

K	Lysine
MGP	Matrix gla protein
mL	Milliliter
mM	Millimolar
mRNA	Messenger RNA
MSX2	Msh homeobox 2
NAADP	Nicotinic acid adenine dinucleotide phosphate
NAC	N-acetyl-L-cysteine
NaCl	Sodium chloride
NaOH	Sodium hydroxide
NBD	N-terminal binding domain
NCX	Na^+/Ca^{2+} exchanger
NF-kB	Nuclear factor κ-light chain enhancer of activated B cells
NHE	Na^+/H^+ exchanger
nM	Nanomolar
NOX	Nicotinamide adenine dinucleotide phosphate oxidase
OASF	Orai-activating small fragment
P/S	Proline/serine
PBS	Phosphate buffered saline
pH_i	Intracellular pH
PI3K	Phosphatidylinositide 3-kinase
PLC-β	Phospholipase C-β
PM	Plasma membrane
PPi	Pyrophosphate
PVDF	Polyvinylidene difluoride
qPCR	Quantitative polymerase chain reaction
RIPA	Radioimmunoprecipitation assay
ROS	Reactive oxygen species
RT-PCR	Real-time polymerase chain reaction
Runx2	Runt-related transcription factor 2
S	Serine
SAM	Sterile alpha motif
SD	Standard deviation
SDS	Sodium dodecyl sulfate
SDS-PAGE	Sodium dodecyl sulfate polyacrylamide gel electrophoresis
SERCA	Sarco/endoplasmatic reticulum Ca^{2+}-ATPase
SGK1	Serum & glucocorticoid inducible kinase 1
SOAR	STIM-Orai activating region
SOCE	Store-operated Ca^{2+} entry
SOX9	SRY-Box 9
SP	Single peptide
SPSS	Statistic package for social science
STIM	Stromal interaction molecule
T	Threonine
TAE	Tris-acetate-EDTA

TBS	Tris-buffered saline
TBST	Tris-buffered saline containing 1% Tween 20
TEMED	N,N,N'N'-Tetramethylethylenediamine
TM	Transmembrane
TRPC	Transient receptor potential cation channel
V1aR	Vasopressin 1a receptor
V1bR	Vasopressin 1b receptor
V2R	Vasopressin 2 receptor
VSMCs	Vascular smooth muscle cells

1 Introduction

1.1 Arginine Vasopressin (AVP)

1.1.1 Physiology of AVP

Vasopressin or arginine vasopressin (AVP), also termed antidiuretic hormone (ADH), is a neurohypophysial nonapeptide hormone (Antoni, 2017) (Figure 1.1). AVP is mainly synthesized in the hypothalamus, smaller quantities are derived from other tissues such as the adrenal glands, the sympathetic ganglia and the testis (Chang et al., 2020, Laycock, 2009). AVP is transported down the neuron's axons through the hypothalamus-pituitary tract and ultimately excreted in the posterior pituitary gland, where it is stored (Struck et al., 2005, Mavani et al., 2015).

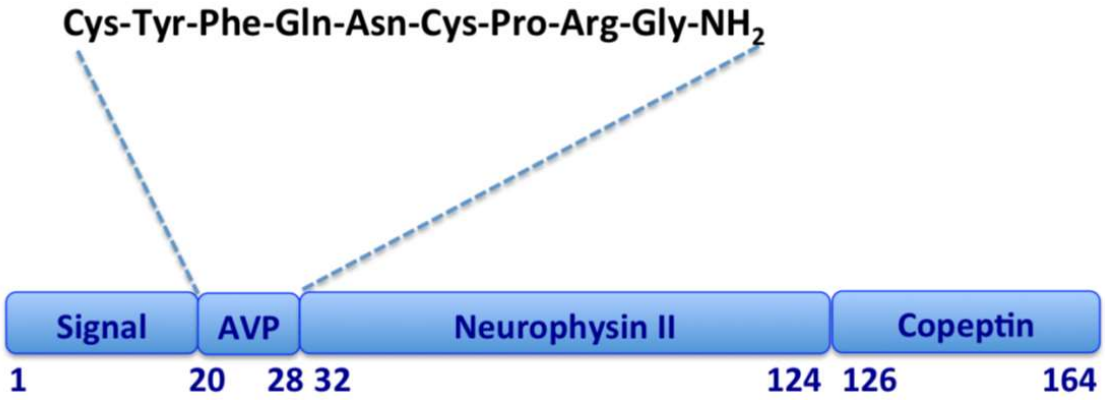

Figure 1.1 The chemical structure of arginine vasopressin (AVP) and its precursor.
Proteolysis sites occur between the boundaries of the boxes. Adapted from *Ferenc A. Antoni* (Antoni, 2017).

AVP is mainly responsible for the homeostasis of tonicity (Cuzzo et al., 2021). High plasma osmotic pressure is the most potent stimulus for the release and secretion of AVP. The osmotic pressure is monitored by highly sensitive osmoreceptors, which responds to the change of less than 2 mOsm/L (Davies, 1972). Then, the secreted AVP contributes to the reabsorption of water in the kidney, thereby returning the osmotic pressure to baseline. In addition, blood pressure and blood volume can also influence the AVP release, albeit to a lesser extent (Mavani et al., 2015).

AVP is synthesized and produced by precursor peptides, pre-provasopressin that is cleaved by a four-enzyme cascade into AVP, neurophysin II and copeptin (Figure 1.1). The primary functions of AVP are to regulate water reabsorption and to cause vasoconstriction (Cuzzo et al., 2020). Neurophysin II has a complex structure and serves as a carrier protein for AVP transport (Morgenthaler et al., 2008). Copeptin is a 39-amino acid glycopeptide cleaved from the C-terminal portion of the pre-provasopressin, which still plays an unknown role in the circulation (Dobsa and Edozien, 2013).

1.1.2 AVP receptors

AVP mediates significant physiological functions through interacting with specific membrane receptors. Vasopressin receptors are divided into three subtypes (V1a, V1b and V2 receptor) (Morel et al., 1992, Sugimoto et al., 1994, Lolait et al., 1992), all belonging to the G protein-coupled receptor (GPCR) family (Zhang et al., 2016). V1a and V1b receptors activate phospholipase by coupling to Gq proteins, while V2 receptors activate adenylyl cyclase via Gs proteins (Birnbaumer, 2000). These three receptors exhibit unique tissue distribution and have different functions. V1a receptors are located in many tissues, including vascular smooth muscle cells (VSMCs), hepatocytes, platelets, myocardium, and myometrium, where they regulate vasoconstriction, hepatic glycogenolysis, platelet aggregation, myocardial hypertrophy, and uterine contraction (Oh, 2008). Furthermore, V1a receptors are also expressed in many regions of the central nervous system, where they can affect circadian rhythms (Li et al., 2009), psychiatric disorders (Mittapalli et al., 2010), as well as social behavior, cognition and emotion (Albers, 2015). The V1b receptors are primarily found in the anterior pituitary and they modulate adrenocorticotropic hormone (ACTH) secretion (Oh, 2008). The V2 receptors are expressed in the kidney tubules, prominently in the collecting ducts, where they mainly mediate antidiuresis of vasopressin (Tanoue et al., 2004).

1.1.3 AVP and calcification

AVP has been considered a stimulator of vascular calcification (Nishiwaki-Yasuda et al., 2007). It has been reported that AVP induces calcification through stimulating Na-dependent Pi transport in rat A-10 VSMCs (Nishiwaki-Yasuda et al., 2007). Moreover, vasopressin may evoke Ca^{2+} influx into VSMCs (Ding et al., 2011), which is partly secondary to the activation of the transient receptor potential channel TRPC6 (Ding et al., 2011) and/or voltage-gated K^+ channels suppression, following the activation of voltage-gated Ca^{2+} channels (Tsai et al., 2020, Brueggemann et al., 2009, Mackie and Byron, 2008). As demonstrated in other cell types, vasopressin may stimulate store-operated Ca^{2+} entry (SOCE) (Jones et al., 2008, Piron and Villereal, 2013). AVP elicits its physiological and pathological functions primarily through interactions with the three receptor subtypes (V1a, V1b and V2 receptor) (Aoyagi et al., 2009). V1a receptors are known to initiate Ca^{2+} signaling following treatment of VSMCs with AVP (Jeffries et al., 2010, Byron, 1996). V1a receptors activate intracellular Ca^{2+} signaling via coupling to Gq proteins, which subsequently stimulate phospholipase C-β (PLC-β) enzymes and release inositol 1,4,5-triphosphate (IP_3) and diacylglycerol (DAG) (Dorn et al., 1997).

Oxidative stress may participate in the pathogenesis of calcification by triggering osteogenic signaling (Mazzini and Schulze, 2006, Shao et al., 2006). Vasopressin is widely regarded as an oxidation inducer in the cerebrovascular system and VSMCs (Faraco et al., 2014, Ding et al., 2011). The Na^+/H^+ exchanger1 (NHE1) is well-known to contribute to luminal acidification of intracellular vesicles that may further be involved in the generation of oxidative stress (Hackam et al., 1997, Singh et al., 2017). Vesicular luminal acidification is, on the other hand, required for phosphate-triggered vascular calcification (Alesutan et al., 2015).

Despite accumulated evidence on the effect of AVP on vascular calcification, the mechanisms in vasopressin-induced vascular calcification remained incompletely understood. Thus, in this study, we explored whether ORAI1-dependent SOCE and NHE1/reactive oxygen species (ROS) participate in the vasopressin-evoked phenotypic transition of VSMCs and vascular calcification.

1.2 Vascular calcification

1.2.1 Classification and outcomes of vascular calcification

Vascular calcification arises from the pathological deposition of calcium-phosphate in the form of hydroxyapatite crystals into the vascular system (Paloian and Giachelli, 2014). It is a major pathophysiological mechanism that is associated with adverse cardiovascular events (Haarhaus et al., 2017, Fadini et al., 2007, Towler et al., 2006, Blacher et al., 2001, London et al., 2003, Foley et al., 1998, Mizobuchi et al., 2009). Vascular calcification is accelerated in certain clinical disorders, such as premature aging, hypertension, diabetes, chronic kidney disease (CKD), and atherosclerosis (Lee et al., 2020).

Depending on the localization of calcium deposition on the vessel wall, vascular calcification is mainly classified into two subtypes, including intimal vascular calcification and medial vascular calcification (Cozzolino et al., 2019). It can also occur in valvular calcification and calciphylaxis (Lee et al., 2020). Detected by microscopy, intimal calcification reveals irregular, discrete, plague-like calcification (Cozzolino et al., 2019). Calcification in the intima is in connection with atherosclerosis, which can result in stenosis and the formation of thrombi, then leading to myocardial infarction or ischemia in both coronary and peripheral arteries (Shi et al., 2020, Tüysüz and Dedemoğlu, 2020). In contrast to calcification in the intima layer, medial calcification exhibits tram-tract in radiographic and ultrasonographic images, with non-narrow diffuse calcification (Cozzolino et al., 2019). Medial calcification occurs independently of atherosclerosis and is detectable in the premature aging, hypertension, diabetes and CKD population (Demer and Tintut, 2008). Medial calcification leads to the loss of elasticity in the arteries and subsequent arterial stiffening (Tüysüz and Dedemoğlu, 2020).

1.2.2 Mechanisms of vascular calcification

Over the past century, vascular calcification was once considered to be a passive process, resulting from oversaturation of plasma with Ca^{2+} and phosphate. Currently, it is characterized as an active and highly regulated biomineralization event (Liberman et al., 2013), involving dedifferentiation and

reprogramming of VSMCs into an osteo-/chondrogenic phenotype (Zhu et al., 2021, Ma et al., 2019).

Vascular calcification may be initiated by several different, non-mutually exclusive mechanisms (Speer and Giachelli, 2004, Giachelli, 2004). First, inhibitors of mineralization, such as pyrophosphate (PPi) and matrix gla protein (MGP), are expressed *in vivo*. Calcification occurs due to the loss or deficiency of these anti-calcification molecules (Tóth et al., 2020). Second, previous evidence has revealed that isolated SMCs undergo a significant osteogenic transition capable of precipitation both *in vivo* and *in vitro* under various stressors (Steitz et al., 2001). Osteogenic transcription factors such as core-binding factor α-1 (CBFA1), msh homeobox 2 (MSX2), and SRY-Box 9 (SOX9), as well as tissue-nonspecific alkaline phosphatase (ALPL) are involved in remodeling of VSMCs, which is decisive for vascular calcification (Kapustin et al., 2015, Lang et al., 2014a, Lang et al., 2013, Steitz et al., 2001). Additionally, a host of studies provide evidence that there is a correlation between VSMCs apoptosis and vascular calcification (Proudfoot et al., 2001, O'Neill et al., 2011). Cell death can cause the release of phospholipid-rich membrane debris and apoptotic bodies, which may serve as nucleation of apatite in calcium phosphate deposits (Proudfoot et al., 2000). Fourth, in the normal state, calcium and phosphate are under homeostatic regulation. The imbalance of calcium and phosphate (normally referred to hypercalcemia or hyperphosphatemia) promotes the precipitation of calcium and phosphate (Goyal and Jialal, 2021). Furthermore, bone remodeling has been expressed as a complicated process in which four phases that are resorption, reversal, formation as well as mineralization are involved, and nucleational complexes are released leading to an increased risk of ectopic mineralization (Wu et al., 2014). At last, matrix vesicles are secreted and released under pathological states and environmental stressors. Previous studies have indicated that matrix degradation is a vital step to trigger vascular calcification (Pai and Giachelli, 2010, Chen et al., 2011).

1.2.3 The role of phosphate in the pathogenesis of vascular calcification

Disturbed mineral homeostasis and impaired renal phosphate elimination are the main determinants of vascular calcification in CKD (Cannata-Andia et al., 2011, Zhu et al., 2021). The mechanisms of phosphate-induced calcification have been explored. Elevated phosphate levels directly stimulate vascular calcification by triggering the phenotypic modulation of VSMCs into osteoblast-like cells in patients with CKD (Cannata-Andia et al., 2011, Giachelli, 2004). The existing experimental studies have demonstrated that phosphate may regulate osteogenic differentiation and mineralization of VSMCs through the sodium-dependent phosphate co-transporter, Pit-1 (Schlieper et al., 2016, Jono et al., 2000). Extracellular phosphate signaling or increased intracellular phosphate promotes VSMCs to undergo phenotypic switching, expressing increased transcript levels of osteogenic genes, such as Runt-related transcription factor 2 (Runx2), ALPL as well as osteocalcin, and contributes to Ca^{2+}/PO_4^{3-} loading of matrix vesicles (Cannata-Andia et al., 2011, Yang et al., 2004). In addition, once nucleation of apatite initiated by cell apoptosis or necrosis occurs, increased $Ca^{2+}\times PO_4^{3-}$ accelerates the growth of apatite crystals through a thermodynamic mechanism, thereby driving matrix mineralization (Yang et al., 2004).

1.3 Ca^{2+} signaling

1.3.1 Intracellular Ca^{2+}

Fluctuations in intracellular Ca^{2+} concentration are required in the regulation of a broad range of cellular functions, such as secretion, contraction, exocytosis, cell proliferation, migration, and death (Lang et al., 2012, Berna-Erro et al., 2012). Particularly, intracellular Ca^{2+} disturbance plays an important role in the development and progression of VSMC calcification (Nguyen et al., 2020). Two sources are responsible for elevations in cytosolic Ca^{2+} concentration: the release of Ca^{2+} from endoplasmic reticulum (ER)-stores and extracellular Ca^{2+} entry across the plasma membrane (PM) through Ca^{2+} channels (Shaw and Feske, 2012). Ca^{2+}-mobilizing messengers, such as IP_3 (Berridge and Irvine, 1989), cyclic adenosine 5'-diphosphate-ribose (cADPR) (Lee, 1997) and nicotinic acid adenine dinucleotide phosphate (NAADP) (Cancela et al., 1999), induce calcium

release from intracellular stores. However, Ca^{2+} influx from extracellular space must be involved to trigger complete activation of cellular processes and to maintain the Ca^{2+} signal.

Ca^{2+} gradients in human cells are established by three PM Ca^{2+} transporters (Na^{+}/Ca^{2+}-exchangers), three different ER Ca^{2+} pump isoforms (sarco/endoplasmatic reticulum Ca^{2+}-ATPase) and four different PM pump isoforms (PM Ca^{2+} ATPases) (Brandman et al., 2007). Additionally, Ca^{2+} channels have been suggested to play an important role in Ca^{2+} entry into the cytosol from extracellular space and intracellular stores (Shaw and Feske, 2012). Ca^{2+} release-activated Ca^{2+} (CRAC) channels, one kind of receptor-operated Ca^{2+} entry, are stimulated when calcium is released from intracellular stores (Cahalan et al., 2007, Sage, 1992). The channels consist of Orai proteins that form the pores of the CRAC channels. Orai proteins are localized in the PM. They are activated by Ca^{2+} sensors stromal interaction molecule (STIM) proteins located in the ER. Since the activation of CRAC channels and the subsequent Ca^{2+} influx are controlled by the ER filling state, this Ca^{2+} signaling pathway is also called SOCE or – using an older term – capacitative Ca^{2+} entry.

1.3.2 Stromal interaction molecule (STIM) proteins

There are two highly conserved homologs of STIM proteins (STIM1 and STIM2) in mammals. STIM1 is a single-transmembrane protein with 685 amino acids, which consists of an about 22 kDa N-terminal domain (STIM1-N) located in the lumen of ER, a single transmembrane (TM) moiety and an approximately 51 kDa cytosolic C-terminal portion (STIM1-C) (Lunz et al., 2019) (Figure 1.2). The ER-luminal domain possesses the single peptide (SP), the canonical and hidden EF-hand (cEF and hEF, respectively) as well as a sterile alpha motif (SAM) (Lunz et al., 2019, Stathopulos et al., 2008). The cEF domain forms a helix-loop-helix structure that is responsible for Ca^{2+} binding within the loop in a resting state, while hEF plays a significant role in stability of the cEF through hydrogen bonding (Stathopulos et al., 2008, Zheng et al., 2011, Rosado et al., 2015). The SAM domain can oligomerize in response to ER Ca^{2+} depletion, which is critical for SOCE initiation (Zheng et al., 2011). The STIM1-C is composed of three coiled-

coil (CC) regions (CC1, CC2, CC3), a proline/serine-rich (P/S) and a polybasic lysine rich (K rich) tail. Additionally, several vital Orai-activating modules have been termed in C-terminus, including Orai-activating small fragment (OASF), CRAC-activating domain (CAD) and STIM-Orai activating region (SOAR), all modules having CC2 and CC3 (Moccia et al., 2015). A host of studies have revealed that the STIM1-C redistributes STIM1 oligomers into ER puncta close to the PM following Ca^{2+} store depletion, and then couples to and activates Orai1 through conformational switch (Park et al., 2009, Muik et al., 2008, Stathopulos et al., 2006).

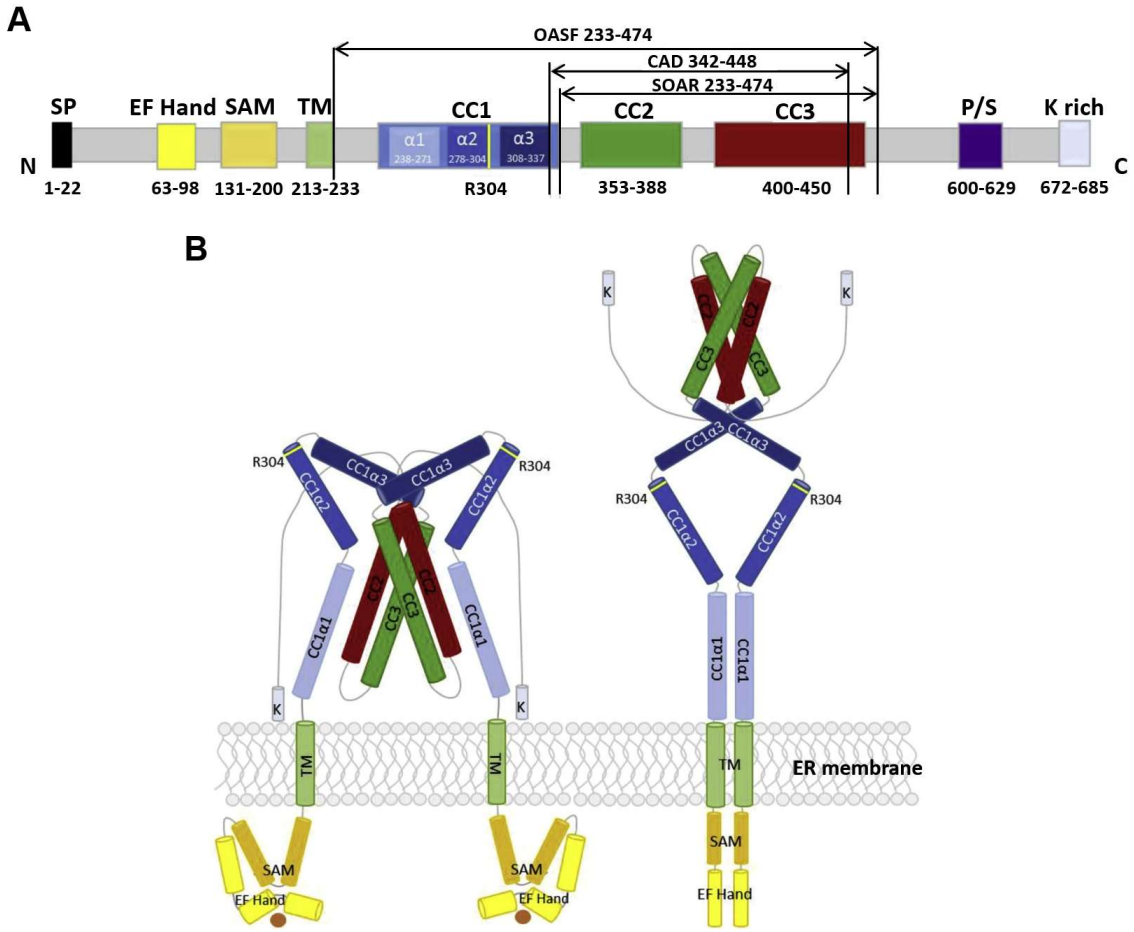

Figure 1.2 The structure of STIM1.
(A). Schematic illustration of the full-length structure of STIM1 with the essential regions for binding with Orai, including OASF, CAD and SOAR. **(B).** Different schematic models of STIM1 in resting (left) and activated (right) state. SP, single peptide; SAM, sterile α motif domain; TM, transmembrane; CC1, coiled-coil region 1; CC2, coiled-coil region 2; CC3, coiled-coil region 3; P/S, proline/serine-rich; K rich, polybasic lysine rich; OASF, Orai-activating small

fragment; CAD, CRAC-activating domain; SOAR, STIM-Orai activating region; ER, endoplasmic reticulum. (Lunz et al., 2019)

STIM1 has been reported to be the main activator of SOCE (Rosado et al., 2015). STIM2 is about 45 percent identical with STIM1, but STIM2 is mainly responsible for sustaining basal Ca^{2+} levels, rather than triggering SOCE (Pani et al., 2012, Gruszczynska-Biegala et al., 2011).

1.3.3 Orai proteins

Three highly conserved isoforms of Orai (Orai1-3, also called CRACM1-3) exist in mammals. The three homologs of Orai are all well-known to form CRAC channels. Among the three Orai proteins, the combination of Orai1 and STIM1 has the strongest efficacy to stimulate SOCE, while Orai2 and Orai3 have weaker or undetectable efficacy (Mercer et al., 2006, Wang et al., 2017). As shown in the Figure 1.3 A-B, Orai1 consists of four transmembrane proteins (TM1-4) containing 301 amino acids, with one intracellular and two extracellular loops as well as both N- and C-termini residing in the cytoplasm (Feske et al., 2006, Navarro-Borelly et al., 2008). A conserved sequence, called “extended transmembrane Orai1 N-terminal” (ETON, aa73-90), is important for the interaction of Orai1 with STIM1 (Fahrner et al., 2013). The residue R91 may act as an inner channel gate (Yamashita et al., 2020). The Ca^{2+}-accumulating region (CAR) increases Ca^{2+} permeation via three aspartate residues (D110, D112, D114) at a low Ca^{2+} concentration (Sallinger et al., 2020). Hydrophobic residues (L273 and L276) promote STIM1 binding and channel activation (Sallinger et al., 2020). It was believed that tetramers of Orai1 subunits form the CRAC channels (Maruyama et al., 2009, Penna et al., 2008). However, Hou *et al* showed in 2012 that the crystal structure of the CRAC channel may be a hexameric structure (Hou et al., 2012). As depicted in the Figure 1.3 C, the ion pore, surrounded by three layers of transmembrane helices, is located in the center of the hexamer (Shim et al., 2015). The first layer is formed by TM1 of each subunit, and the second layer is surrounded by TM2 and TM3 helixes, and TM4 domain constitutes the outmost layer. Importantly, intracellular N- and C- terminal domains are the functional binding regions for STIM1-Orai1 combination (McNally et al., 2013). It

is notable that the CAD of STIM1 weakly binds to the site in the Orai1 N-terminal binding domain (NBD), but with higher affinity binds to the site in the Orai1 C-terminal binding domain (CBD) (Palty et al., 2015, Derler et al., 2013).

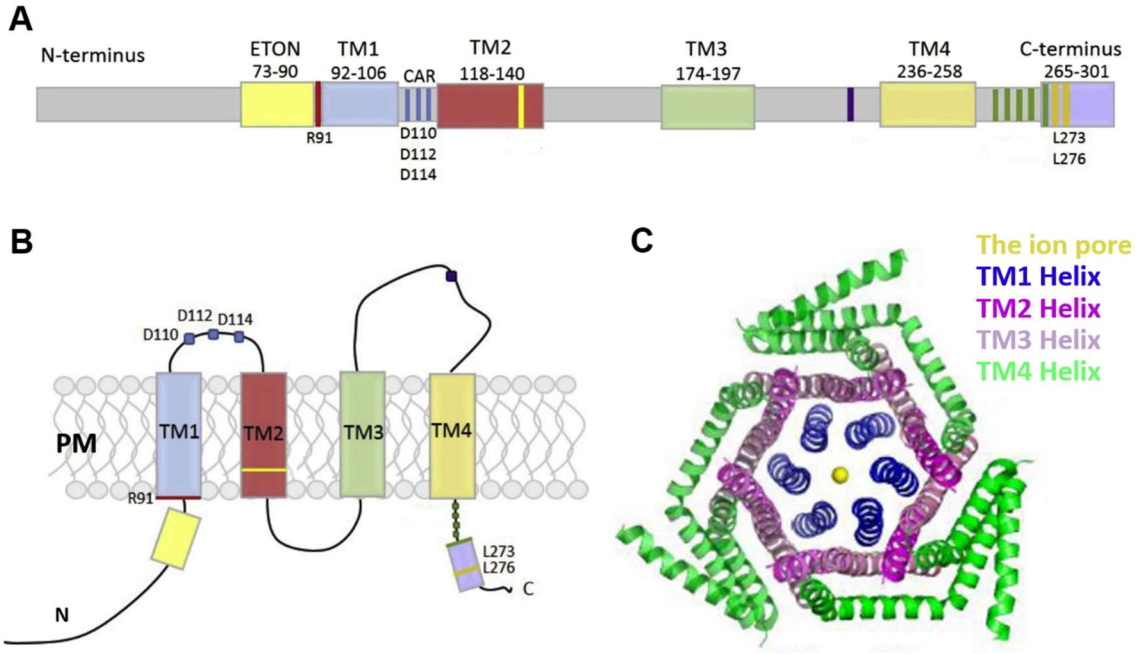

Figure 1.3 The structure of Orai1.
(A). Schematic representation of the overall structure of Orai1 with the important regions, including N-terminus and C-terminus, the ETON region (aa73-90), R91, CAR (D110, D112, D114), four TM domains (TM1, aa92-106; TM2, aa118-140; TM3, aa174-197; TM4, aa236-258) and hydrophobic residues (L273, L276). **(B).** Topology of Orai1 monomer. Orai1 includes four TM domains, N- and C- termini and essential residues like in (A) (Lunz et al., 2019). **(C).** A top view of hexameric Orai1 channel structure (Shim et al., 2015). ETON, extended transmembrane Orai1 N-terminal; aa, amino acids; TM, transmembrane; CAR, Ca^{2+}-accumulating region; PM, plasma membrane.

1.3.4 Store-operated Ca^{2+} entry (SOCE)

SOCE is a ubiquitous Ca^{2+} influx channel that is triggered by the depletion of intracellular Ca^{2+} stores. SOCE is implicated in many cell functions, such as vascular calcification (Zhu et al., 2021, Ma et al., 2019), neuro degeneration (Kawamata et al., 2014), platelet activity (Zhou et al., 2021, Pelzl et al., 2020) and carcinogenesis (Shuba, 2019). PM-localized Orai1 and ER-localized STIM1 have been proven to be the primary components of SOCE (Ambudkar et al., 2017). In the resting state of the cell, when ER Ca^{2+} stores are replete, STIM1 is diffusely distributed in the ER membrane where Ca^{2+} is combined with the luminal EF-

hand of STIM1. Following the emptying of Ca^{2+} stores, Ca^{2+} dissociation from the EF-hand of STIM1 drives a destabilization-coupled oligomerization process of STIM1 and induces conformational rearrangements of STIM1. Subsequently, STIM1 oligomers are rapidly relocated and accumulated at ER-PM junctional sites, which appears as the puncta formation of STIM1 (Shim et al., 2015, Liou et al., 2007). Then, Orai1 is also redistributed within the PM and recruited at the apposed positions to STIM1. This juxtaposition enables the interaction between Orai1 and STIM1 to occur, resulting in the activation of SOCE channels (Luik et al., 2008) (Figure 1.4).

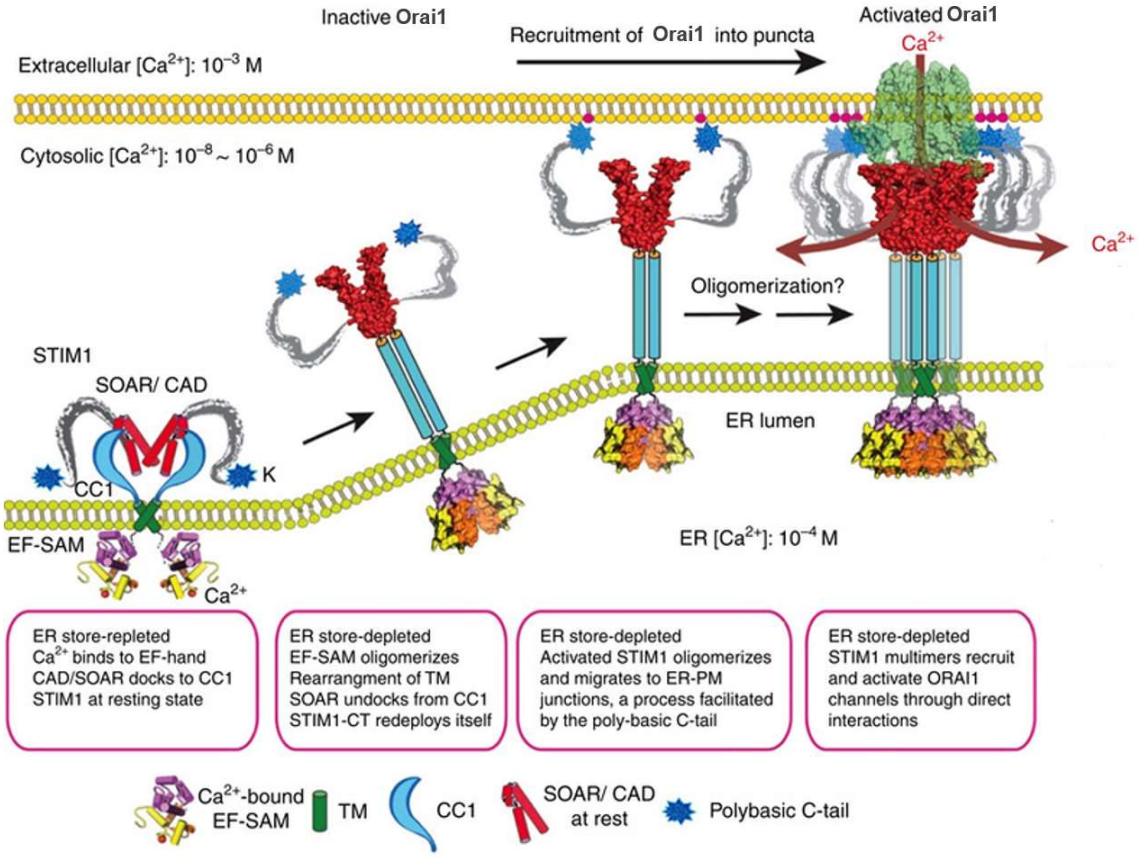

Figure 1.4 Activation steps of SOCE.
In the resting state, the ER is filled with Ca^{2+}. Following store depletion, Ca^{2+} unbinding leads to the oligomerization of STIM1 and then redistribution of oligomers at ER-PM junctions, causing the formation of STIM1 puncta. Activated STIM1 recruits Orai1 into puncta and stimulates Orai1 channels. STIM1, stromal interaction molecule1; SAM, sterile α motif domain; CC1, coiled-coil region 1; SOAR, STIM-Orai activating region; CAD, CRAC-activating domain; K, polybasic C-tail; TM, transmembrane; PM, plasma membrane; ER, endoplasmic reticulum. Adapted from *Guolin Ma* (Ma et al., 2015).

1.4 The relationship of Na^+/H^+ exchanger NHE1, Na^+/Ca^{2+} exchanger NCX1 and reactive oxygen species (ROS)

1.4.1 The distribution of NHE isoforms

The intracellular ionic milieu is maintained by the balance of ion channels, transporters and pumps, which is critical for the maintenance of homeostasis in living cells (Nakamura et al., 2005). NHEs are membrane proteins that regulate intracellular pH (pH_i) through simultaneously transporting the influx of a Na^+ and the efflux of a H^+ (Pedersen and Counillon, 2019). There are ten known NHE subtypes (NHE1-NHE10) in mammals, with specific tissue distribution and important physiological functions (Vallés et al., 2015). NHE1-5 reside on the PM. NHE1 is in the PM of most tissues and the predominant isoform found in the mammalian myocardium (Karmazyn et al., 1999). NHE2 and NHE3 predominantly target in the apical membrane in epithelial cells of the kidney and intestine (Malo and Fliegel, 2006). NHE4 is primarily expressed in the stomach, but is also identified in other tissues, like the intestine, kidney, brain, uterus and skeletal muscle (Orlowski et al., 1992). NHE5 is mainly localized in the brain tissue, followed by lower levels in the spleen, testis, and skeletal muscle (Attaphitaya et al., 1999). NHE6-9 are found in intracellular compartments, including Golgi, endosomes and lysosomes, and are involved in regulating organelle pH (Nakamura et al., 2005). NHE10, a newly identified subtype, is found in the osteoclasts, which is essential for the osteoclast differentiation and survival (Vallés et al., 2015).

1.4.2 The structure of NHE1

The NHE1 isoform is the first identified and the most frequently studied in the NHE family. NHE1 is composed of 815 amino acids, with 500-amino acids at the N-terminus and 315-amino acids at the C-terminus. NHE1 has two domains, consisting of an N-terminal 12 transmembrane domain that mediates ion translocation and a large hydrophilic C-terminal domain that plays a regulatory role in ion transport by phosphorylation (Fliegel, 2019) (Figure 1.5).

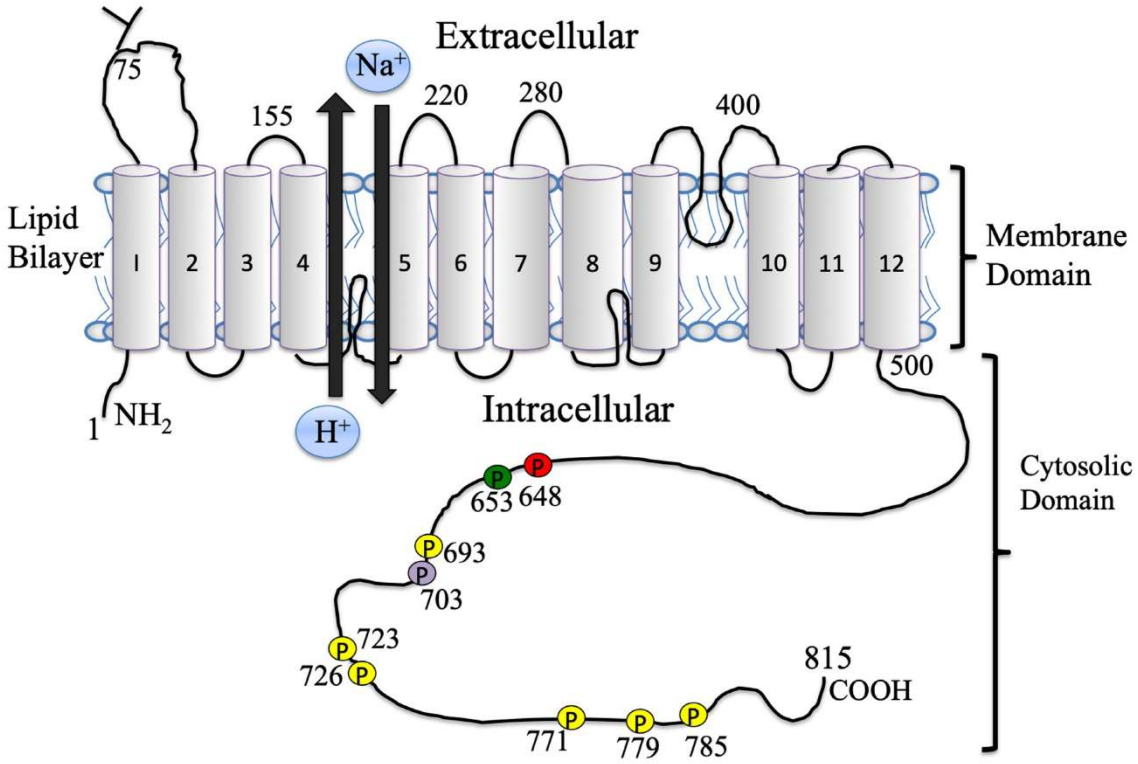

Figure 1.5 The structure of NHE1.
1-12 denotes transmembrane domains. The schematic model depicting some representative amino acids on extramembrane loops. Phosphorylation sites are presented–yellow for ERK, red for AKT, green for B-Raf, and purple for $p90^{rsk}$. ERK, extracellular signal-regulated kinase; AKT, protein kinase B; $p90^{rsk}$, ribosomal protein s6 kinase. (Fliegel, 2019)

1.4.3 The cooperation between NHE1 and NCX1

Various studies have indicated that NHE1 has diverse physiological functions, the most basic roles of which are the balance of cellular pH and volume. NHE1 participates in normal cell growth, proliferation, migration, differentiation and apoptosis (Slepkov et al., 2007), while abnormal expression of NHE1 is also involved in cancer, organ ischemia and hypertension (Malo and Fliegel, 2006, Bobulescu et al., 2005). It is worth noting when NHE1 influences hypertension, the reverse transport by NCXs is also involved, leading to intracellular Ca^{2+} overload and VSMC contraction (Bobulescu et al., 2005). The function of PM NCX proteins is to regulate Ca^{2+} in exchange for Na^{+} through Ca^{2+}-efflux (forward mode) or Ca^{2+}-influx (reverse mode), the direction depending on ionic concentration and membrane potential (Khananshvili, 2014). Three subtypes of

NCXs are distributed in unique tissues, with NCX1 being widely expressed in various tissues, including arteries, kidney, heart and other organs (Iwamoto et al., 2005, Wang et al., 2021). In addition, NCX is closely related to mineralization through delivery of Ca^{2+} into the matrix in osteoblasts (Stains et al., 2002). In tumors, calcification is also induced via the cooperation of NHE1 and reverse transport of NCX1 (Liskova et al., 2019).

1.4.4 NHE1 and ROS

Oxidative stress is an important driver of vascular calcification in CKD and atherosclerosis (Hawkins, 2018, Byon et al., 2008). Oxidative stress can induce osteogenic differentiation and VSMC calcification through phosphatidylinositide 3-kinase (PI3K)/ protein kinase B (AKT)/ Runx2 signaling (Byon et al., 2008). Oxidative stress also contributes to bone morphogenetic protein 2/4 (BMP-2/4) signaling and then pro-calcific matrix remodeling (Shao et al., 2006). Several studies have demonstrated that ROS accumulation is linked to NHE1 activation (Rothstein et al., 2002, Snabaitis et al., 2002, Garciarena et al., 2008). The loss of NHE1 expression in *Nhe1*$^{-/-}$ mice has been shown to suppress oxidative stress, as described by reduced expressions of redox-related proteins (Prasad et al., 2013). It is also reported that ROS activates NHE1 activity through extracellular signal-regulated kinase (ERK)1/2 signaling (Wei et al., 2001). Presumably, NHE1 interacts with ROS.

1.5 Serum and glucocorticoid inducible kinase 1 (SGK1)

1.5.1 Importance of SGK1

SGK1 belongs to the “AGC” kinase family of serine/threonine protein kinases that were originally defined due to the similar structure with protein kinases A, protein kinases G and protein kinases C at their catalytic domains (Pearce et al., 2010). The family contains at least 60 members, such as well-studied AKT and less well-studied SGK (Pearce et al., 2010). SGK1 and AKT family share a large homologous sequence and analogous function (Lang et al., 2006, Kobayashi and Cohen, 1999). However, SGK1 differs from AKT because SGK1 lacks the pleckstrin homology domain that directly binds to phosphatidylinositol 3,4,5

trisphosphate (Milburn et al., 2003, Kobayashi and Cohen, 1999). As illustrated in Figure 1.6 (Della-Morte et al., 2018), SGK1 contains 431 amino acids. Activation of SGK1 relies on phosphorylation of SGK1 at threonine 256 (T256) and serine 422 (S422). The enzymatic site of SGK-1 is located at lysine 127 (K127) of the ATP-binding site. The shuttling of SGK-1 between nucleus and cytoplasm is mediated through the interaction of importin-α with the nuclear localization signal (NLS) of essential domains of SGK1 protein.

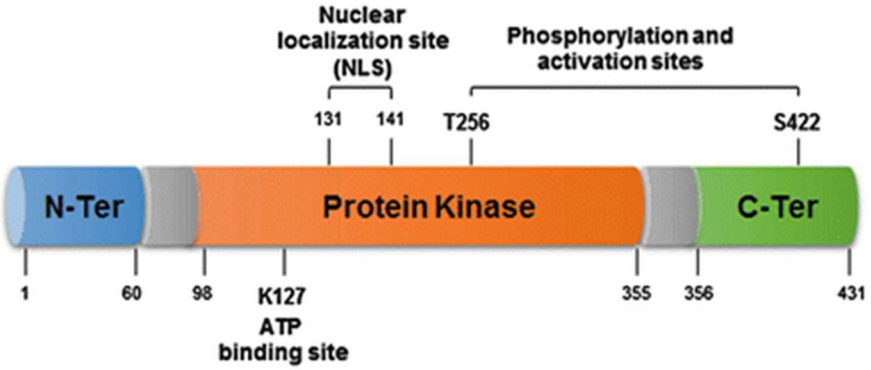

Figure 1.6 The structure of SGK1.
The schematic model illustrating the main domain structure of SGK1. Shown are ATP-binding site K127, NLS, as well as two key phosphorylation sites T256 and S422. K127, lysine 127; NLS, nuclear localization site; T256, threonine 256; S422, serine 422; C-Ter, COOH-terminus; N-Ter, NH_2-terminus. (Della-Morte et al., 2018)

SGK1 is ubiquitously expressed in all examined mammalian tissues (Zhang et al., 2020). SGK1 expression is stimulated by a wide spectrum of stimuli, including glucocorticoids, insulin, growth factors, cytokines, dehydration, saline ingestion, oxidative stress, Ca^{2+} chelation, cell swelling, excessive glucose concentrations, and deoxyribonucleic acid (DNA) damage (Lang and Stournaras, 2013, Lang et al., 2014b). Furthermore, previous studies have revealed that SGK1 participates in the modulation of ion channels, such as voltage-gated Na^+ channel SCN5A (Boehmer et al., 2003), epithelial Na^+ channel ENaC (Van Beusecum et al., 2019), voltage-gated K^+ channels KCNQ1/KCNE1 (Seebohm et al., 2008), and transient receptor potential channels TRPV4, 5 and 6 (Lang et al., 2018b). Recently, SGK1 has been shown to stimulate the CRAC channel Orai1 and its sensor STIM1 (Wester et al., 2019, Zhu et al., 2021). SGK1 is also a regulator of a variety of carriers, such as Na^+/H^+ exchangers NHE1 (Voelkl et

al., 2013) and NHE3 (Wang et al., 2007), Na^+-K^+-2Cl^--cotransporter NKCC2, glucose carriers SGLT1, GLUT1 and GLUT4 (Lang et al., 2018b).

1.5.2 SGK1 and SOCE

Ca^{2+} is a highly important intracellular second messenger, involved in a range of fundamental biological processes, including cell growth, proliferation, differentiation, death and exocytosis (Hwang et al., 2012). It is also well-recognized that Ca^{2+} signaling is implicated in the formation and function of osteoblastic cells and osteoclastic cells (Hwang et al., 2012, Hwang and Putney, 2011). Increased cytosolic Ca^{2+} concentration is caused by the release from ER Ca^{2+} stores and Ca^{2+} influx from extracellular space. In most non-excitable cell types, SOCE is the main pathway of extracellular Ca^{2+} entry, which is primarily mediated by Orai1 and STIM1 (Hwang et al., 2012, Ambudkar et al., 2017). Previous work has shown that SGK1 upregulates the Orai1 abundance through phosphorylating ubiquitin ligase Nedd4-2 (Eylenstein et al., 2011) and enhances the transcription of Orai1 and STIM1 by the activation and translocation of nuclear factor κ-light chain enhancer of activated B cells (NF-κB) (Borst et al., 2012). SGK1 is a pro-calcific regulator depending on the transcriptional activity of NF-κB, resulting in osteo-/chondrogenic transdifferentiation of VSMCs and vascular calcification (Ma et al., 2019). In fact, SGK1-dependent regulation of Orai1/STIM1 retains SGK1-sensitive functions, including stimulation of vascular calcification, cell proliferation, and migration (Ma et al., 2019, Hwang et al., 2012).

1.5.3 SGK1 and NHE1/ROS

SGK1 upregulates a myriad of carriers, including the expression and activity of Na^+/H^+ exchanger NHE1 (Voelkl et al., 2012) and the epithelial NHE3 (Yun et al., 2002). It has been demonstrated that SGK1 activates osteogenic regulation of VSMCs, which in turn leads to vascular calcification (Chilukoti et al., 2013). In HL-1 cardiomyocytes, a 24-h treatment with glucocorticoids elevates the expression of Na^+/H^+ exchanger NHE1, whereas the transcription and activity of NHE1 are abrogated by SGK1 inhibitor EMD638683 (Voelkl et al., 2013). A previous study showed that the activation of NHE1 triggers the development and

progression of heart failure and left ventricular hypertrophy in different animal models, while longtime treatment with NHE1 inhibitor cariporide significantly attenuates these diseases and prolongs the lifespan, indicating the potential therapeutic effect of NHE1 inhibitors on chronic diseases (Baartscheer, 2006, Darmellah et al., 2007). Additionally, the role of Na^+/H^+ exchanger in mineralizing osteoblasts has been disclosed (Liu et al., 2011). In particular, NHE1 further regulates nicotinamide adenine dinucleotide phosphate oxidase (NOX) activity and accordingly ROS generation (Garciarena et al., 2008), which stimulates osteogenic differentiation and VSMC calcification (Byon et al., 2008). In addition, NHE1 exports intracellular H^+ in exchange for Na^+, which results in the overload of cytosolic Na^+ (Orlowski and Grinstein, 2004). In the following, the PM ion transporter NCX1 exchanges Ca^{2+} for intracellular Na^+ driven by the Na^+ electrochemical gradient (Khananshvili, 2014). NCX1 is an important protein that participates in Ca^{2+} entry via reverse mode in arterial smooth muscle (Dong et al., 2006).

1.6 Aim of the study

To the best of our knowledge, nothing is known about a role of SOCE, NHE1 and ROS generation in vasopressin-induced vascular smooth muscle cell calcification. Thus, the current study addresses the following purposes:

To explore whether vasopressin modified ORAI/STIM isoform expressions, SOCE, NHE1 expression, ROS generation and thus osteogenic signaling, HAoSMCs were treated without and with vasopressin. Vasopressin is known as a stimulator of vascular calcification (Nishiwaki-Yasuda et al., 2007). As shown in other cell types, vasopressin may stimulate SOCE (Jones et al., 2008, Piron and Villereal, 2013). Furthermore, NHE1 exports intracellular H^+ in exchange for Na^+, which results in the overload of cytosolic Na^+ (Orlowski and Grinstein, 2004). In the following, the PM ion transporter NCX1 exchanges Ca^{2+} for intracellular Na^+ driven by the Na^+ electrochemical gradient (Khananshvili, 2014). Oxidative stress interacting with NHE1 may participate in the pathogenesis of calcification by triggering osteogenic signaling (Mazzini and Schulze, 2006, Shao et al., 2006, Prasad et al., 2013, Wei et al., 2001).

2 Materials and methods

2.1 Materials

2.1.1 Antibodies and primers

Table 2.1: List of used antibodies.

Target	Lot No.	Source	Dilution	Supplier
Purified anti-GAPDH antibody	2118S	Rabbit	1:1000	Cell Signaling Technology, Danvers, USA
Purified anti-ORAI1 antibody	13130-1-AP	Rabbit	1:1000	Proteintech, Rosemont, USA
Purified anti-STIM1 antibody	4916S	Rabbit	1:1000	Cell Signaling Technology, Danvers, USA
Purified anti-SGK1 antibody	12103S	Rabbit	1:1000	Cell Signaling Technology, Danvers, USA
Purified anti-SGK1(phospho S422) antibody	ab55281	Rabbit	1:1000	Abcam, Cambridge, UK
Purified anti-NHE1 antibody	PRS4377	Rabbit	1:1000	Sigma-Aldrich, St. Louis, USA
Purified anti-rabbit horseradish peroxidase (HRP)-conjugated antibody	7074S		1:2500	Cell Signaling Technology, Danvers, USA

Table 2.2: List of used primers.

Primer	Orientation	Sequence (5'– > 3' orientation))
ORAI1	Forward	CACCTGTTTGCGCTCATGAT
	Reverse	GGGACTCCTTGACCGAGTTG
ORAI2	Forward	CAGCTCCGGGAAGGAACGTC
	Reverse	CTCCATCCCATCTCCTTGCG
ORAI3	Forward	CTTCCAATCTCCCACGGTCC
	Reverse	GTTCCTGCTTGTAGCGGTCT
STIM1	Forward	AAGAAGGCATTACTGGCGCT
	Reverse	GATGGTGTGTCTGGGTCTGG
STIM2	Forward	AGGGGATTCGCCTGTAACTG
	Reverse	GGTTTACTGTCGTTGCCAGC
CBFA1	Forward	GCCTTCCACTCTCAGTAAGAAGA
	Reverse	GCCTGGGGTCTGAAAAAGGG
MSX2	Forward	TGCAGAGCGTGCAGAGTTC
	Reverse	GGCAGCATAGGTTTTGCAGC
SOX9	Forward	AGCGAACGCACATCAAGAC

	Reverse	CTGTAGGCGATCTGTTGGGG
ALPL	Forward	GGGACTGGTACTCAGACAACG
	Reverse	GTAGGCGATGTCCTTACAGCC
SGK1	Forward	AGGAGGATGGGTCTGAACGA
	Reverse	GGGCCAAGGTTGATTTGCTG
V1aR	Forward	CCTTCAAGACTGTGTTCAAAGC
	Reverse	TCCTTCCACATACCCGTACTG
V1bR	Forward	CTCATCTGCCATGAGATCTGTAA
	Reverse	CCACATCTGGACACTGAAGAA
V2R	Forward	ATTCATGCCAGTCTGGTGC
	Reverse	TCACGATGAAGTGTCCTTGG
NHE1	Forward	ACCTGGTTCATCAACAAGTTCCG
	Reverse	TTCACAGCCAACAGGTCTACCA
NCX1	Forward	ACAAGAGGTATCGAGCTGGC
	Reverse	ATGCCATTTCTCGCCTAGC
GAPDH	Forward	TCAAGGCTGAGAACGGGAAG
	Reverse	TGGACTCCACGACGTACTCA

2.1.2 Biochemicals and reagents

Table 2.3: List of biochemicals and reagents used in the project.

Name	Supplier
2',7'–dichlorofluorescein diacetate (DCFDA)	Sigma-Aldrich, St. Louis, USA
4-(2-Hydroxyethyl)-piperazine-1-ethanesulfonic acid (HEPES)	Carl Roth, Karlsruhe, Germany
Acrylamide/Bis-solution 30% (29:1)	Carl Roth, Karlsruhe, Germany
SeaKem® LE agarose	Lonza, Rockland, ME, USA
Alkaline phosphatase assay kit	Abcam, Cambridge, UK
Bio-Rad protein assay dye reagent Concentrate	Bio-Rad Laboratories, München, Germany
Calcium chloride ($CaCl_2$)	Sigma-Aldrich, St. Louis, USA
Cariporide	Sigma-Aldrich, St. Louis, USA
Cell dissociation reagent	Gibco, Grand Island, USA
Chloroform	Carl Roth, Karlsruhe, Germany
Developer and replenisher	Kodak, USA
Dimethyl sulfoxide (DMSO)	Carl Roth, Karlsruhe, Germany
Dulbecco's phosphate buffered saline (PBS)	Sigma-Aldrich, St. Louis, USA
Pierce™ enhanced chemiluminescence (ECL) western blotting substrate	Thermo Fisher Scientific, USA
Ethylene glycol tetraacetic acid (EGTA)	VWR, Leuven, Belgium
Ethanol 99.98%	Carl Roth, Karlsruhe, Germany
Fetal bovine serum (FBS)	Gibco, Grand Island, USA

Fixer and Replenisher	Kodak, USA
Fura-2/AM	Invitrogen, Goettingen, Germany
Glucose	Sigma-Aldrich, St. Louis, USA
Glycine	Carl Roth, Karlsruhe, Germany
GoScript™ reverse transcription kit	Promega, Hilden, Germany
GoTaq® qPCR master mix kit	Promega, Hilden, Germany
GSK-650394	Sigma-Aldrich, St. Louis, USA
Halt Protease and Halt Phosphatase Inhibitor Cocktail	Thermo Fisher Scientific, Danvers, USA
Hydrochloric acid (HCl)	Carl Roth, Karlsruhe, Germany
Isopropanol	Carl Roth, Karlsruhe, Germany
Magnesium sulfate ($MgSO_4$)	Sigma-Aldrich, St. Louis, USA
Human Vascular Smooth Muscle Cell Basal Medium (also called “Medium 231”)	Gibco, Grand Island, USA
Methanol	Sigma-Aldrich, St. Louis, USA
MRS1845	Tocris, Bristol, UK
N-acetyl-L-cysteine (NAC)	Sigma-Aldrich, St. Louis, USA
Non-fat milk powder	Carl Roth, Karlsruhe, Germany
Paraformaldehyde	Carl Roth, Karlsruhe, Germany
Penicillin/Streptomycin	Invitrogen, Karlsruhe, Germany
PeqGold TriFast	PeqLab, Erlangen, Germany
Potassium chloride (KCl)	Carl Roth, Karlsruhe, Germany
Protein marker	Thermo Fisher Scientific, Danvers, USA
QuantiChrom™ Calcium Assay Kit	BioAssay Systems, Hayward, CA
Radioimmunoprecipitation assay (RIPA) lysis buffer	Cell Signaling Technology, Danvers, USA
Roti®-Load 1 (4x)	Carl Roth, Karlsruhe, Germany
Sodium dodecyl sulfate (SDS)	Carl Roth, Karlsruhe, Germany
Sodium chloride (NaCl)	Carl Roth, Karlsruhe, Germany
Sodium hydrogen phosphate (Na_2HPO_4)	Carl Roth, Karlsruhe, Germany
Sodium hydroxide (NaOH)	Carl Roth, Karlsruhe, Germany
SYBR® Safe DNA Gel Stain	Invitrogen, Eugene, Oregon, USA
RG7713	MedChemExpress, New Jersey, USA
N,N,N’N’-Tetramethylethylenediamine (TEMED)	Carl Roth, Karlsruhe, Germany
Thapsigargin	Invitrogen, Darmstadt, Germany
Tris-base	Carl Roth, Karlsruhe, Germany
Trypsin	Gibco, Paisley, UK
Tween 20	Carl Roth, Karlsruhe, Germany
Vasopressin	Sigma-Aldrich, Steinheim, Germany

2.1.3 Solutions, medium and buffers

Table 2.4: List of solutions, medium and buffers used in the project.

Solutions, Medium and Buffers	Compounds and handling	
Cell culture medium	Human Vascular Smooth Muscle Cell Basal Medium (also called “Medium 231”)	445 mL
	FBS	50 mL
	Penicillin/Streptomycin solution	5 mL
70% Ethanol solution	99.98% Ethanol	70 mL
	dd H_2O	30 mL
2% Agarose gels	Agarose	4 g
	SYBR® Safe DNA Gel Stain	6 µL
	Tris-acetate-EDTA (TAE) buffer	200 mL
1.5 M Tris (pH 8.8)	Tris-base	36.33 g
	dd H_2O	200 mL
1.0 M Tris (pH 6.8)	Tris-base	24.22 g
	dd H_2O	200 mL
10% Ammonium persulphate (APS)	APS	10 g
	dd H_2O	100 mL
10% Sodium dodecyl sulfate (SDS)	SDS	10 g
	dd H_2O	100 mL
10×SDS running buffer (pH 8.3)	Tris-base	30.3 g
	Glycine	144 g
	SDS	10 g
	dd H_2O	1 L
1×SDS running buffer	10×SDS running buffer	100 mL
	dd H_2O	900 mL
10×Transfer buffer	Tris-base	30.3 g
	Glycine	144 g
	dd H_2O	1 L
1×Transfer buffer	10×Transfer buffer	100 mL
	Methanol	200 mL
	dd H_2O	700 mL
10×Tris-buffered saline (TBS) (pH 7.6)	Tris-base	24.2 g
	NaCl	80 g
	dd H_2O	1 L
1×TBST	10×TBS	100 mL
	Tween 20	1 mL
	dd H_2O	900 mL
10% Resolving gel (per 5 mL)	H_2O	1.9 mL
	Acrylamide/Bis-solution 30% (29:1)	1.7 mL
	1.5 M Tris (pH8.8)	1.3 mL
	10% SDS	0.05 mL
	10% APS	0.05 mL
	TEMED solution	0.002 mL
	H_2O	3.4 mL

5% Stacking gel (per 5 mL)	Acrylamide/Bis-solution 30% (29:1)	0.83 mL
	1.5 M Tris (pH8.8)	0.63 mL
	10% SDS	0.05 mL
	10% APS	0.05 mL
	TEMED solution	0.005 mL
5% non-fat milk	Non-fat milk	5 g
	1×TBST	100 mL
Standard HEPES solution (pH 7.4)	NaCl	3.653 g
	KCl	0.1864 g
	$MgSO_4 \cdot 7H_2O$	0.15 g
	HEPES	3.84 g
	Na_2HPO_4	0.142 g
	Glucose	0.45 g
	$CaCl_2 \cdot 2H_2O$	0.074 g
	dd H_2O	500 mL
Ca^{2+}-free HEPES solution (pH 7.4)	NaCl	3.653 g
	KCl	0.1864 g
	$MgSO_4 \cdot 7H_2O$	0.15 g
	HEPES	3.84 g
	Na_2HPO_4	0.142 g
	Glucose	0.45 g
	EGTA	0.0951 g
	dd H_2O	500 mL
1% Alizarin red S solution (pH 4.0)	Alizarin red S	1 g
	dd H_2O	100 mL

2.1.4 Consumables and instruments

Table 2.5: List of used consumables and instruments.

Name	Supplier
Agarose gel electrophoresis chamber	BioRad, München, Germany
Axiorvert 100	Carl Zeiss, Oberkochen, Germany
BioPhotometer	Eppendorf, Hamburg, Germany
BioTek™ PowerWave™ Microplate Spectrophotometer	BioTek, Bad Friedrichshall, Germany
Cell culture plate 6, 12, 24, 96 well	Corning incorporated, München, Germay
CFX96 real-time system	Bio-Rad, München, Germany
Cover glasses	VWR, Leuven, Belgium
Cuvettes, Uvette	Eppendorf, Hamburg, Germany
Electronic pipette controller	Peqlab Biotech, Erlangen, Germany
Electrophoresis and blotting system	Bio-Rad, München, Germany
Eppendorf 5331 MasterCycler gradient thermal cycler	Eppendorf, Hamburg, Germany

Eppendorf 5417R refrigerated centrifuge	Eppendorf, Hamburg, Germany
Eppendorf tube 0.5, 1.5, 2.0 mL	Eppendorf, Hamburg, Germany
Flow cytometry machine, FACS Calibur™	BD Biosciences, Heidelberg, Germany
Heidolph Polymax 1040	Heidolph
Heraeus cell culture hood	Thermo Fisher Scientific, Langenselbold, Germany
Heraeus cell culture incubator	Thermo Fisher Scientific, Langenselbold, Germany
pH meter	SI Analytics, Mainz, Germany
Platform shaker	Heidolph Instruments GmbH, Schwabach, Germany
Polyvinylidene difluoride (PVDF) transfer membrane	Bio-Rad, München, Germany
qPCR 96 well plate	VWR, Leuven, Belgium
Roller mixer	Phoenix Instrument GmbH, Garbsen, Germany
Scanner	Epson, Nagano, Japan
Corning® Costar® Stripette® serological pipettes 5, 10, 25 mL	Corning incorporated, München, Germay
Sterile tips 10, 100, 200, 1000 µL	BioZyme, USA
Sterile tubes 15, 50 mL	Greiner bio-one, Frickenhausen, Germany
Tissue culture flask 75mL	SARSTEDT, Nübrecht, Germany
Vortex-Genie2	Scientific Industries, New York, USA

2.1.5 Software

Table 2.6: List of used software.

Software	Supplier
ImageJ	Version 1.52, National Institutes of Health, Bethesda, MD, USA
Metafluor	Version 7.5, Universal Imaging, Downingtown, PA, USA
FlowJo	Version V10, TreeStar, CA, USA
SPSS	Version 22.0, SPSS Inc., Chicago, IL, USA
GraphPad Prism	Version 8.0.2, San Diego, California, USA
Endnote	Version X8, Clarivate Analytics, USA

2.2 Methods

2.2.1 Cell culture

Human aortic smooth muscle cells (HAoSMCs, Thermo Fisher Scientific) were routinely maintained in Medium 231 (Gibco) supplemented with 10% fetal

bovine serum (FBS, Gibco) and 1% Penicillin/Streptomycin (Invitrogen). HAoSMCs were cultured at 37ºC in a humidified incubator containing 5% CO_2. Culture medium was replaced every 2 or 3 days. HAoSMCs of 4 to 10 passages were used for experiments upon 80% confluency (Zhu et al., 2021).

2.2.2 Treatments

Where indicated, the cells were treated with 100 nM vasopressin (Sigma-Aldrich) (Nishiwaki-Yasuda et al., 2007) in the following experiments. To investigate a role of Orai1 in vasopressin-evoked vascular calcification, HAoSMCs were pre-incubated with V1a receptor inhibitor RG7713 (10 nM, MedChemExpress) (Zhu et al., 2021), with SGK1 blocker GSK-650394 (1 μM, Sigma-Aldrich) (Borst et al., 2012) and/or with Orai1 blocker MRS1845 (10 μM, Tocris) (Ma et al., 2019, Korchak et al., 2007) prior to vasopressin exposure. Furthermore, to explore a role of NHE1 expression and ROS generation in vasopressin-induced vascular calcification, HAoSMCs were pre-incubated with NHE1 inhibitor cariporide (10 μM, Sigma-Aldrich) (Chatterjee et al., 2014) and/or with ROS scavenger N-acetyl-L-cysteine (NAC, 0.5 mM, Sigma-Aldrich) (Xu et al., 2019) before vasopressin exposure.

2.2.3 Quantitative polymerase chain reaction (qPCR)

2.2.3.1 RNA extraction

RNase-free EP tubes and tips were prepared in advance. Total RNA of each sample was extracted using 1 mL TriFast (Peqlab). After dissociation of cells at room temperature, 200 μL trichloromethane per 1 mL TriFast were added, followed by a vigorous vibration for 15 s. After incubating for 5 min at room temperature, the samples were centrifuged at 12,000 ×g at 4°C for 15 min. The upper colorless aqueous phase was transferred to a new EP tube. RNA was precipitated using isopropanol. After that, RNA was washed twice to remove DNA using 70% Ethanol and the supernatant was discarded. RNA pellet was air-dried at ambient temperature for 10-15 min. Then, 20-50 μL RNase-free water was added to solubilize the RNA at 65°C for 10-15 min.

The concentration of RNA was obtained using the BioPhotometer (Eppendorf) at the wavelengths 260 nm and 280 nm when diluted in RNase-free water at a ratio of 1:69.

2.2.3.2 cDNA synthesis

Reverse transcription of total RNA was conducted using GoScript™ Reverse Transcriptase System (Promega) according to the manufacturer's instructions. After DNase digestion, 3 µg of total RNA were prepared in RNase-free water to reach the volume to 9 µL, and then 1 µL Oligo$(dT)_{15}$ primers and 1 µL random primers were added. The mixture was placed on the PCR machine at 70°C for 5 min. Following, 4 µL GoScript™ 5× Reaction Buffer, 2.5 µL $MgCl_2$, 1 µL PCR Nucleotide Mix, 1 µL GoScript™ Reverse Transcriptase and 0.5 µL Recombinant RNasin® Ribonuclease Inhibitor were added and mixed well. The mixture was incubated at 25°C for 5 min, 42°C for 60 min and followed at 70°C for 15 min.

2.2.3.3 qPCR

A total volume for qPCR was 15 µL using 100 ng of cDNA, 2× GoTaq® qPCR Master Mix (Promega), 500 nM forward and reverse primer (Thermo Fischer Scientific) as well as RNase-free water. Cycling conditions were as follows: initial denaturation at 95°C for 3 min, followed by 40 cycles of 95°C for 15 s, 58°C for 30 s and 72°C for 30 s. The primers for amplification used in this study were provided in Table 2.2.

The real-time qPCR was conducted on a CFX96 Real-Time System (Bio-Rad). All experiments were carried out in duplicate. The relative mRNA expression was obtained by using the $2^{-\Delta\Delta Ct}$ methods normalized to the control group (Zhu et al., 2020, Zhu et al., 2021).

qPCR samples for V1aR, V1bR, V2R primers were also visualized via 2% agarose gel electrophoresis stained with SYBR® Safe DNA Gel Stain.

2.2.4 Western blotting

HAoSMCs were collected and centrifuged for 5 min at 300 ×g and 4°C. The pellet was washed three times with cold phosphate buffered saline (PBS) and lysed with 40 µL ice-cold RIPA lysis buffer (Cell Signaling Technology) containing Halt Protease and Halt Phosphatase Inhibitor Cocktail (Thermo

Fisher Scientific). The protein concentration was quantified using the Bradford assay (BioRad). The equal amounts of proteins were resolved on 10% sodium dodecyl sulfate (SDS)-polyacrylamide gel (PAGE), followed by electro-transferring onto polyvinylidene difluoride (PVDF) membranes for 80 min. Nonspecific binding sites were blocked with 5% non-fat milk for 1 h before overnight incubation with primary anti-Orai1 antibody (1:1000, Proteintech), anti-STIM1 antibody (1:1000, Cell Signaling Technology), anti-SGK1 antibody (1:1000, Cell Signaling Technology), anti-SGK1 (phospho S422) antibody (1:1000, Abcam), anti-NHE1 antibody (1:1000, Sigma-Aldrich) or anti-GAPDH antibody (1:2000, Cell Signaling Technology) at 4°C. The blots were washed with TBST three times and subsequently incubated with corresponding secondary antibody conjugated with horseradish peroxidase (HRP) (1:2500, Cell Signaling Technology) for 2 h at ambient temperature. After additional washes (TBST), the bands were captured using an enhanced chemiluminescence (ECL) detection reagent (Thermo Fisher Scientific). ImageJ software (National Institutes of Health) was used for semi-quantified analysis of the obtained blots, and the results were normalized to GAPDH. Protein marker (Thermo Fisher Scientific) was used for detecting apparent protein sizes (Zhu et al., 2020).

2.2.5 Cytosolic Ca^{2+} measurements

Cytosolic Ca^{2+} concentrations ($[Ca^{2+}]_i$) were detected using Fura-2/AM fluorescence (Schmid et al., 2012). Cells were loaded on chambered glass coverslips and treated with vasopressin in the absence or presence of GSK-650394 or MRS1845 at indicated concentrations. The cells were incubated with 2 μM Fura-2/AM (Invitrogen) for 30-45 min in the incubator at 37°C. The fluorescence excitation was at 340 nm and 380 nm, and emission at 505 nm through an objective (Fluor 40×/1.30 oil) built in an inverted phase-contrast microscope (Axiovert 100, Zeiss). The change of $[Ca^{2+}]_i$ was estimated from the ratio of 340 nm/380 nm excitation wavelengths. Data (n = 20-35 cells) were collected using specialized Metafluor software (Universal Imaging). SOCE was determined as follows: standard HEPES solution for 3 min, Ca^{2+}-free HEPES solution for 3 min for Ca^{2+} removal from extracellular space, Ca^{2+}-free HEPES

solution with thapsigargin for 7 min to inhibit the sarco/endoplasmatic reticulum Ca^{2+}-ATPase (SERCA) with thapsigargin (1 μM, Invitrogen) and subsequent Ca^{2+} re-addition for 7 min in the continued presence of thapsigargin. The increase of slope (delta ratio/s) and peak (delta ratio) of Fura-2/AM fluorescence following re-addition of Ca^{2+} were used to quantify Ca^{2+} entry. The solutions, including standard HEPES solution and Ca^{2+}-free HEPES solution (shown in Table 2.4), were prepared as described before (Zhu et al., 2020, Zhu et al., 2021).

2.2.6 Detection of ROS generation

Intracellular ROS was determined using a flow cytometry. Harvested HAoSMC cells were washed and incubated at a final concentration of 10 μM 2',7'-dichlorofluorescein diacetate (DCFDA) (Sigma-Aldrich) in the dark for 30 min at 37°C. After that, cells were washed three times with PBS and subsequently resuspended in 500 μL PBS. ROS production was immediately measured by flow cytometry (BD Biosciences). At an excitation wavelength of 488 nm and an emission wavelength of 530 nm on a FACS machine, the fluorescence intensity of DCFDA was detected and measured. The geometric mean analysis was conducted using FlowJo_V10 software (TreeStar).

2.2.7 Alkaline phosphatase (ALP) activity assay

HAoSMCs were treated with 100 nM vasopressin for 7 days in the presence or absence of SGK1 blocker GSK-650394, ORAI1 inhibitor MRS1845, NHE1 inhibitor cariporide or ROS scavenger NAC at indicated concentrations. Fresh media with agents were changed every 2 to 3 days. Commercial ALP assay kit (Abcam) was used for the measurement of ALP activity in VSMCs according to the manufacturer's protocols. We measured the ALP activity at optical density 405 nm using a microplate reader (BioTek). The results were normalized to total protein concentration in each sample, as determined by the Bradford method (Bio-Rad Laboratories) (Zhu et al., 2020, Zhu et al., 2021).

2.2.8 Calcium content and alizarin red S staining

Calcium content assay was performed following vasopressin treatment of HAoSMCs for 14 days. Cells were decalcified in 0.6 M hydrochloric acid (HCl) for 24 h at 4°C. Calcium content was measured by the QuantiChrom^{TM} Calcium Assay Kit (BioAssay Systems). HAoSMCs were lysed with 0.1 M sodium hydroxide (NaOH)/0.1% SDS. Calcium content was expressed as units per mg of protein (U/mg protein) (Bio-Rad Laboratories). To visualize calcium deposits, alizarin red S staining was performed after 100 nM vasopressin and 1 mM $CaCl_2$ (Sigma-Aldrich) treatment for 14 days. Fresh Medium 231 with agents was replaced every 2-3 days. Cells were fixed in 4% paraformaldehyde for 45 min and then stained with 1% alizarin red (pH 4.0) for 50 min. The red mineralized nodules were the calcified areas (Zhu et al., 2020, Zhu et al., 2021).

2.2.9 Measurement of medium pH and bicarbonate concentration

To measure the pH of the medium, HAoSMCs were seeded in the 6-well plates for 24 h. Then, cells were treated with vasopressin for 24 h in the absence or presence of NHE1 inhibitor cariporide. The pH of the culture medium was monitored using a pH meter at 0, 1, 2, 6, 12, 24 h.

The corresponding values of bicarbonate concentrations in the medium can be calculated according to the Henderson-Hasselbalch equation as follows:

$$pH = 6.1 + \log\left(52 \frac{\text{mg/mL } NaHCO_3}{\%\ CO_2} - 1\right) \text{ (Esser, 2010)}$$

2.2.10 Statistical analysis

All data are expressed as mean ± standard deviation (SD), *n* means the replication number of experiments. Statistical analysis was performed using statistic package for social science (SPSS, Version 22.0) and GraphPad Prism (Version 8.0.2). The probability of significant differences within two groups was conducted using unpaired *t* test (Student's *t* test). Statistical analysis of multiple groups was carried out using analysis of variance (ANOVA) followed by Dunnett's and Tukey's test. A p value ≤ 0.05 was considered as statistically significant.

3 Results

3.1 Vasopressin-stimulated ORAI1 expression and SOCE in HAoSMCs

3.1.1 Vasopressin exposure increased the expression of osteogenic genes, calcium deposition and ALP activity in HAoSMCs

To investigate whether vasopressin influences osteogenic signaling in HAoSMCs, cells were exposed to various concentrations (0, 10, 50, 100, 200 nM) of AVP for 24 h. Since CBFA1, MSX2, SOX9 and ALPL are implicated in VSMC osteogenic transdifferentiation, we selected them as detection markers (Steitz et al., 2001, Holmar et al., 2020, Durham et al., 2018). As indicated from Figure 3.1, qPCR results demonstrated that treatment with AVP upregulated transcript levels of osteogenic transcription factors *CBFA1* (Figure 3.1A), *MSX2* (Figure 3.1B), and *SOX9* (Figure 3.1C), as well as *ALPL* (Figure 3.1D) in a concentration-dependent manner in HAoSMCs, reaching statistical significance at 100 nM vasopressin (Figure 3.1A-D). Alizarin red S staining (Figure 3.2A), calcium content (Figure 3.2B) and ALP activity (Figure 3.2C) showed that vasopressin exposure increased calcium deposition (Figure 3.2A-B) and ALP activity (Figure 3.2C) in HAoSMCs in a concentration-dependent manner, effects again requiring 100 nM vasopressin to reach statistical significance. Dependent on the above results, HAoSMCs were incubated with 100 nM AVP for the subsequent experiments.

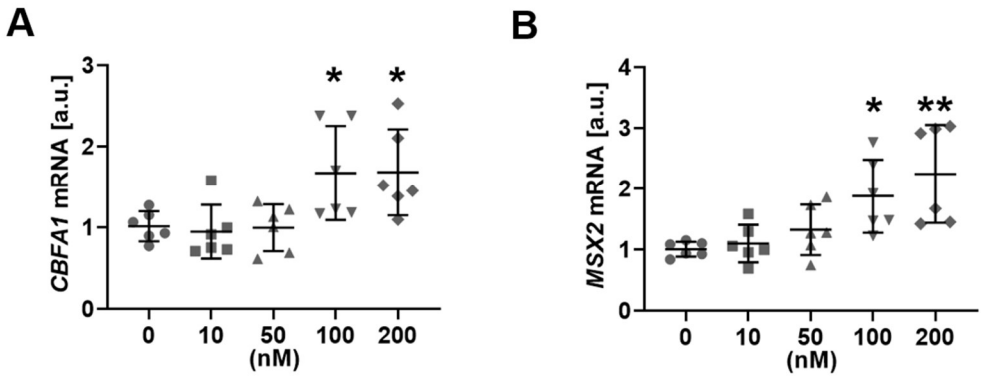

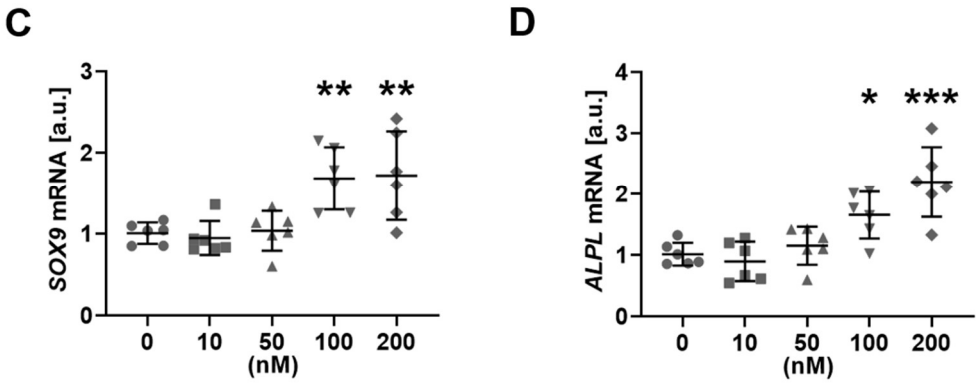

Figure 3.1 Effects of vasopressin on osteogenic genes *CBFA1*, *MSX2*, *SOX9* and *ALPL* transcription in HAoSMCs.
Osteogenic switching genes *CBFA1* **(A)**, *MSX2* **(B)**, *SOX9* **(C)** and *ALPL* **(D)** transcript levels in HAoSMCs after a 24-h culture without and with 10 - 200 nM vasopressin. Values are means ± SD. *(p < 0.05), **(p < 0.01), ***(p < 0.001) indicates statistically significant difference to absence of vasopressin (ANOVA). n=6 for each group. Adapted from *Xuexue Zhu* (Zhu et al., 2021).

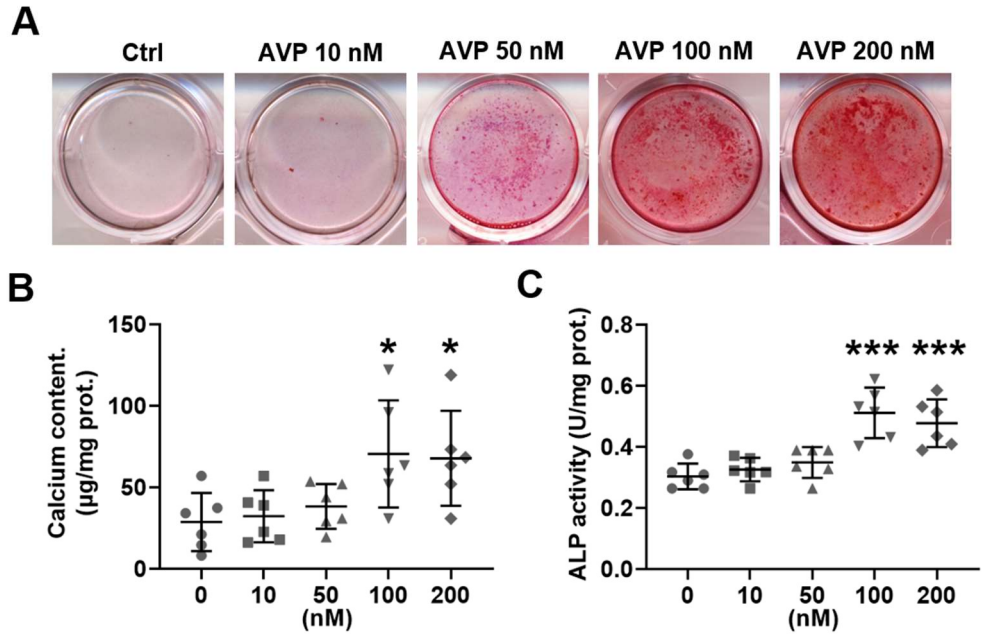

Figure 3.2 Effects of vasopressin on calcium deposition and ALP activity in HAoSMCs.
(A). Representative alizarin red S staining in HAoSMCs in response to different concentrations (10 - 200 nM) of vasopressin and 1 mM $CaCl_2$ for 14 days. **(B).** Calcium content of HAoSMCs after a 14-day culture without and with 10 - 200 nM vasopressin. **(C).** ALP activity of HAoSMCs after a 7-day treatment without and with 10 - 200 nM vasopressin. Values are means ± SD. *(p < 0.05), ***(p <

0.001) indicates statistically significant difference to 0 nM vasopressin (ANOVA). *n*=6 for each group. Adapted from *Xuexue Zhu* (Zhu et al., 2021).

3.1.2 Vasopressin sensitivity of ORAIs/STIMs and SOCE in HAoSMC cells

To test the potential effect of vasopressin on SOCE, transcript levels and protein abundance of the CRAC channel ORAI isoforms, and thus ORAI-activating Ca^{2+} sensor STIMs were evaluated. A 24-h incubation of HAoSMCs with 100 nM vasopressin significantly increased the transcript levels of *ORAI1* (Figure 3.3A) and *ORAI2* (Figure 3.3B), as well as *STIM1* (Figure 3.3D) and *STIM2* (Figure 3.3E). However, the expression levels of *ORAI3* (Figure 3.3C) were unchanged following 100 nM vasopressin treatment. ORAI1 and STIM1 have been identified as the primary components of SOCE (Ambudkar et al., 2017). Therefore, we further measured the protein expressions of ORAI1 and STIM1. We observed that a 24-h exposure of HAoSMCs to 100 nM vasopressin significantly upregulated the protein abundance of ORAI1 (Figure 3.3F-G) and STIM1 (Figure 3.3F, H).

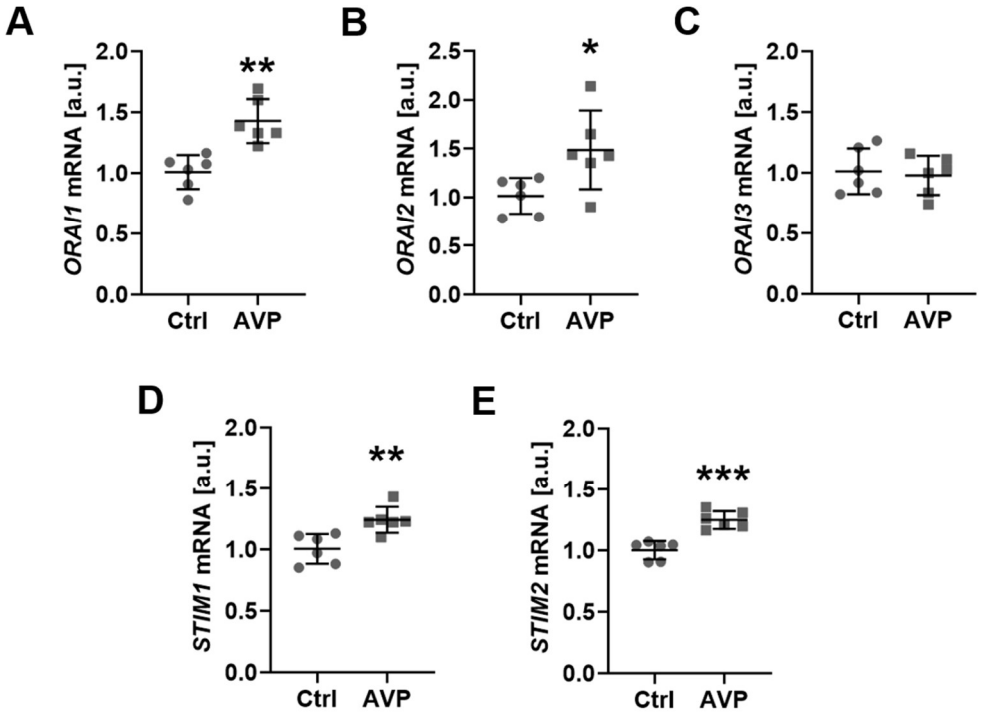

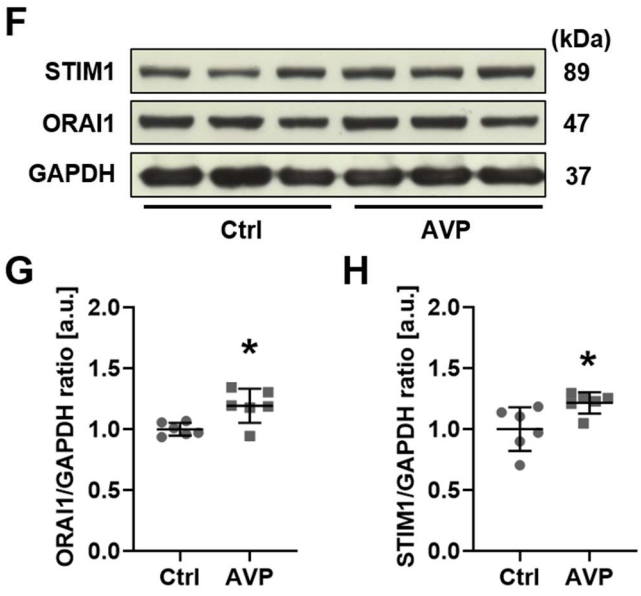

Figure 3.3 Effects of vasopressin on ORAIs and STIMs in HAoSMCs. **(A-E).** The transcript levels of *ORAI1* **(A)**, *ORAI2* **(B)**, *ORAI3* **(C)**, *STIM1* **(D)** and *STIM2* **(E)** in HAoSMCs following a 24-h culture without (Ctrl) and with (AVP) 100 nM vasopressin. **(F).** Representative immunoblots showing the protein expressions of ORAI1 and STIM1 in vehicle (Ctrl) and 100 nM vasopressin (AVP)-treated HAoSMCs for 24 h. Scatter dot plots showing that the quantitative analysis of ORAI1 **(G)** and STIM1 **(H)** protein levels. Values are means ± SD. *($p < 0.05$), **($p < 0.01$), ***($p < 0.001$) indicates statistically significant difference to absence of vasopressin (unpaired *t*-test). n=6 for each group. Figures A-E were adapted from *Xuexue Zhu* (Zhu et al., 2021).

To assess the direct effect of vasopressin on SOCE, we used Fura-2 fluorescence to measure $[Ca^{2+}]_i$. As expected, Fura-2 fluorescence analysis indicated that the enhanced expressions of ORAIs and STIMs went paralleled to alterations of $[Ca^{2+}]_i$ after 100 nM vasopressin incubation (Figure 3.4). To determine SOCE (Figure 3.4A), the AVP-treated HAoSMCs were first incubated using standard HEPES solution to remove excess Fura-2 dye and then Ca^{2+}-free HEPES solution was added to reach a nominal Ca^{2+}-free circumstance. After that, Ca^{2+}-free solution containing thapsigargin (1 μM), which is an irreversible inhibitor of the SERCA, was perfused. Subsequently, extracellular Ca^{2+} was re-added in the presence of thapsigargin. We found that there was no significant difference in a rapid increase caused by intracellular Ca^{2+} store depletion following a 24-h treatment with 100 nM vasopressin (Figure 3.4A, B, D). However,

compared with control group, vasopressin dramatically increased SOCE after a 24-h incubation with 100 nM vasopressin (Figure 3.4A, C, E).

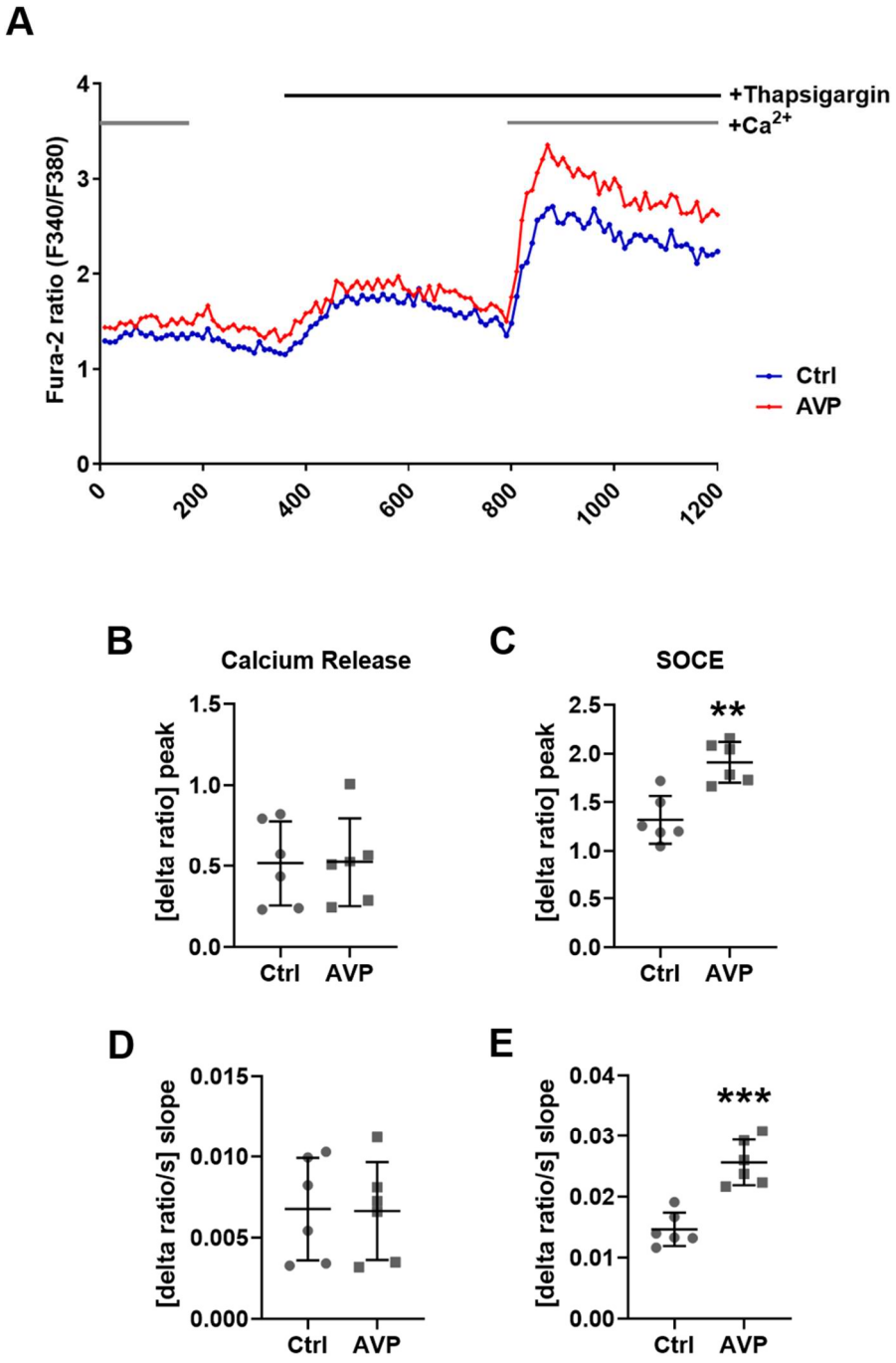

Figure 3.4 Effects of vasopressin on SOCE in HAoSMC cells.
(A). Representative tracings reflecting the average of Fura-2 fluorescence-ratio from 6 experiments in fluorescence spectrometry. HAoSMCs loaded with 2 μM Fura-2/AM were incubated with 1 mM Ca^{2+} HEPES solution, followed by Ca^{2+}-free HEPES solution, Ca^{2+}-free HEPES solution with thapsigargin (1 μM), as well

as the addition back of extracellular Ca^{2+} following a 24-h culture without (Ctrl) and with (AVP) 100 nM vasopressin. The peak **(B)** and slope **(D)** increase of fura-2 fluorescence-ratio after the addition of Ca^{2+}-free HEPES solution with thapsigargin (1 µM) following exposure to without (Ctrl) and with (AVP) 100 nM vasopressin for 24 h in HAoSMCs. The peak **(C)** and slope **(E)** increase of fura-2 fluorescence-ratio following the addition back of extracellular Ca^{2+} after a 24-h treatment without (Ctrl) and with (AVP) 100 nM vasopressin in HAoSMCs. Values are means ± SD. **(p < 0.01), ***(p < 0.001) indicates statistically significant difference to absence of vasopressin (unpaired t-test). n=6 for each group. Adapted from *Xuexue Zhu* (Zhu et al., 2021).

3.1.3 MRS1845-sensitivity of the vasopressin effect on SOCE in HAoSMC cells

MRS1845 is a selective SOCE inhibitor by blocking ORAI1 (Korchak et al., 2007, van Kruchten et al., 2012). In order to investigate whether the ORAI1 inhibitor MRS1845 affected the effect of vasopressin on SOCE and to determine the optimal concentration of MRS1845, HAoSMCs were exposed to 100 nM vasopressin in the absence or presence of MRS1845 with increasing concentrations (0, 1, 5, 10 µM) for 24 h. qPCR results revealed that 5 µM MRS1845 significantly inhibited vasopressin-induced transcription of osteogenic genes *CBFA1* (Figure 3.5A) and *MSX2* (Figure 3.5B), while 10 µM MRS1845 effectively attenuated the upregulation of *SOX9* (Figure 3.5C) and *ALPL* (Figure 3.5D) transcription by vasopressin.

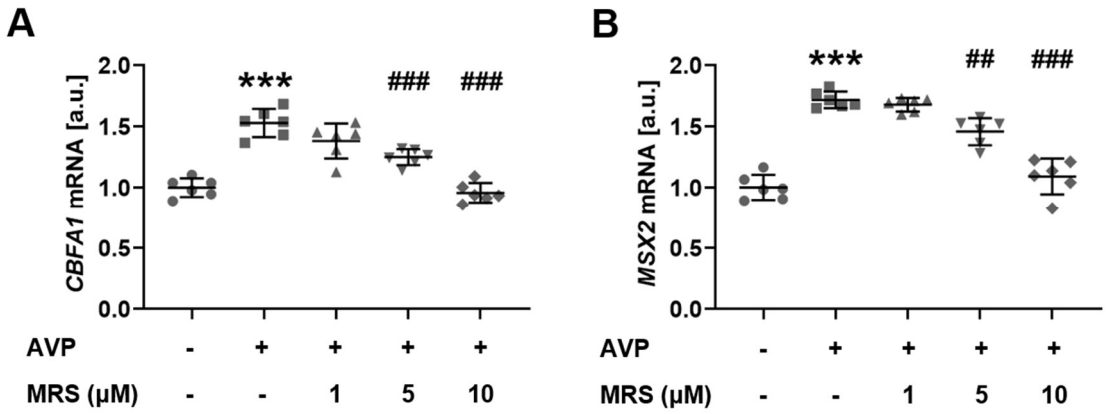

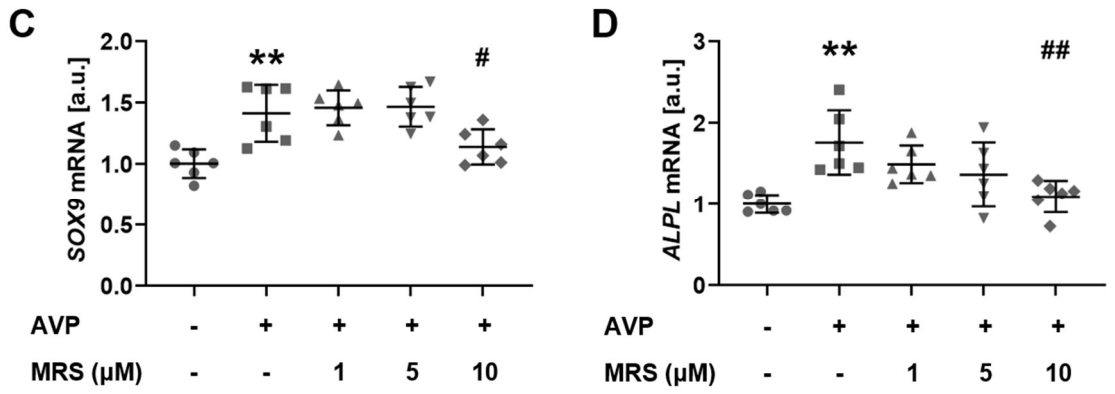

Figure 3.5 Effects of increasing concentrations of ORAI1 blocker MRS1845 on osteogenic genes *CBFA1*, *MSX2*, *SOX9* and *ALPL* transcription in HAoSMCs.
HAoSMCs were pretreated with increasing concentrations (0, 1, 5, 10 μM) of ORAI1 blocker MRS1845 (MRS) for 30 min and subsequently incubated with 100 nM vasopressin (AVP) for 24 h. Non-treated cells functioned as a negative control (Ctrl). Transcript levels of osteogenic genes *CBFA1* **(A)**, *MSX2* **(B)**, *SOX9* **(C)** and *ALPL* **(D)** were assessed by qPCR in HAoSMCs. Values are means ± SD. **($p < 0.01$), ***($p < 0.001$) indicates statistically significant difference to absence of vasopressin, $^{\#}$($p < 0.05$), $^{\#\#}$($p < 0.01$), $^{\#\#\#}$($p < 0.001$) indicates statistically significant difference to vasopressin treatment alone (ANOVA). n=6 for each group.

Therefore, in the subsequent experiments, HAoSMC cells were pretreated with 10 μM MRS1845 for 30 min prior to 100 nM vasopressin incubation. Our findings revealed that the addition of MRS1845 significantly repressed SOCE both in the absence and presence of vasopressin (Figure 3.6A, C, E). Notably, vasopressin stimulated SOCE even in the presence of MRS1845 (Figure 3.6A, C, E), an observation pointing to the stimulation of MRS1845-insensitive SOCE. In addition, we found that MRS1845 did not affect intracellular Ca^{2+} store release induced by thapsigargin (Figure 3.6A, B, D).

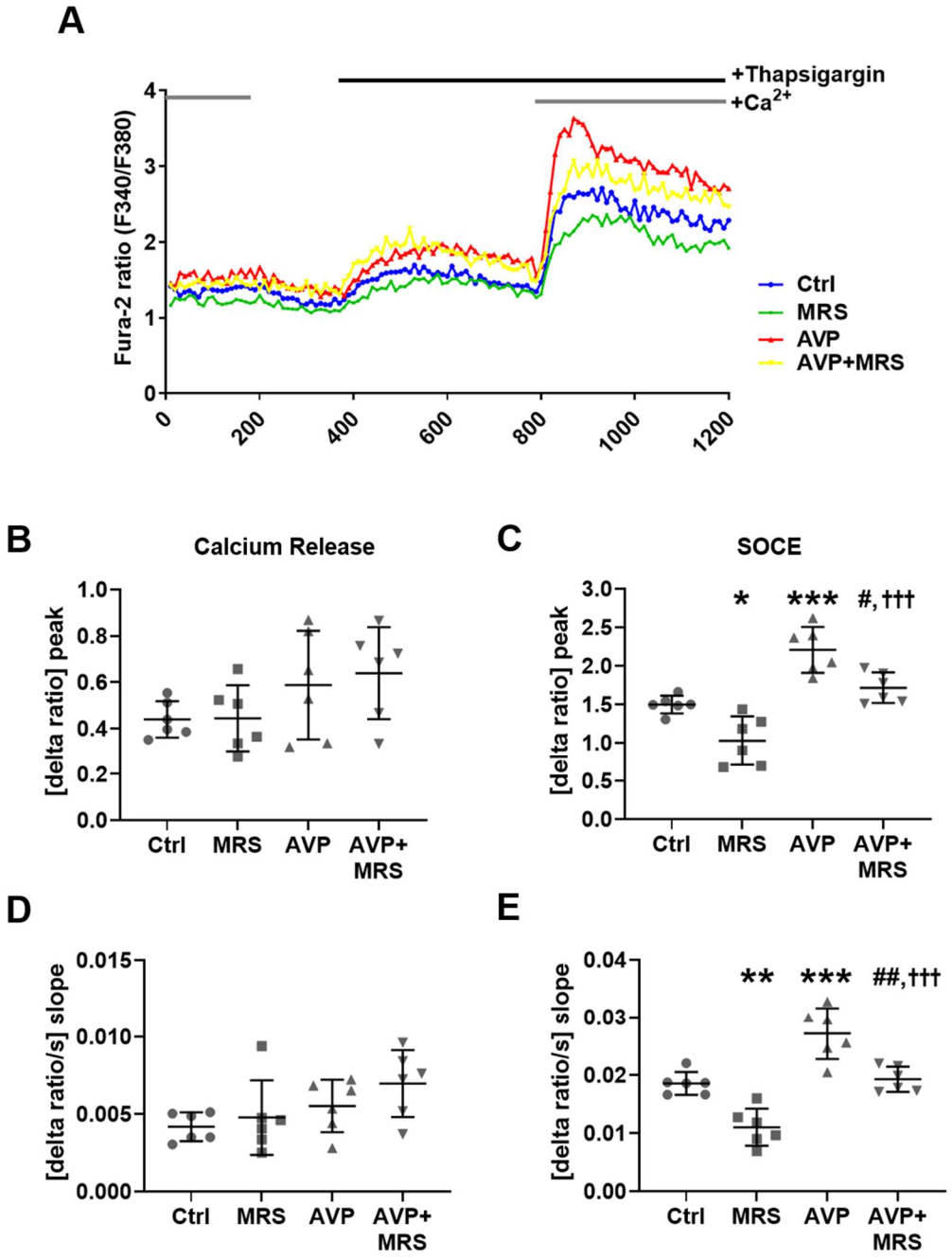

Figure 3.6 Sensitivity of vasopressin-induced SOCE in response to ORAI1 blocker MRS1845 in HAoSMCs.

(A). Representative tracings reflecting the treatment results of Fura-2 fluorescence-ratio from 6 experiments. HAoSMCs loaded with 2 μM Fura-2/AM were incubated with 1 mM Ca^{2+} HEPES solution, followed by Ca^{2+}-free HEPES solution, Ca^{2+}-free HEPES solution with the presence of thapsigargin (1 μM), as well as the addition back of extracellular Ca^{2+} following a 24-h treatment without (Ctrl) and with (AVP) 100 nM vasopressin in the absence or presence of 10 μM ORAI1 inhibitor MRS1845 (MRS). The peak **(B)** and slope **(D)** increase of fura-2 fluorescence-ratio after the addition of thapsigargin (1 μM) into Ca^{2+}-free HEPES

solution following a 24-h exposure to without (Ctrl) and with (AVP) 100 nM vasopressin in the absence or presence of 10 μM ORAI1 blocker MRS1845 (MRS) in HAoSMCs. The peak **(C)** and slope **(E)** increase of fura-2 fluorescence-ratio after re-addition of extracellular Ca^{2+} following without (Ctrl) and with (AVP) 100 nM vasopressin treatment for 24 h in the absence or presence of 10 μM ORAI1 blocker MRS1845 (MRS) in HAoSMCs. Values are means ± SD. *($p < 0.05$), **($p < 0.01$), ***($p < 0.001$) indicates statistically significant difference to Ctrl, $^{\#}$($p < 0.05$), $^{\#\#}$($p < 0.01$) indicates statistically significant difference to vasopressin treatment alone, †††($p < 0.001$) indicates statistically significant difference to MRS treatment alone (ANOVA). *n*=6 for each group. Adapted from *Xuexue Zhu* (Zhu et al., 2021).

3.1.4 Inhibition of SGK1 blunted vasopressin-induced ORAI1 and STIM1 expression, and SOCE in HAoSMCs

To explore whether the expression of SGK1 is influenced by vasopressin, HAoSMCs were treated with 100 nM vasopressin. A 24-h incubation of HAoSMCs with vasopressin dramatically elevated the transcript levels of *SGK1* (Figure 3.7A). Additionally, we observed that the protein expression of phospho-SGK1 (S422) (Figure 3.7B, C) was significantly increased. In contrast, vasopressin had no effect on the protein expression of total-SGK1 (Figure 3.7B, D).

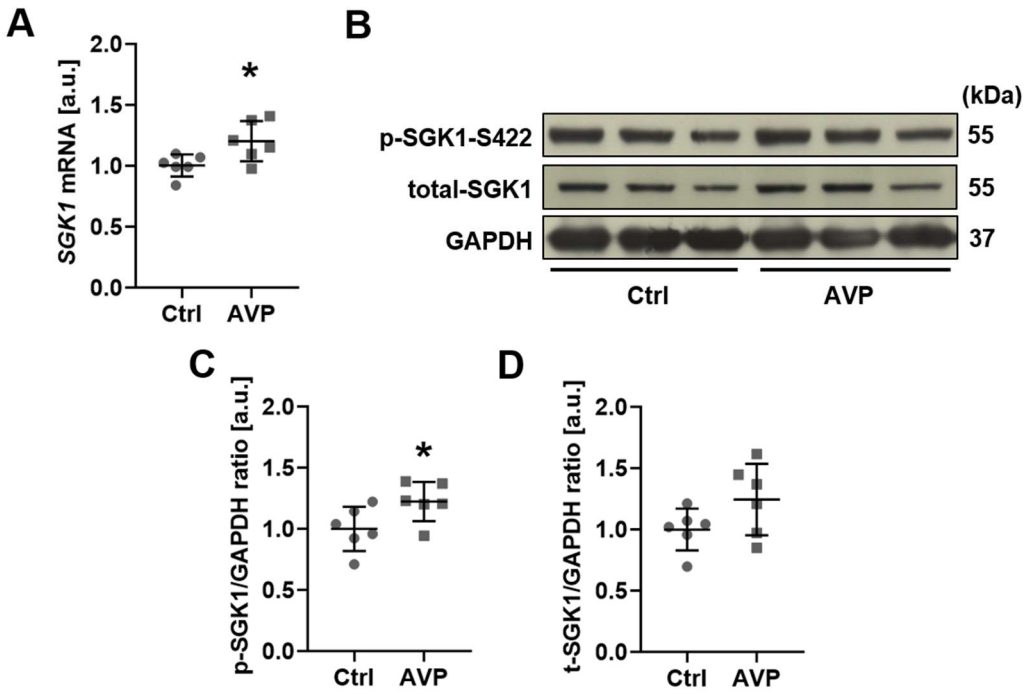

Figure 3.7 Effects of vasopressin on SGK1 expression in HAoSMCs.
(A). *SGK1* transcript levels in HAoSMCs following a 24-h culture without (Ctrl) and with (AVP) 100 nM vasopressin. **(B).** Representative original blots showing

the effects of 100 nM vasopressin on phospho-SGK1 (S422) and total-SGK1 protein abundance in HAoSMCs after vasopressin incubation for 24 h. **(C).** Scatter dot plots showing the quantification of phospho-SGK1 (S422) protein levels. **(D).** Quantitative analysis of total-SGK protein levels. Values are means ± SD. *(p < 0.05) indicates statistically significant difference to absence of vasopressin (unpaired t-test). n=6 for each group.

We wanted to further examine whether SGK1 (Ma et al., 2019) is involved in the stimulation of ORAI1 and STIM1 expressions by vasopressin and treated cells with increasing concentrations (0, 0.1, 0.5, 1 μM) of the SGK1 inhibitor GSK-650394. qPCR results showed that 1 μM GSK-650394 suppressed vasopressin-induced the transcription of osteogenic genes *CBFA1* (Figure 3.8A), *MSX2* (Figure 3.8B), *SOX9* (Figure 3.8C) as well as *ALPL* (Figure 3.8D). Based on these results, in the following experiments, HAoSMCs were pre-incubated with 1 μM GSK-650394 for 30 min before 100 nM vasopressin treatment.

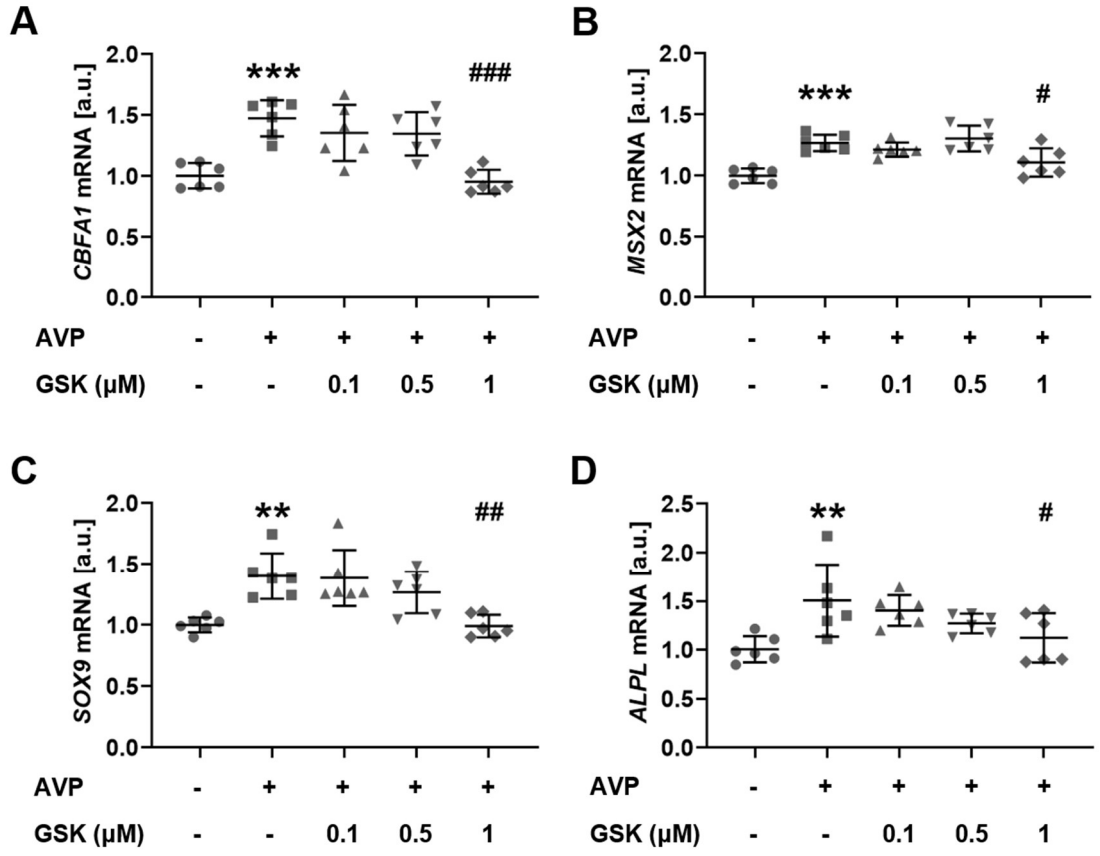

Figure 3.8 Effects of increasing concentrations of SGK1 inhibitor GSK-650394 on osteogenic genes *CBFA1*, *MSX2*, *SOX9* and *ALPL* transcription in HAoSMCs.

HAoSMCs were exposed to various concentrations (0, 0.1, 0.5, 1 μM) of SGK1 inhibitor GSK-650394 (GSK) for 30 min prior to 100 nM vasopressin (AVP) treatment for 24 h. Non-treated cells were used as a negative control (Ctrl). Transcript levels of osteogenic switching genes *CBFA1* **(A)**, *MSX2* **(B)**, *SOX9* **(C)** and *ALPL* **(D)** were determined with qPCR in HAoSMCs. Values are means ± SD. **($p < 0.01$), ***($p < 0.001$) indicates statistically significant difference to Ctrl, $^{\#}$($p < 0.05$), $^{\#\#}$($p < 0.01$), $^{\#\#\#}$($p < 0.001$) indicates statistically significant difference to vasopressin treatment alone (ANOVA). n=6 for each group.

We found that SGK1 inhibition by 1 μM GSK-650394 prevented the upregulation of *ORAI1* (Figure 3.9A) and *STIM1* (Figure 3.9B) transcription induced by vasopressin. Also, immunoblots showed that 1 μM GSK-650394 pre-incubation obviously counteracted vasopressin-challenged upregulation of protein abundance of ORAI1 (Figure 3.9C, D) and STIM1 (Figure 3.9C, E) in HAoSMCs. Meanwhile, GSK-650394 pretreatment had no effect on the expressions of ORAI1 and STIM1 in the control-cultured HAoSMCs.

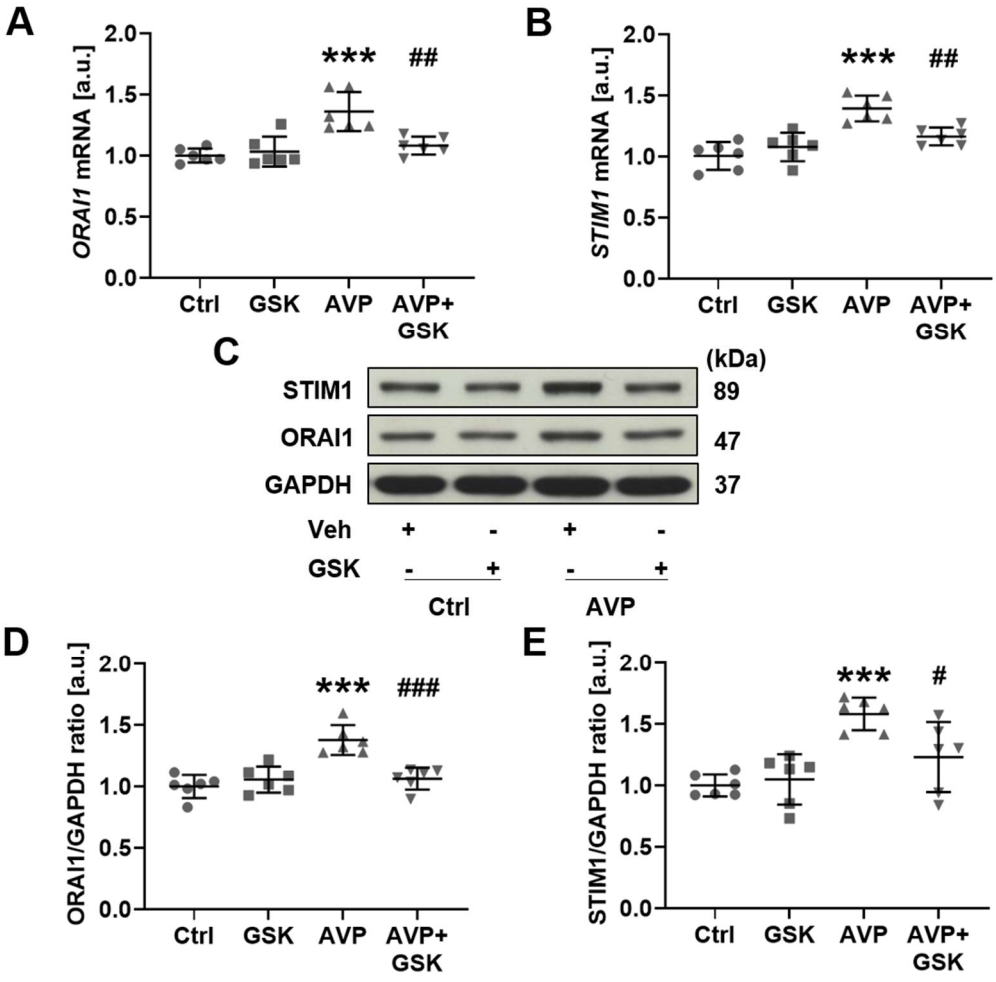

Figure 3.9 Sensitivity of vasopressin-induced ORAI1 and STIM1 expression in response to SGK1 inhibitor GSK-650394 in HAoSMCs.
The mRNA levels of *ORAI1* **(A)** and *STIM1* **(B)** following a 24-h treatment without (Ctrl) and with (AVP) 100 nM vasopressin in the absence or presence of 1 μM SGK1 inhibitor GSK-650394 (GSK) in HAoSMCs. **(C).** Representative immunoblots showing protein abundance of ORAI1 and STIM1 following a 24-h culture without (Ctrl) and with (AVP) 100 nM vasopressin in the absence or presence of 1 μM SGK1 inhibitor GSK-650394 (GSK). **(D).** Scatter dot plots showing the quantification of ORAI1. **(E).** Quantitative analysis of STIM1 protein level. Values are means ± SD. ***($p < 0.001$) indicates statistically significant difference to absence of vasopressin, #($p < 0.05$), ##($p < 0.01$), ###($p < 0.001$) indicates statistically significant difference to vasopressin treatment alone (ANOVA). *n*=6 for each group. Figures A-B were adapted from *Xuexue Zhu* (Zhu et al., 2021).

Furthermore, the inhibition of SGK1 blunted the vasopressin-stimulated upregulation of SOCE (Figure. 3.10A, C, E). Similarly, 1 μM GSK-650394 remarkably inhibited SOCE both in the absence or presence of vasopressin (Figure. 3.10A, C, E). Vasopressin obviously enhanced SOCE even in the presence of SGK1 inhibitor GSK-650394 (Figure 3.10A, C, E), suggesting that SOCE is only partially dependent on SGK1. In addition, we demonstrated that GSK-650394 did not significantly modify calcium release induced by thapsigargin (Figure 3.10A, B, D).

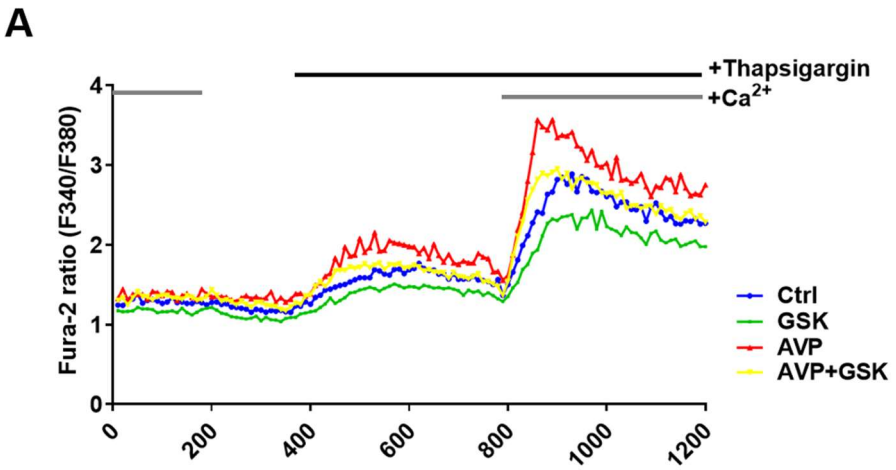

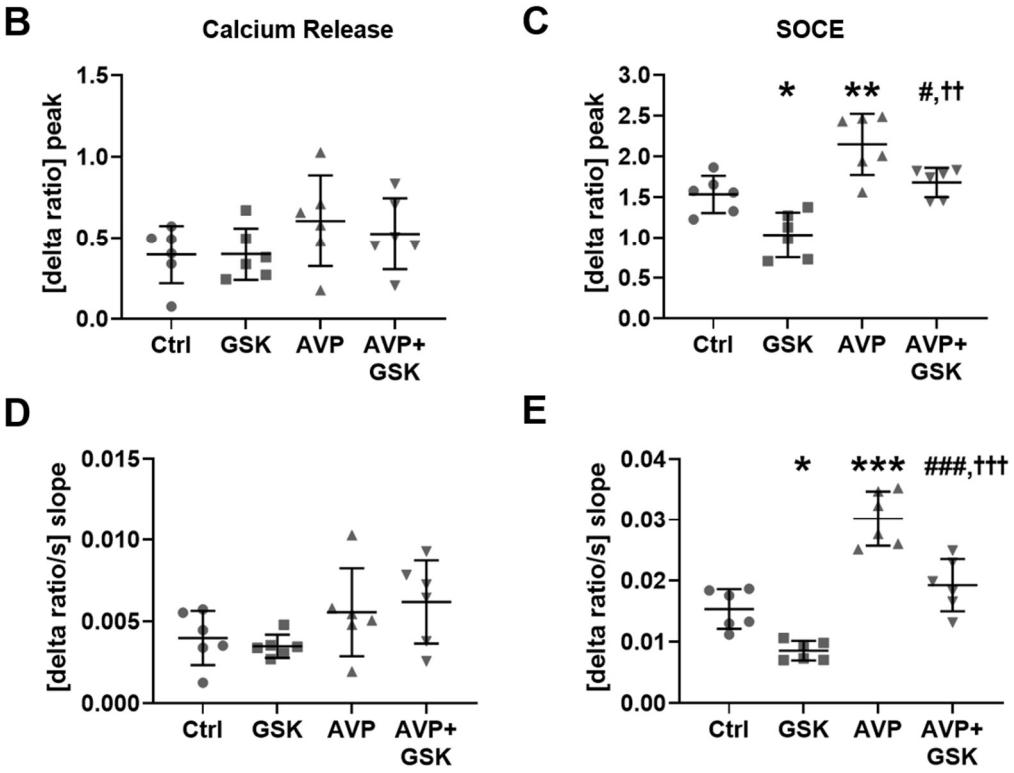

Figure 3.10 Sensitivity of the vasopressin effect on SOCE in response to SGK1 inhibitor GSK-650394 in HAoSMCs.
(A). Representative tracings representing the average values of Fura-2 fluorescence-ratio from 6 experiments in fluorescence spectrometry. After a 24-h exposure to without (Ctrl) and with (AVP) 100 nM vasopressin in the absence or presence of pretreatment with 1 μM SGK1 inhibitor GSK-650394 (GSK), HAoSMCs loaded with 2 μM Fura-2/AM were incubated with 1 mM Ca^{2+} HEPES solution, followed by Ca^{2+}-free HEPES solution, Ca^{2+}-free HEPES solution with the presence of thapsigargin (1 μM), as well as the re-addition of extracellular Ca^{2+}. The peak **(B)** and slope **(D)** increase of fura-2-fluorescence-ratio after the addition of Ca^{2+}-free HEPES solution with thapsigargin (1 μM) following a 24-h treatment without (Ctrl) and with (AVP) 100 nM vasopressin in the absence or presence of 1 μM SGK1 inhibitor GSK-650394 (GSK) in HAoSMCs. The peak **(C)** and slope **(E)** increase of fura-2-fluorescence-ratio following re-addition of extracellular Ca^{2+} after a 24-h exposure of HAoSMCs to without (Ctrl) and with (AVP) 100 nM vasopressin in the absence or presence of 1 μM SGK1 inhibitor GSK-650394 (GSK). Values are means ± SD. *($p < 0.05$), **($p < 0.01$), ***($p < 0.001$) indicates statistically significant difference to Ctrl, $^{\#}$($p < 0.05$), $^{\#\#\#}$($p < 0.001$) indicates statistically significant difference to vasopressin treatment alone, ††($p < 0.01$), †††($p < 0.001$) indicates statistically significant difference to GSK treatment alone (ANOVA). n=6 for each group. Adapted from *Xuexue Zhu* (Zhu et al., 2021).

3.1.5 Inhibition of SGK1 and ORAI1 blunted vasopressin-induced osteogenic signaling and calcification in HAoSMCs

In order to confirm whether the observed increase of ORAIs and STIMs transcription and SOCE stimulated by vasopressin in HAoSMCs leads to the expected vasopressin-induced osteo-/chondrogenic signaling, HAoSMCs were pretreated with SGK1 blocker GSK-650394 or ORAI1 inhibitor MRS1845 for 30 min, followed by 100 nM vasopressin incubation for 24 h. Transcript levels of osteogenic genes *CBFA1*, *MSX2*, *SOX9*, and *ALPL* were evaluated using qPCR. Herein, we found that exposure of HAoSMCs to vasopressin increased transcript levels of *CBFA1* (Figure 3.11A), *MSX2* (Figure 3.11B), *SOX9* (Figure 3.11C), and *ALPL* (Figure 3.11D), which were significantly prevented by GSK-650394 or MRS1845 treatment (Figure 3.11A-D). Moreover, alizarin red S staining and calcium content assay showed that vasopressin incubation of HAoSMCs for 14 days enhanced calcium deposit, which was markedly blunted by GSK-650394 or MRS1845 (Figure 3.11E-F). Similar results were obtained for ALP activity. Exposure of HAoSMCs to vasopressin for 7 days increased ALP activity, which was attenuated by GSK-650394 or MRS1845 treatment (Figure 3.11G).

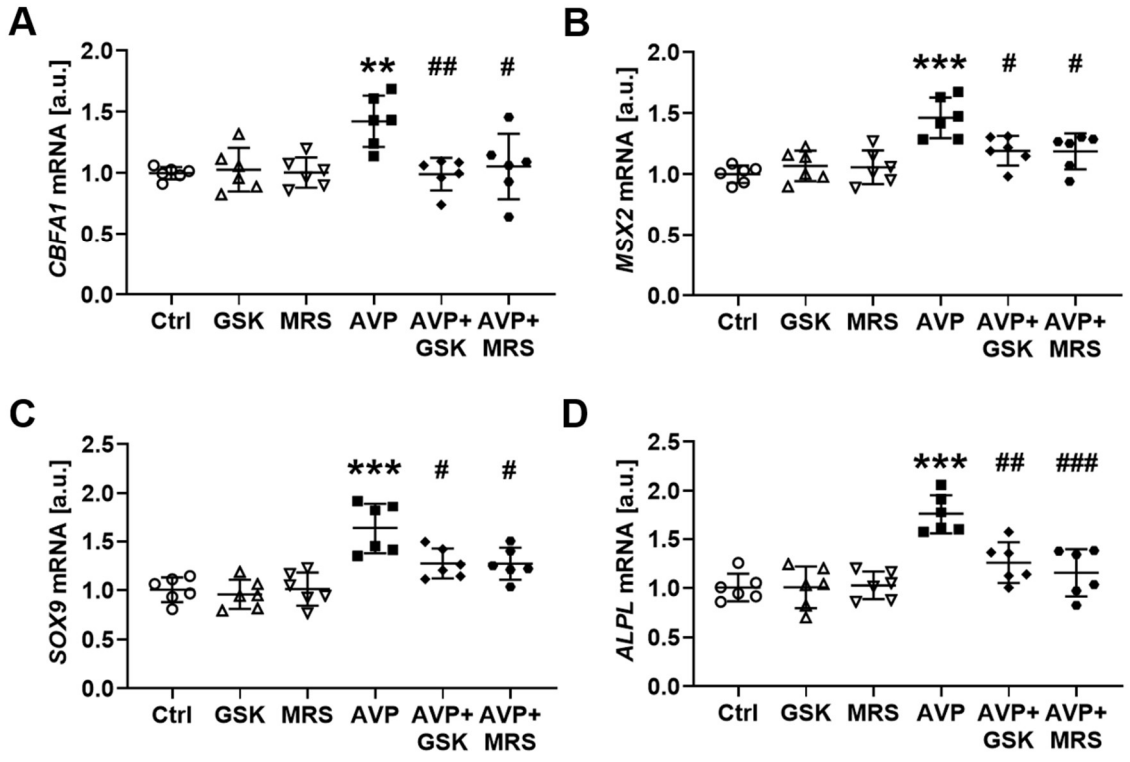

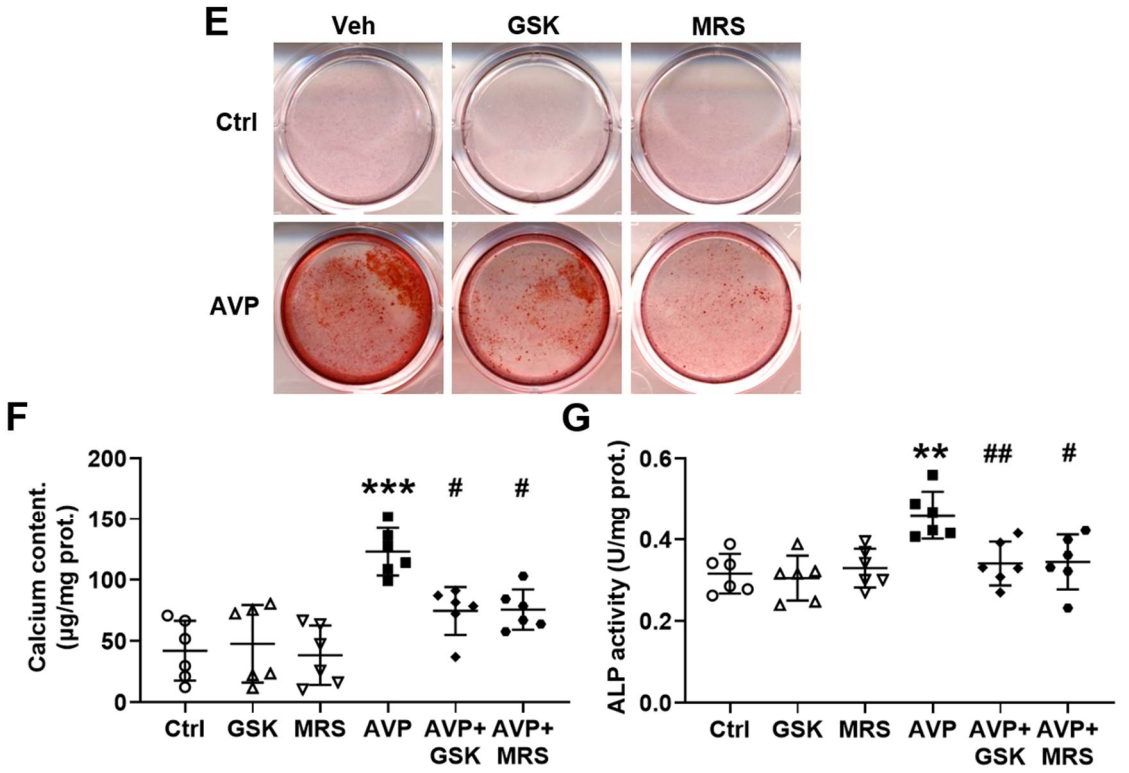

Figure 3.11 Sensitivity of vasopressin-induced osteogenic signaling and calcification in HAoSMCs to SGK1 inhibitor GSK-650394 and ORAI1 blocker MRS1845.

(A-D). HAoSMCs were pretreated in the absence or presence of 1 µM SGK1 inhibitor GSK-650394 (GSK) or 10 µM ORAI1 blocker MRS1845 (MRS) for 30 min, and then stimulated with 100 nM vasopressin (AVP) for 24 h. Non-treated cells functioned as a negative control (Ctrl). Transcript levels of osteogenic switching markers *CBFA1* **(A)**, *MSX2* **(B)**, *SOX9* **(C)** and *ALPL* **(D)** were determined by qPCR. **(E).** HAoSMCs were stimulated without (Ctrl) and with (AVP) 100 nM vasopressin and 1 mM $CaCl_2$ in the absence (Veh) or presence of 1 µM SGK1 inhibitor GSK-650394 (GSK) or 10 µM ORAI1 blocker MRS1845 (MRS) for 14 days. Original images of alizarin red S staining depicting calcium deposits. **(F).** Scatter dot plots of calcium content in HAoSMCs after stimulating without (Ctrl) and with (AVP) 100 nM vasopressin in the absence or presence of 1 µM SGK1 inhibitor GSK-650394 (GSK) or 10 µM ORAI1 blocker MRS1845 (MRS) for 14 days. **(G).** Scatter dot plots of ALP activity in HAoSMCs after pretreatment with 1 µM SGK1 inhibitor GSK-650394 (GSK) or 10 µM ORAI1 blocker MRS1845 (MRS) for 30 min before without (Ctrl) and with (AVP) 100 nM vasopressin for 7 days. Values are means ± SD. **($p < 0.01$), ***($p < 0.001$) indicates statistically significant difference to absence of vasopressin, #($p < 0.05$), ##($p < 0.01$), ###($p < 0.001$) indicates statistically significant difference to vasopressin treatment alone (ANOVA). n=6 for each group. Adapted from *Xuexue Zhu* (Zhu et al., 2021).

3.1.6 Vasopressin receptors transcripts in HAoSMCs

To investigate whether vasopressin receptor subtypes exist in HAoSMCs and which subtype of vasopressin receptor is responsible for the effects described above, agarose gel electrophoresis of qPCR products were employed to visualize vasopressin receptor subtype expression. As depicted in Figure 3.12A, V1a and V2 receptor subtypes are both expressed in HAoSMCs. Importantly, V1a receptor is known to activate cellular Ca^{2+} signaling (Jeffries et al., 2010), while V2 receptor mediates antidiuresis (Tanoue et al., 2004). Therefore, additional experiments were conducted to explore whether the V1a receptor participates in the effect of vasopressin on ORAI1 expression. Herein, HAoSMCs were pre-incubated with increasing concentrations (0, 1, 5, 10 nM) of V1aR inhibitor RG7713, followed by treatment with 100 nM vasopressin for 24 h. qPCR results showed that 10 nM RG7713 significantly suppressed vasopressin-induced the transcript levels of *ORAI1* (Figure 3.12B). Based on this result, HAoSMCs were exposed to 100 nM vasopressin for 24 h in the absence and presence of 10 nM RG7713 in the subsequent experiment. qPCR data implied that the suppression of V1a receptor by RG7713 prevented vasopressin-induced upregulation of *ORAI1* transcript levels in HAoSMC cells, whereas RG7713 did not significantly change *ORAI1* transcription in the control-cultured HAoSMCs (Figure 3.12C).

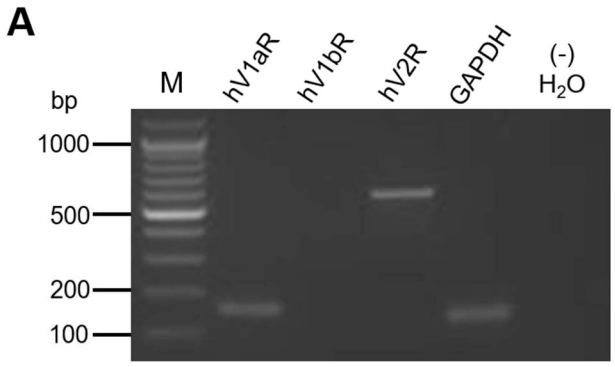

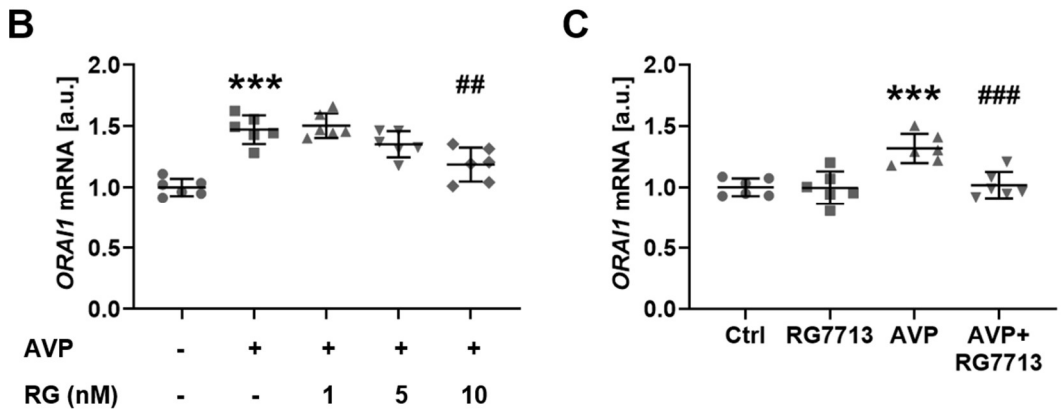

Figure 3.12 Vasopressin receptor transcripts in HAoSMCs.
(A). Representative gel illustrating the mRNA-abundance of vasopressin receptor subtype V1aR, V1bR and V2R in HAoSMCs. GAPDH and ddH_2O acted as positive and negative controls, respectively. **(B).** The mRNA levels of *ORAI1* in HAoSMCs following a 24-h incubation without (Ctrl) and with (AVP) 100 nM vasopressin in the absence or presence of various concentrations (0, 1, 5, 10 nM) of V1aR inhibitor RG7713 (RG). **(C).** The mRNA level of *ORAI1* in HAoSMCs following a 24-h culture without (Ctrl) and with (AVP) 100 nM vasopressin in the absence or presence of 10 nM V1aR inhibitor RG7713. Values are means ± SD. ***($p < 0.001$) indicates statistically significant difference to Ctrl, $^{\#\#}$($p < 0.01$), $^{\#\#\#}$($p < 0.001$) indicates statistically significant difference to vasopressin treatment alone (ANOVA). n=6 for each group. Figures A and C were adapted from *Xuexue Zhu* (Zhu et al., 2021).

3.2 Requirement of Na^+/H^+ exchanger NHE1 and oxidative stress for vasopressin-induced osteogenic signaling and calcification in HAoSMCs

3.2.1 Vasopressin exposure enhanced oxidative stress, calcium deposition and ALP activity in HAoSMCs

It is accepted that oxidative stress is involved in osteoblastic differentiation of VSMCs and calcification (Briet and Burns, 2012). Here, we wanted to test whether ROS were involved in vasopressin-mediated calcification in HAoSMCs. Flow cytometry analysis implied that vasopressin increased ROS accumulation in HAoSMCs (Figure 3.13A-B).

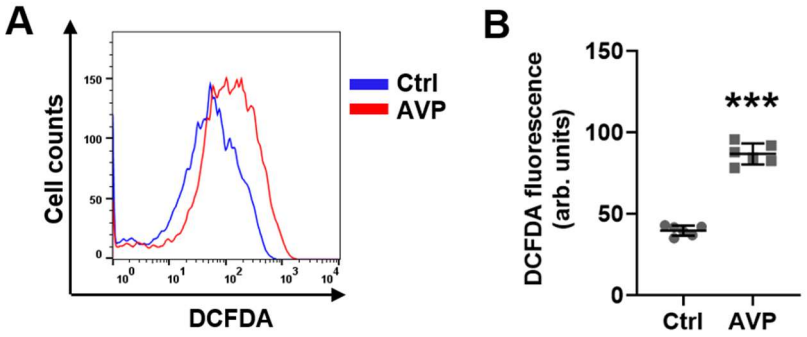

Figure 3.13 Effect of vasopressin on ROS generation in HAoSMCs.
(A). Representative overlay histograms from flow cytometry analysis using 2',7'-dichlorofluorescein diacetate (DCFDA) illustrating ROS generation without (Ctrl) and with (AVP) 100 nM vasopressin stimulation for 24 h. **(B).** Scatter dot plots showing the quantification of ROS production. Values are means ± SD. ***(p < 0.001) indicates statistically significant difference to Ctrl (unpaired t-test). n=6 for each group.

To test whether the ROS scavenger NAC (Xu et al., 2019) influenced the effect of vasopressin on calcium deposit and determine the optimal concentration of NAC in HAoSMCs, increasing concentrations (0, 0.1, 0.2, 0.5, 1 mM) of NAC were pretreated for 30 min, followed by 100 nM vasopressin stimulation for 24 h. Treatment of HAoSMCs with NAC significantly decreased vasopressin-induced *NHE1* transcript level in a concentration-dependent manner, reaching a statistically significant effect at 0.5 mM NAC (Figure 3.14A).

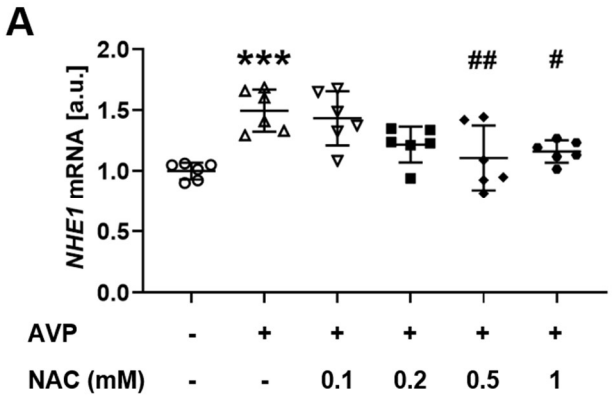

Figure 3.14 Effects of increasing concentrations of the ROS scavenger N-acetyl-L-cysteine on *NHE1* transcription in HAoSMCs.
(A). HAoSMCs were exposed to various concentrations (0, 0.1, 0.2, 0.5, 1 mM) of N-acetyl-L-cysteine (NAC) for 30 min prior to without (Ctrl) and with (AVP) 100 nM vasopressin for 24 h. The mRNA level of *NHE1* in HAoSMCs were assessed using qPCR. Values are means ± SD. ***(p < 0.001) indicates statistically

significant difference to Ctrl, $^{\#}(p < 0.05)$, $^{\#\#}(p < 0.01)$ indicates statistically significant difference to vasopressin treatment alone (ANOVA). *n*=6 for each group.

Based on our findings, HAoSMCs were pre-incubated with 0.5 mM NAC for 30 min before incubation with 100 nM vasopressin in the following experiments. Alizarin red S staining (Figure 3.15A), calcium content (Figure 3.15B) and ALP activity (Figure 3.15C) showed that blockade of ROS with NAC significantly relieved vasopressin-triggered calcium deposition and ALP activity, indicating the important role of oxidative stress in VSMC calcification.

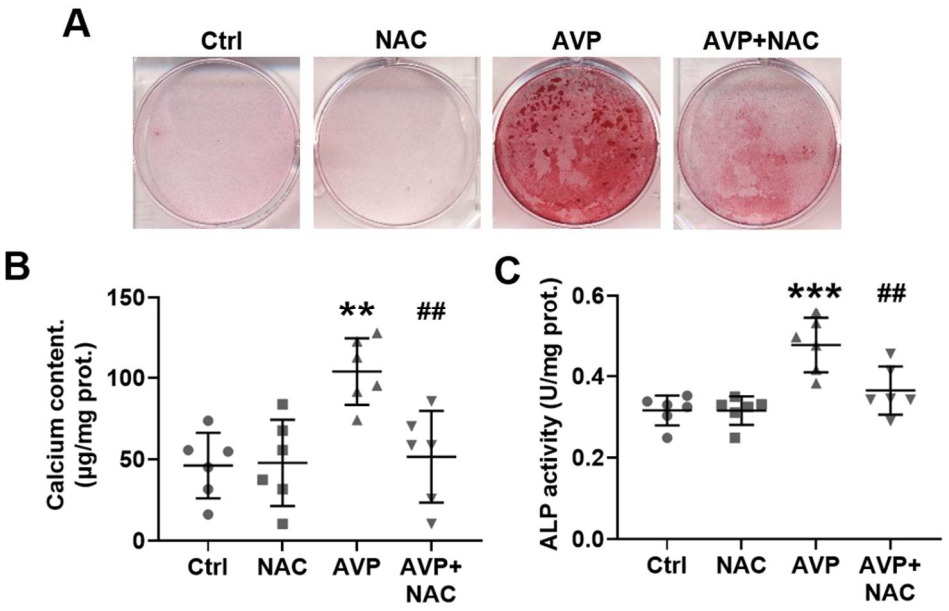

Figure 3.15 Sensitivity of vasopressin-induced calcification of HAoSMCs in response to ROS scavenger N-acetyl-L-cysteine.
(A). HAoSMCs were incubated without (Ctrl) and with (AVP) 100 nM vasopressin and 1 mM $CaCl_2$ in the absence or presence of 0.5 mM ROS scavenger N-acetyl-L-cysteine (NAC) for 14 days. Representative images of alizarin red S staining depicting calcium deposits. **(B).** Scatter dot plots of calcium content in HAoSMCs after stimulation without (Ctrl) and with (AVP) 100 nM vasopressin in the absence or presence of 0.5 mM ROS scavenger N-acetyl-L-cysteine (NAC) for 14 days. **(C).** Scatter dot plots of ALP activity in HAoSMCs after pre-incubating with 0.5 mM ROS scavenger N-acetyl-L-cysteine (NAC) for 30 min before without (Ctrl) and with (AVP) 100 nM vasopressin for 7 days. Values are means ± SD. $^{**}(p < 0.01)$, $^{***}(p < 0.001)$ indicates statistically significant difference to Ctrl (ANOVA), $^{\#\#}(p < 0.01)$ indicates statistically significant difference to vasopressin treatment alone (ANOVA). *n*=6 for each group.

3.2.2 Vasopressin exposure increased NHE1 expression, calcium deposition and ALP activity in HAoSMCs

NHE1 is overexpressed in mineralizing osteoblasts (Liu et al., 2011). NHE1 is almost inactive in normal cells when pH_i is neutral, whereas it is activated as long as the pH_i becomes acidic (Koltai, 2018). The main function of NHE1 is to export intracellular H^+ in exchange for Na^+, resulting in the overload of cytosolic Na^+ (Orlowski and Grinstein, 2004, Reshkin et al., 2013, Ghashghaeinia et al., 2019). Following, the PM ion transporters NCX exchange Ca^{2+} for intracellular Na^+ through its reverse mode by sensing the Na^+ electrochemical gradient (Khananshvili, 2014). We investigated whether NCX assists the NHE1 signaling in participating in vasopressin-induced vascular calcification in HAoSMCs. Our results indicated that mRNA levels of *NCX1* were dramatically upregulated by 100 nM vasopressin, as evidenced by qPCR (Figure 3.16A). In addition, the mRNA level (Figure 3.16B) and protein abundance (Figure 3.16C) of NHE1 demonstrated that exposure of HAoSMCs to 100 nM vasopressin elevated the expression of NHE1.

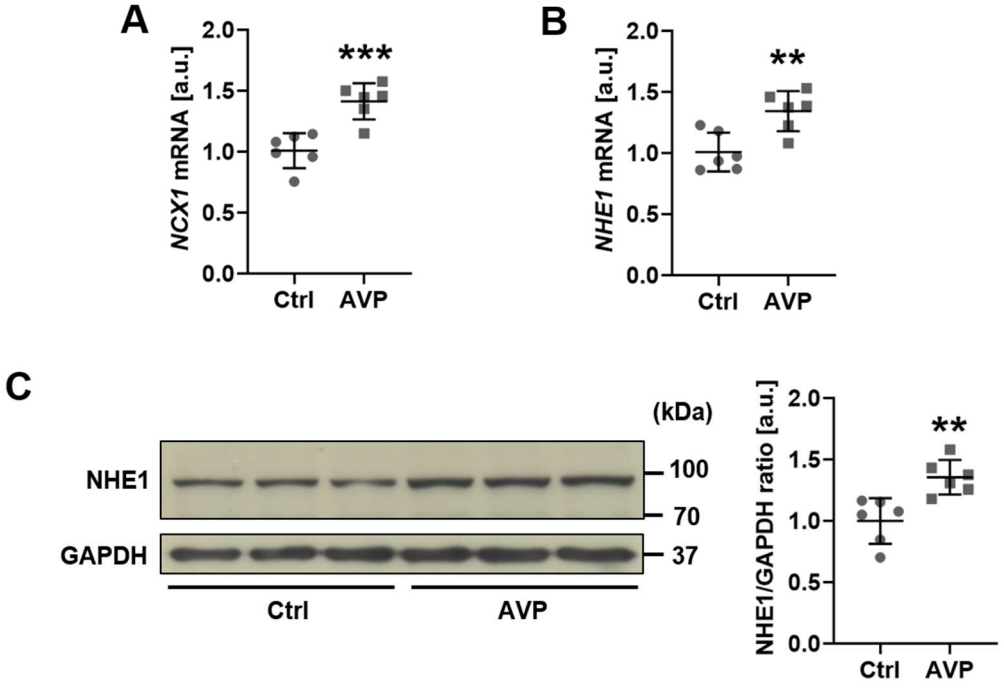

Figure 3.16 Effects of vasopressin on NHE1 expression in HAoSMCs.
(A-B). The mRNA levels of *NCX1* **(A)** and *NHE1* **(B)** were assessed by qPCR in HAoSMCs following a 24-h culture without (Ctrl) and with (AVP) 100 nM vasopressin. **(C).** Original immunoblots and quantitative analysis showing the

protein levels of NHE1 after without (Ctrl) and with (AVP) 100 nM vasopressin treatment for 24 h. Values are means ± SD. **($p < 0.01$), ***($p < 0.001$) indicates statistically significant difference to Ctrl (unpaired *t*-test). *n*=6 for each group.

To explore whether the NHE1 inhibitor cariporide (Chatterjee et al., 2014) affected the effect of vasopressin on calcium deposition and determine the optimal concentration of cariporide, HAoSMCs were incubated with 100 nM vasopressin in the absence and presence of the NHE1 inhibitor cariporide with increasing concentrations (0, 1, 5, 10, 20 µM). We found that incubation with cariporide significantly downregulated vasopressin-induced expressions of osteogenic genes in a concentration-dependent manner. qPCR results showed that cariporide inhibited vasopressin-stimulated upregulation of *CBFA1* (Figure 3.17A) and *SOX9* (Figure 3.17C), to reach statistical significance, 5 µM cariporide was required. Whereas, cariporide effectively prevented vasopressin-induced expressions of *MSX2* (Figure 3.17B) and *ALPL* (Figure 3.17D), an effect reaching statistical significance at 10 µM cariporide. Thus, the optimal effective concentration was observed with 10 µM cariporide.

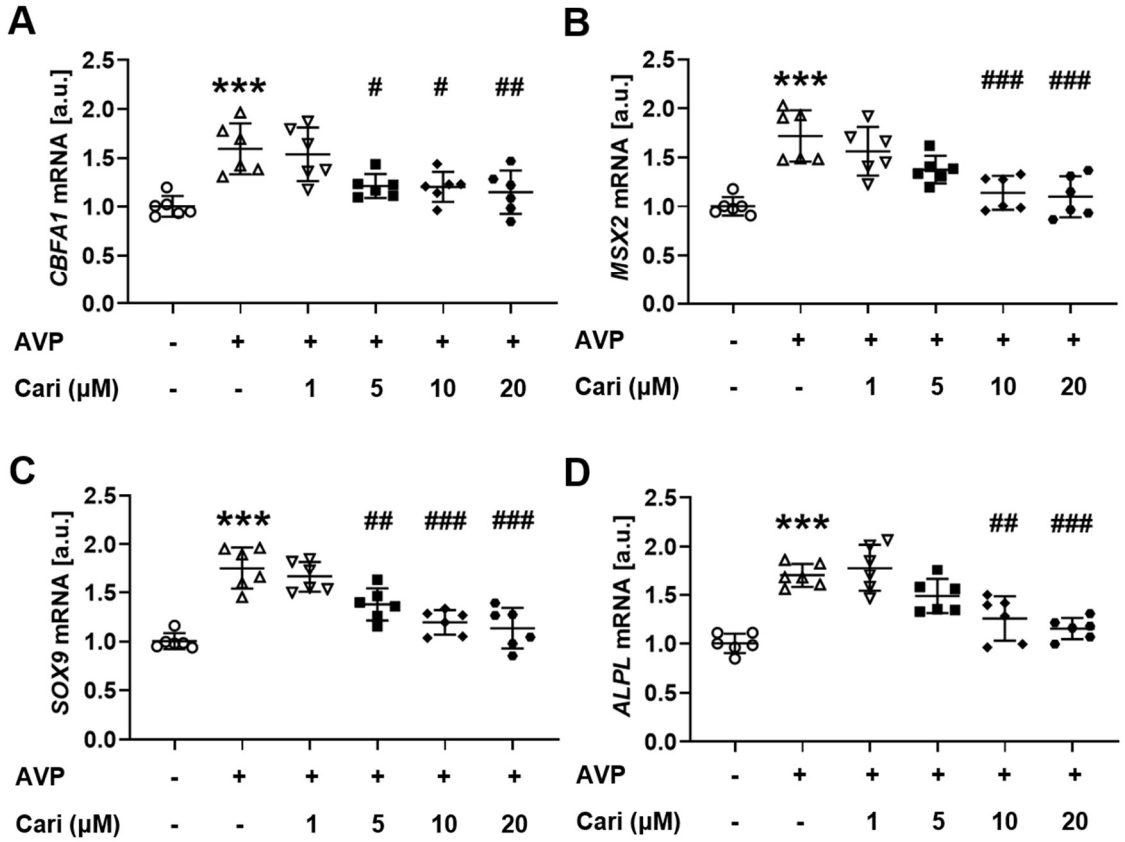

Figure 3.17 Effects of increasing concentrations of the NHE1 inhibitor cariporide on osteogenic genes *CBFA1*, *MSX2*, *SOX9* and *ALPL* transcription in HAoSMCs.
HAoSMCs were exposed to various concentrations (0, 1, 5, 10, 20 μM) of cariporide (Cari) for 30 min before 100 nM vasopressin (AVP) for 24 h. Non-treated cells acted as a negative control (Ctrl). Osteogenic transcription factors *CBFA1* **(A)**, *MSX2* **(B)**, *SOX9* **(C)** and *ALPL* **(D)** transcript levels in HAoSMCs were evaluated by qPCR. Values are means ± SD. ***($p < 0.001$) indicates statistically significant difference to Ctrl, $^{\#}(p < 0.05)$, $^{\#\#}(p < 0.01)$, $^{\#\#\#}(p < 0.001)$ indicates statistically significant difference to vasopressin treatment alone (ANOVA). *n*=6 for each group.

Based on our findings, HAoSMCs were pre-incubated with 10 μM cariporide for 30 min before 100 nM vasopressin exposure in the following experiments. Alizarin red S staining (Figure 3.18A), calcium content (Figure 3.18B) and ALP activity (Figure 3.18C) revealed that cariporide obviously diminished vasopressin-triggered calcium deposition and ALP activity, suggesting a significant role of NHE1 and NCX1 in VSMC calcification. Notably, medium pH (Figure 3.19A) and bicarbonate concentration (Figure 3.19B) were not changed after treating with vasopressin and/or cariporide at different time points.

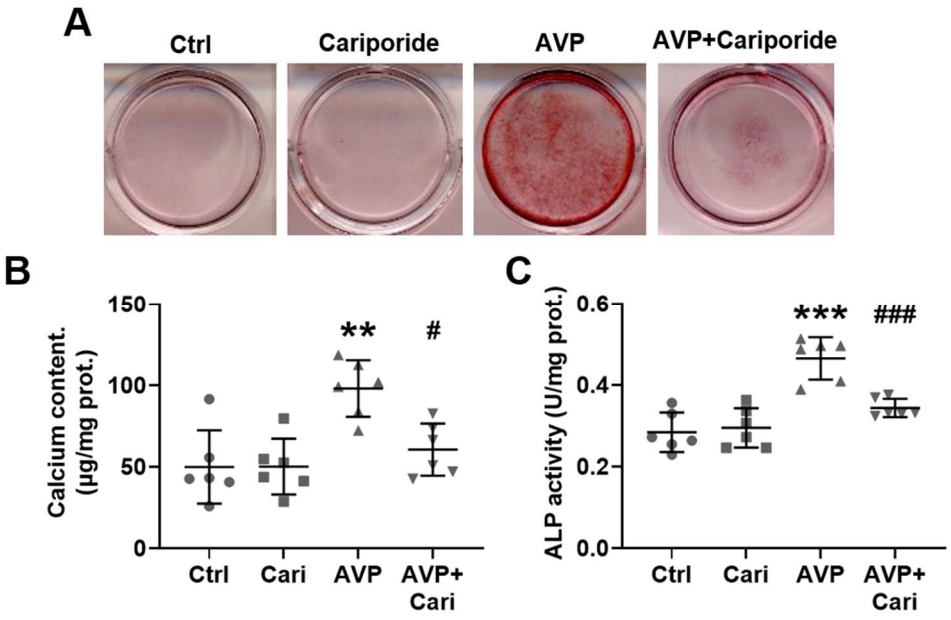

Figure 3.18 Sensitivity of vasopressin-induced calcification in HAoSMCs to NHE1 inhibitor cariporide.
(A). HAoSMCs were stimulated without (Ctrl) and with (AVP) 100 nM vasopressin and 1 mM $CaCl_2$ in the absence or presence of pre-incubation with 10 μM NHE1 inhibitor cariporide (Cari) for 14 days. Representative original images of alizarin

red S staining showing calcium deposits. **(B).** Calcium content of HAoSMCs for 14 days. **(C).** ALP activity of HAoSMCs for 7 days. Values are means ± SD. **($p < 0.01$), ***($p < 0.001$) indicates statistically significant difference to Ctrl (ANOVA), $^{\#}$($p < 0.05$), $^{\#\#\#}$($p < 0.001$) indicates statistically significant difference to vasopressin treatment alone (ANOVA). *n*=6 for each group.

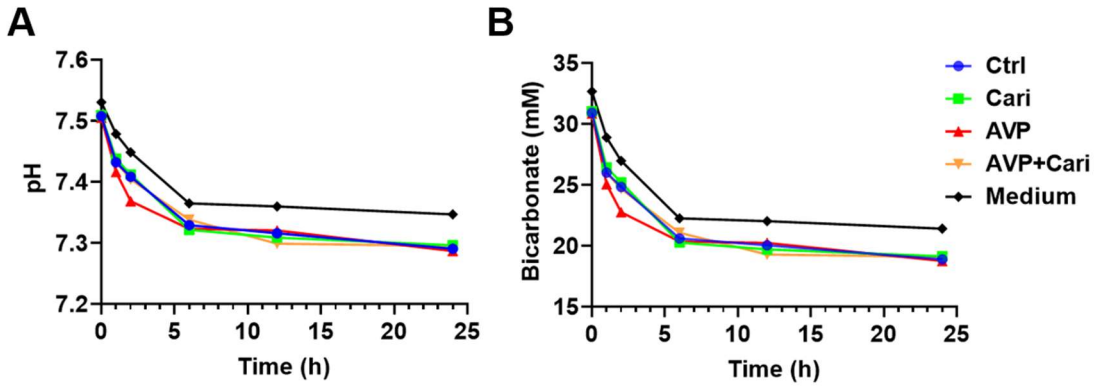

Figure 3.19 Effect of vasopressin on the pH of medium and bicarbonate concentration in response to NHE1 inhibitor cariporide.
(A-B). HAoSMCs were treated without (Ctrl) and with (AVP) 100 nM vasopressin in the absence or presence of 10 μM NHE1 inhibitor cariporide (Cari) for various time points (0, 1, 2, 6, 12, 24 h). The pH of medium **(A)** was measured and the corresponding bicarbonate concentration **(B)** was calculated according to the Henderson-Hasselbalch equation. Medium acted as a cell-free control group. Values are means. *n*=6 for each group.

3.2.3 Interaction of NHE1 with oxidative stress in response to vasopressin stimulation in HAoSMCs

Further, we wanted to examine whether there was a possible interaction between NHE1 and ROS, which may contribute to calcification in vasopressin-treated HAoSMCs. As expected, flow cytometry analysis demonstrated that inhibition of NHE1 by cariporide blocked vasopressin-stimulated ROS accumulation in HAoSMCs (Figure 3.20A-B). In addition, blockade of ROS generation with NAC substantially diminished the mRNA level (Figure 3.20C) and protein level (Figure 3.20D-E) of NHE1 in vasopressin-incubated HAoSMCs. In conclusion, we provided evidence that a positive feedback loop of NHE1 and ROS was formed in vasopressin-stimulated VSMC calcification.

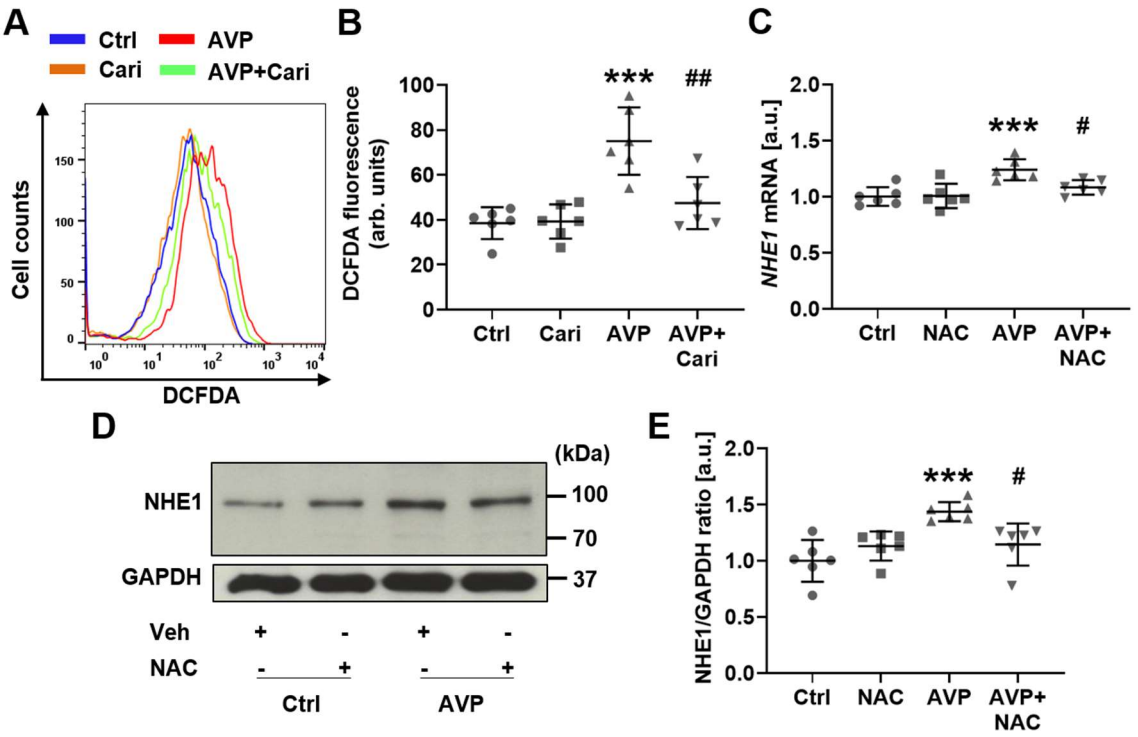

Figure 3.20 Interaction of NHE1 with ROS in HAoSMCs in response to vasopressin.
(A). The HAoSMCs were pre-incubated with 10 μM cariporide (Cari) for 30 min before without (Ctrl) and with (AVP) 100 nM vasopressin for another 24 h. Representative overlay histograms from flow cytometry analysis using 2',7'-dichlorofluorescein diacetate (DCFDA) illustrating ROS generation. **(B).** Scatter dot plots showing the quantification of ROS production. **(C).** The mRNA levels of *NHE1* were measured by qPCR in HAoSMCs following without (Ctrl) and with (AVP) 100 nM vasopressin in the absence or presence of pretreatment with 0.5 mM ROS scavenger N-acetyl-L-cysteine (NAC) for 24 h. **(D).** Representative immunoblots showing the protein abundance of NHE1 in HAoSMCs after without (Ctrl) and with (AVP) 100 nM vasopressin exposure in the absence (Veh) or presence of pretreatment with 0.5 mM ROS scavenger N-acetyl-L-cysteine (NAC) for 24 h. **(E).** Scatter dot plots showing quantitative analysis of NHE1 protein levels. Values are means ± SD. ***($p < 0.001$) indicates statistically significant difference to Ctrl, $^{\#}$($p < 0.05$), $^{\#\#}$($p < 0.01$) indicates statistically significant difference to vasopressin treatment alone (ANOVA). n=6 for each group.

3.2.4 Inhibition of NHE1 and oxidative stress blunted vasopressin-induced osteogenic signaling in HAoSMCs

In order to further determine whether inhibition of NHE1 expression and ROS accumulation affected vasopressin-mediated osteo-/chondrogenic signaling in HAoSMCs, cells were preconditioned with NHE1 inhibitor cariporide or ROS scavenger NAC for 30 min prior to 100 nM vasopressin culture for 24 h. The

mRNA levels of osteogenic genes *CBFA1*, *MSX2*, *SOX9*, and *ALPL* were detected with qPCR in HAoSMCs. We observed that vasopressin exposure upregulated transcript levels of osteogenic genes *CBFA1* (Figure 3.21A), *MSX2* (Figure 3.21B), *SOX9* (Figure 3.21C), and *ALPL* (Figure 3.21D), which were effectively suppressed by NHE1 inhibitor cariporide or ROS scavenger NAC (Figure 3.21A-D).

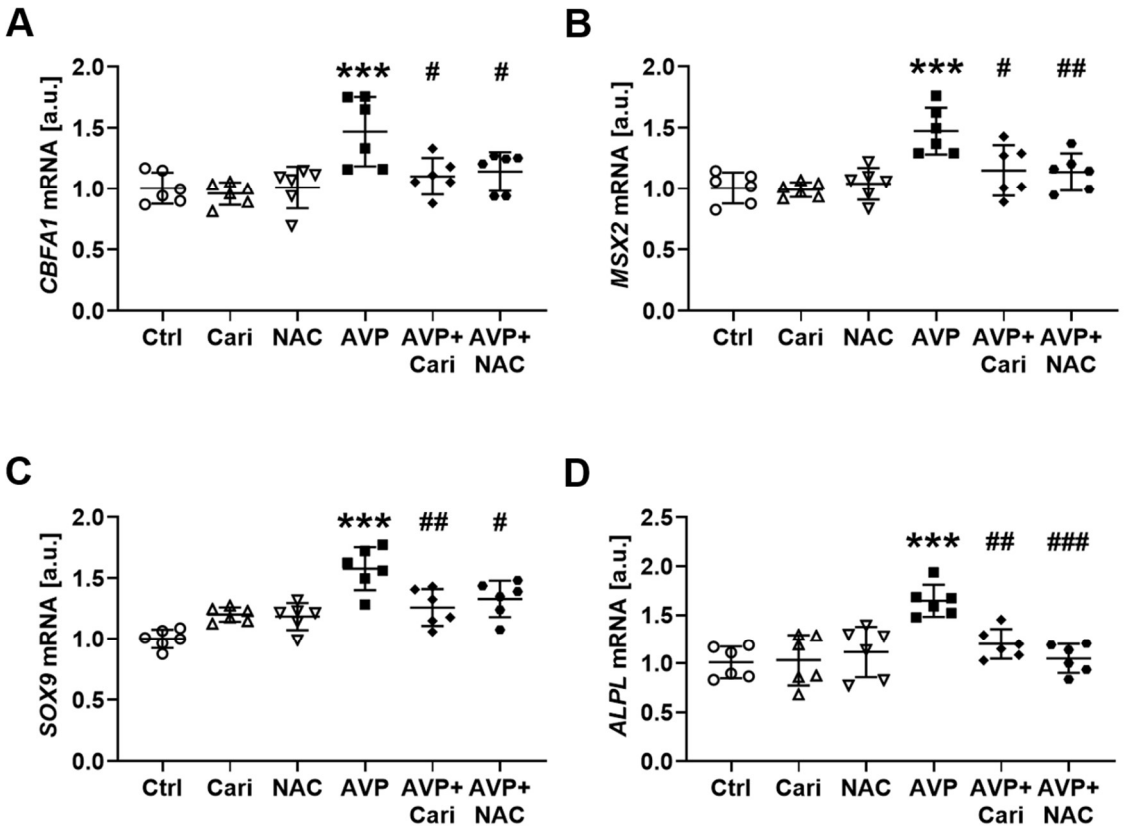

Figure 3.21 Sensitivity of vasopressin-induced osteogenic signaling in HAoSMCs to NHE1 inhibitor cariporide and ROS scavenger N-acetyl-L-cysteine.
HAoSMCs were pretreated in the absence or presence of 10 µM NHE1 inhibitor cariporide (Cari) or 0.5 mM ROS scavenger N-acetyl-L-cysteine (NAC) for 30 min before without (Ctrl) and with (AVP) 100 nM vasopressin treatment for another 24 h. Osteogenic switching markers *CBFA1* **(A)**, *MSX2* **(B)**, *SOX9* **(C)** and *ALPL* **(D)** transcript levels were measured using qPCR. Values are means ± SD. ***($p < 0.001$) indicates statistically significant difference to Ctrl, #($p < 0.05$), ##($p < 0.01$), ###($p < 0.001$) indicates statistically significant difference to vasopressin treatment alone (ANOVA). n=6 for each group.

3.2.5 Inhibition of SGK1 blunted vasopressin-induced NHE1 expression, calcium deposition and ALP activity in HAoSMCs

In order to investigate whether the stimulation of NHE1 expression by vasopressin required SGK1, HAoSMCs were pre-incubated with SGK1 blocker GSK-650394 for 30 min, followed by 100 nM vasopressin treatment for 24 h. Western blotting showed that GSK-650394 pretreatment obviously impeded the increased protein levels of NHE1 triggered by vasopressin (Figure 3.22A-B). Similarly, inhibition of SGK1 by GSK-650394 appreciably blunted the vasopressin-induced upregulation of *NHE1* transcript levels (Figure 3.22C). In addition, alizarin red S staining (Figure 3.22D), calcium content (Figure 3.22E) and ALP activity (Figure 3.22F) showed that repression of SGK1 with GSK-650394 significantly relieved aberrant calcium deposition and ALP activity induced by vasopressin.

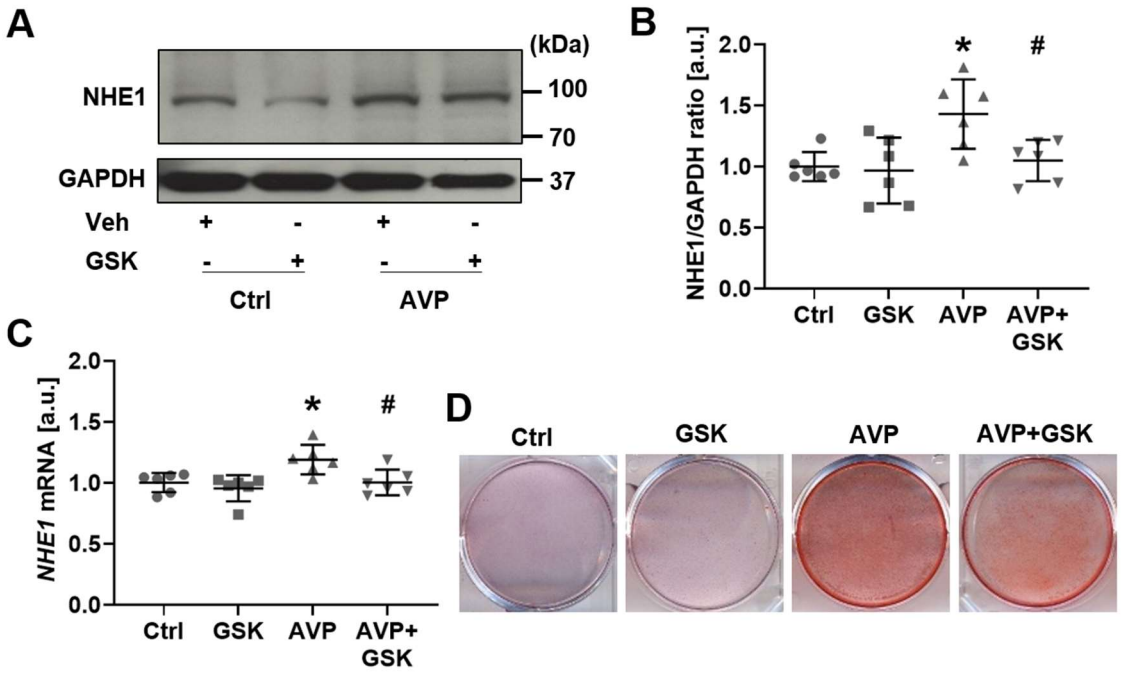

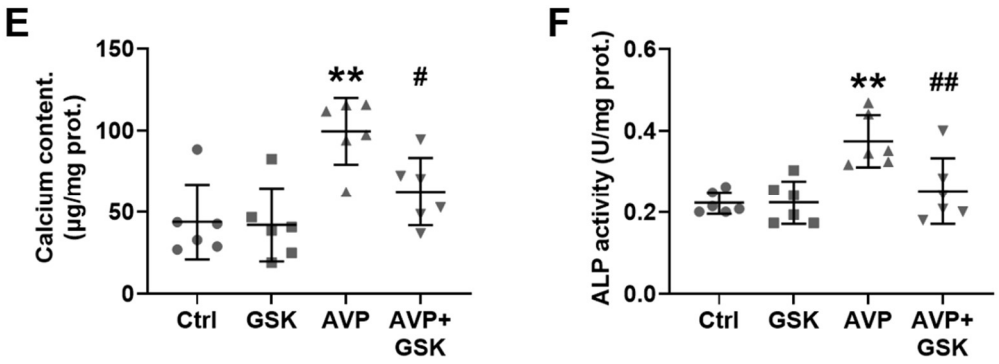

Figure 3.22 Sensitivity of vasopressin-induced NHE1 expression and calcification in response to SGK1 inhibitor GSK-650394 in HAoSMCs.
(A-B). Representative immunoblots **(A)** and quantitative analysis **(B)** showing the protein levels of NHE1 after without (Ctrl) and with (AVP) 100 nM vasopressin treatment for 24 h in the absence or presence of 1 µM SGK1 inhibitor GSK-650394 (GSK). **(C).** The mRNA levels of *NHE1* were detected by qPCR in HAoSMCs following a 24-h culture without (Ctrl) and with (AVP) 100 nM vasopressin in the absence or presence of SGK1 inhibitor GSK-650394 (GSK). **(D).** HAoSMCs were stimulated without (Ctrl) and with (AVP) 100 nM vasopressin and 1 mM $CaCl_2$ in the absence or presence of 1 µM SGK1 inhibitor GSK-650394 (GSK) for 14 days. Representative images of alizarin red S staining showing calcium deposits. **(E-F).** Calcium content **(E)** and ALP activity **(F)** of HAoSMCs for 14 days **(E)** or 7 days **(F)**. Values are means ± SD. *($p < 0.05$), **($p < 0.01$) indicates statistically significant difference to absence of vasopressin, $^{\#}$($p < 0.05$), $^{\#\#}$($p < 0.01$) indicates statistically significant difference to vasopressin treatment alone (ANOVA). *n*=6 for each group.

3.2.6 Inhibition of SGK1 and NHE1 blunted vasopressin-induced osteogenic signaling in HAoSMCs

In order to confirm whether the SGK1-sensitive NHE1 regulation by vasopressin is relevant for the effects of vasopressin on osteogenic signaling, HAoSMCs were pre-incubated with SGK1 inhibitor GSK-650394 or NHE1 blocker cariporide for 30 min, followed by 100 nM vasopressin treatment for 24 h. We found that vasopressin exposure increased transcript levels of osteogenic genes *CBFA1* (Figure 3.23A), *MSX2* (Figure 3.23B), *SOX9* (Figure 3.23C), and *ALPL* (Figure 3.23D), which were apparently prevented by GSK-650394 or cariporide (Figure 3.23A-D), as evidenced using qPCR.

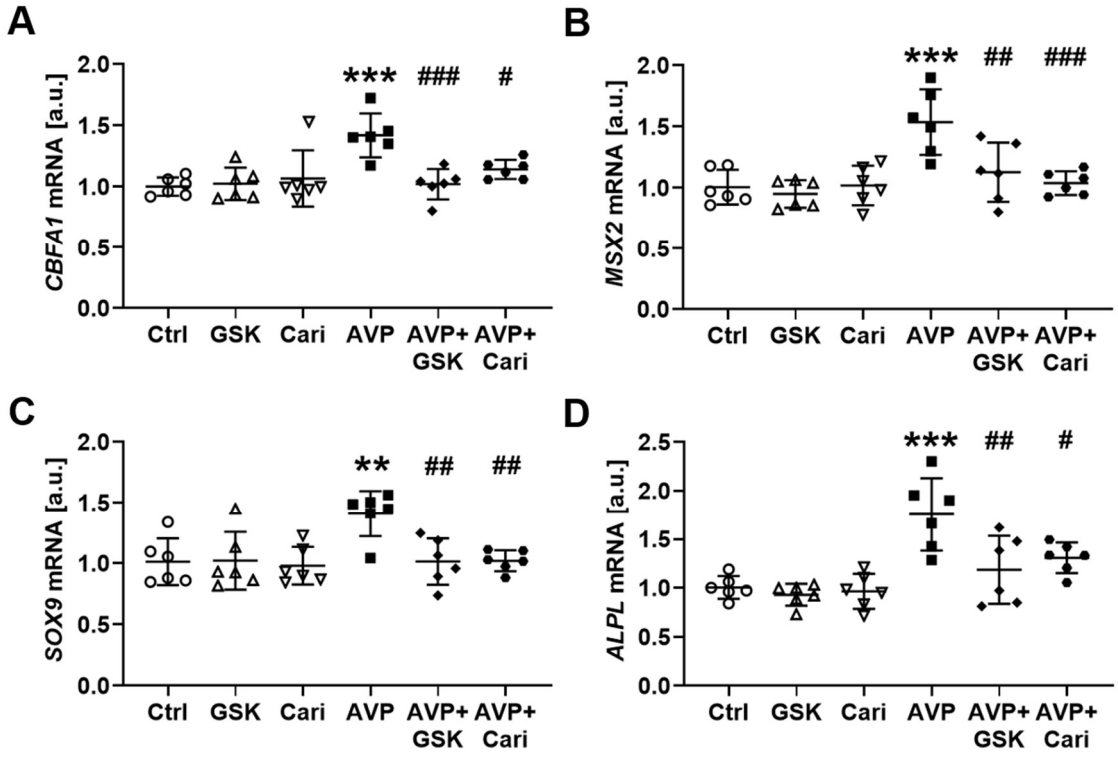

Figure 3.23 Sensitivity of vasopressin-induced osteogenic signaling in HAoSMCs to SGK1 inhibitor GSK-650394 and NHE1 inhibitor cariporide. HAoSMCs were pretreated in the absence or presence of 1 µM SGK1 inhibitor GSK-650394 (GSK) or 10 µM NHE1 inhibitor cariporide (Cari) for 30 min before without (Ctrl) and with (AVP) 100 nM vasopressin treatment for another 24 h. Osteogenic switching markers *CBFA1* **(A)**, *MSX2* **(B)**, *SOX9* **(C)** and *ALPL* **(D)** transcript levels were determined with qPCR. Values are means ± SD. **($p < 0.01$), ***($p < 0.001$) indicates statistically significant difference to Ctrl, $^{\#}$($p < 0.05$), $^{\#\#}$($p < 0.01$), $^{\#\#\#}$($p < 0.001$) indicates statistically significant difference to vasopressin treatment alone (ANOVA). n=6 for each group.

4 Discussion

Vascular calcification is an active biomineralization process, rather than a passive event (Lang et al., 2018a). A host of factors, such as increased calcium and/or phosphate levels, oxidative stress, bone morphogenetic proteins, inflammation and apoptosis, promote the phenotypic transition of VSMCs into osteoblast-like cells and vascular calcification (Huang et al., 2020, Sun et al., 2019, Li et al., 2019). As described before (Sun et al., 2019), the degree of vascular calcification can be evaluated by analysis of osteogenic transdifferentiation, enhanced calcium deposition and increased ALP activity. In the present series, osteogenic signaling and vascular calcification of VSMCs were induced by the combination of vasopressin with Ca^{2+}, as expected from previous work (Nishiwaki-Yasuda et al., 2007). Nonetheless, the cellular and molecular mechanisms of vascular calcification, which are caused by vasopressin, are still elusive. Our observations suggest that vasopressin may induce phenotypic transition of VSMCs and vascular calcification through regulating CRAC channel SOCE and activating a positive regulatory loop of NHE1 and oxidative stress. A summary of this project is depicted in Figure 4.1.

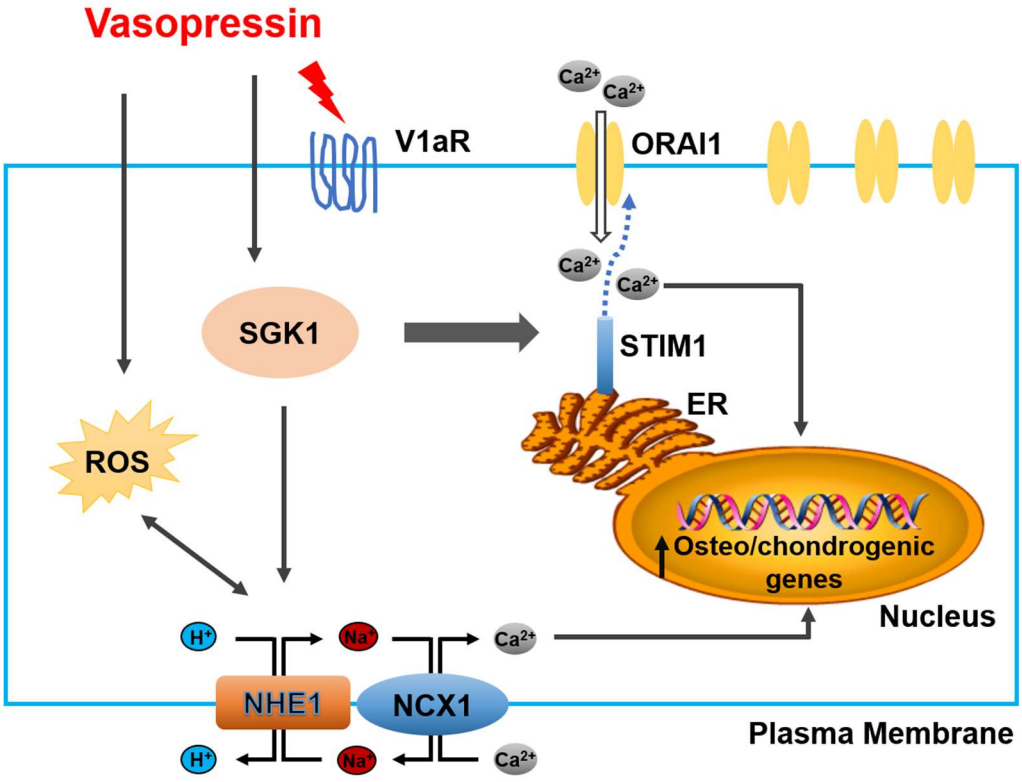

Figure 4.1 A summary schematic model delineating the role of vasopressin on osteogenic signaling and vascular calcification in HAoSMCs.
Vasopressin enhances ORAI1-dependent store-operated Ca^{2+} entry, NHE1 expression and ROS generation via an SGK1-mediated mechanism. In HAoSMCs, exposure to elevated vasopressin enhances SGK1 expression, which is implicated in the orchestration of osteo-/chondrogenic transdifferentiation of VSMCs and vascular calcification. The increased SGK1 expression induces the upregulation of Ca^{2+} channel ORAI1 and its sensor STIM1. V1aR participates in the effect of vasopressin on Ca^{2+} signaling. Vasopressin also increases NHE1 expression and ROS generation, and thus triggers osteogenic signaling and calcification, an effect requiring SGK1. V1aR, vasopressin 1a receptor; SGK1, serum & glucocorticoid inducible kinase 1; STIM1, stromal interaction molecule1; ROS, reactive oxygen species; ER, endoplasmic reticulum; NHE1, Na^+/H^+ exchanger1; NCX1, Na^+/Ca^{2+} exchanger1.

There are three vasopressin receptor subtypes, including V1a, V1b and V2 receptor, distributed in specific tissues (Zhang et al., 2016). The V1a receptor has been identified in VSMCs (Figure 3.12A). The receptor subtype involved here is presumably the V1a receptor, which can be found in HAoSMCs (Figure 3.12A and (Aoyagi et al., 2009)) and is known to activate intracellular Ca^{2+} signaling (Jeffries et al., 2010, Byron, 1996). In this study, V1a receptor has been found to participate in the effect of vasopressin on osteogenic signaling and vascular calcification (Figure 4.1). Normally, the concentration of vasopressin in human plasma ranged from 0.7 - 5.8 pg/mL (0.65 pM - 5.25 pM) (Hummerich et al., 1983). Previous studies have shown that half-maximal activation of V1a receptors is 0.13 ± 0.02 nM (Di Giglio et al., 2017) or of $[Ca^{2+}]_i$ increase is 23 ± 9 nM (Serradeil-Le Gal et al., 1995). The concentration (100 nM) of vasopressin we used to reach significant stimulation is similar to that concentrations previously found to evoke calcification in rat aortic smooth muscle cells (Nishiwaki-Yasuda et al., 2007), but orders of magnitude higher than those observed in human plasma (Hummerich et al., 1983) and those required for half-maximal activation of V1a receptors (Di Giglio et al., 2017) and of $[Ca^{2+}]_i$ increase (Serradeil-Le Gal et al., 1995). Higher concentration (1 μM) of vasopressin appreciably increases intracellular Ca^{2+} concentration (Tran et al., 2015). The potential reasons for higher concentrations required *in vitro* may be due to the long incubation to stimulate osteoblastic phenotype and calcification, moreover, internalization and subsequent

vasopressin degradation may reduce the effective extracellular concentration during culture.

4.1 The effect of vasopressin on ORAI1 expression and SOCE in HAoSMCs

Ca^{2+} signaling is vital for a plethora of cellular functions and is involved in the regulation of osteoblastic transition (Zhang et al., 2020). Activation of SOCE may be responsible for maintaining intracellular Ca^{2+} oscillations, in which Orai and STIM proteins are involved (Dupont and Combettes, 2016). Orai proteins function as the pore-forming subunits of SOCE expressed in the PM, which regulates influx of extracellular Ca^{2+} (Gudlur and Hogan, 2017, Derler et al., 2016), while STIM proteins act as Orai-regulating Ca^{2+} sensors expressed in the ER (Grabmayr et al., 2020). A previous study in hepatocytes has demonstrated that vasopressin treatment stimulates the maintenance of oscillations of cytosolic Ca^{2+} activity (Jones et al., 2008). Our results revealed that the mRNA levels of *ORAI1* and *ORAI2*, as well as of *STIM1* and *STIM2* were markedly elevated upon sustained vasopressin stimulation, but the transcript level of *ORAI3* did not significantly change after exposure to vasopressin. Accumulating evidence has verified that Orai1 and STIM1 are normally essential and sufficient for SOCE activity. However, Orai2 and/or Orai3 are responsible for replacement of Orai1 in Orai1 deficiency (Dupont and Combettes, 2016). STIM2 is used to sustain the Ca^{2+} level due to its lower affinity for ER Ca^{2+} (Pani et al., 2012, Gruszczynska-Biegala et al., 2011). We have shown that the protein levels of ORAI1 and STIM1 were obviously increased after incubating with vasopressin. In addition, vasopressin significantly enhanced SOCE that is mainly mediated by ORAI1 and STIM1.

SGK1 expression is reported to be highly dynamic, and in the cardiovascular system, SGK1 expression is strongly elevated in the regulation of diverse pathophysiological functions (Lang et al., 2006). SGK1 is stimulated by dehydration and it has been shown that the increased SGK1 expression and activity contribute to or even explain a myriad of pathophysiological consequences of suboptimal water intake (Lang et al., 2017). SGK1, on the other hand, is a powerful stimulator of CRAC channel Orai1 activity and expression (Lang et al., 2012, Schmidt et al., 2014). Although SGK1 affects Orai1-mediated

SOCE in phosphate-induced vascular calcification, whether SGK1-dependent stimulation of Orai1 expression is involved in vasopressin-triggered osteogenic phenotypic and vascular calcification remains obscure. For this, HAoSMCs were treated with an effective ORAI1 blocker MRS1845 and SGK1 inhibitor GSK-650394. The concentration of MRS1845 (10 μM) and GSK-650394 (1 μM) in this study was based on previous studies (Borst et al., 2012, Korchak et al., 2007, Zhu et al., 2021) and our results (Figure 3.5 and Figure 3.8). Herein, we observed that *SGK1* transcription and the protein level of phospho-SGK1 (S422) were increased after exposure to vasopressin. The upregulated ORAI1 and STIM1 expression induced by vasopressin were blunted by SGK1 inhibitor GSK-650394. Moreover, GSK-650394 counteracted the vasopressin-induced upregulation of SOCE. Similar results implied that ORAI1 blocker MRS1845 reversed the vasopressin-stimulated upregulation of SOCE. Nevertheless, vasopressin dramatically enhanced SOCE even in the presence of MRS1845 or GSK-650394. These observations may indicate that vasopressin-induced SOCE is either incompletely inhibited by ORAI1 blocker MRS1845 or SGK1 inhibitor GSK-650394, respectively, or is in part influenced by ORAI1 and/or SGK1-insensitive mechanisms.

Unlike most mature cell types, VSMCs have no terminal differentiation characteristics, thereby they can transform their phenotype in response to injuries (Iyemere et al., 2006). The VSMCs transdifferentiation is reflected by osteo-/chondrogenic transcription factors, such as CBFA1, MSX2, SOX9 as well as tissue-nonspecific ALPL, which is used to cleave the calcification inhibitor PPi (Voelkl et al., 2018b). A variety of studies provide evidence that SGK1 is implicated in the orchestration of osteo-/chondrogenic transdifferentiation of VSMCs and vascular calcification (Lang et al., 2018b, Ma et al., 2019, Voelkl et al., 2018a). SGK1 stimulates osteogenic signaling with the upregulation of the osteogenic transcription factors *CBFA1*, *MSX2*, *SOX9*, as well as *ALPL* (Zhu et al., 2021). Importantly, intracellular Ca^{2+} signaling modulated by Orai1 also contributes to specific gene expressions in osteoblasts (Hwang et al., 2012). Here, we found that high vasopressin levels increased the gene expressions related to the osteogenic transformation *CBFA1*, *MSX2*, *SOX9*, and *ALPL*, ALP activity as

well as calcium deposition in HAoSMCs. In addition, we investigated the effect of SGK1 and ORAI1 on phenotypic modulation and mineralization in HAoSMCs. Our data demonstrate that vasopressin-mediated upregulation of osteogenic differentiation markers *CBFA1*, *MSX2*, *SOX9*, and *ALPL*, ALP activity as well as calcium deposition was abolished by SGK1 inhibitor GSK-650394 or ORAI1 blocker MRS1845.

Collectively, vasopressin increases the transcript levels of *ORAI1*, *ORAI2*, *STIM1* and *STIM2*, and thus upregulates SOCE in HAoSMCs. The effect of vasopressin on SOCE contributes to the stimulation of osteogenic signaling and to mineralization, an effect requiring SGK1.

4.2 The effect of vasopressin on NHE1 expression and oxidative stress in HAoSMCs

The activity of NHEs is critical for pH_i homeostasis in various cells, especially under acidic circumstances (Orlowski and Grinstein, 2004). Normally, the NHEs control the electroneutral exchange of intracellular H^+ for extracellular Na^+, therefore protecting cells against the damaging effects of intracellular acidification and maintaining pH_i (Orlowski and Grinstein, 2004). In mineralizing osteoblasts, the expression of NHE1 is enhanced (Liu et al., 2011). Mechanisms linking NHE1 activity to osteogenic signaling may include luminal pH in intracellular vesicles. NHE1 is inserted into phagosomal membranes and may contribute to luminal acidification of intracellular vesicles (Hackam et al., 1997). Luminal acidification has, on the other hand, been shown to be decisive for phosphate-induced vascular smooth muscle cell calcification (Alesutan et al., 2015). The existing evidence drove us to investigate whether NHE1 participates in vasopressin-evoked osteoblastic phenotype and VSMC calcification. To address the role of NHE1 in vasopressin-induced calcification, HAoSMCs were treated with a selective NHE1 inhibitor cariporide. According to our findings (Figure 3.17) and previous work (Chatterjee et al., 2014), the concentration of cariporide we used was 10 μM. In this study, our findings showed that the expression of NHE1 was significantly elevated after exposure of HAoSMCs to vasopressin. Furthermore, dysregulated osteogenic signaling, calcium deposition and ALP activity in

HAoSMCs were blunted by NHE1 inhibitor cariporide. Notably, vasopressin and/or cariporide did not change medium pH and bicarbonate concentration. The abnormally high expression of NHE1 results in intracellular Na^+ overload. Afterwards, NCX1 could transport Ca^{2+} into the cells due to decreased electrochemical gradient of Na^+ (Chou et al., 2015). According to our observations, the transcript level of *NCX1* was increased after vasopressin incubation in HAoSMCs. These data demonstrate that vasopressin treatment stimulates the development of VSMC calcification through upregulating both NHE1 expression and *NCX1* transcript level, and thus excessing Na^+ could be exported in exchange for extracellular Ca^{2+}, subsequently contributing to a rise in intracellular Ca^{2+} concentration.

ROS is known to be a major activator of vascular calcification in CKD (Liakopoulos et al., 2017, Agharazii et al., 2015). Clinical trials have suggested that intervention of oxidative stress may become a target of treatment of calcification, considering the risk of oxidative stress in calcification and cardiovascular diseases (Briet and Burns, 2012). However, the involvement of oxidative stress in vasopressin-associated VSMC calcification has not been defined. For this, 0.5 mM NAC, a well-known ROS scavenger, was used according to our results (Figure 3.14) and previous studies (Xu et al., 2019). In this study, our results showed that ROS generation was markedly increased by vasopressin in HAoSMCs. We also found that treatment of HAoSMCs with ROS scavengers NAC significantly attenuated the vasopressin-triggered osteogenic signaling, calcium deposit and ALP activity. Thus, it is speculated that oxidative stress at least partly mediates VSMC calcification. Our additional results showed that ROS accumulation was elevated by vasopressin in HAoSMCs, which was prevented by NHE1 inhibitor cariporide. ROS scavenger NAC, in turn, blunted vasopressin-stimulated NHE1 expression in HAoSMCs. Thus, NHE1 and ROS may form a positive feedback loop, which is responsible for vasopressin-induced VSMC calcification.

On the basis of earlier studies, SGK1 plays a decisive role in phosphate-stimulated osteogenic signaling and VSMC calcification (Voelkl et al., 2018b, Voelkl et al., 2019). Accordingly, $sgk1^{-/-}$ knockout mice are protected against

vascular calcification (Voelkl et al., 2018b). Moreover, SGK1 has been shown to be involved in upregulation of NHE1 expression and activity (Klug et al., 2021, Voelkl et al., 2012, Lang et al., 2014b). However, it is unclear whether SGK1 participates in vasopressin-evoked increase of NHE1 expression. In the present series, our findings verified that pharmacological inhibition of SGK1 suppressed vasopressin-induced NHE1 expression, osteogenic signaling and calcium deposition.

Taken together, vasopressin incubation stimulates NHE1 expression, *NCX1* transcript level and ROS production, and thus triggers osteogenic signaling and calcification, effects requiring SGK1.

4.3 Limitations and outlook

These interpretations are however limited, as the findings are only observed in calcified cells, which may not fully reflect vascular calcification. The mechanisms of vasopressin on vascular calcification *in vivo* have not been verified. Also, NHE1 is vital for pHi homeostasis (Akram et al., 2006), nevertheless, we did not determine the pHi and NHE1 activity after exposure HAoSMCs to vasopressin in response to an ammonium pulse due to limited experimental conditions. Despite these limitations, our observations suggest an important role of sustained vasopressin stimulation in osteo-/chondrogenic transdifferentiation of VSMCs and vascular calcification *in vitro*.

Therefore, further studies are needed to elucidate the role of NHE1 induced by vasopressin on vascular calcification, including the pHi and NHE1 activity. Moreover, further work including animal experiments and clinical studies is needed to confirm the association of vasopressin and vascular calcification.

5 Summary

Vascular calcification is one of the main risk factors of cardiovascular morbidity and mortality in patients with chronic kidney disease (CKD). Vascular calcification is an active process involving the upregulation of osteogenic transcription factors, including core-binding factor α-1 (CBFA1), msh homeobox 2 (MSX2), SRY-Box 9 (SOX9) and alkaline phosphatase (ALPL). Although vasopressin was originally believed to help prevent water loss, it could be a risk factor in several kidney diseases, including CKD. The present study was designed to explore the effect of vasopressin on osteogenic signaling and calcification, as well as its downstream mechanisms.

In this study, human aortic smooth muscle cells (HAoSMCs) were cultured and used in all experiments from passages 4 to 10. Transcript levels were measured using qRT-PCR, protein abundance utilizing western blotting, reactive oxygen species (ROS) generation with 2',7'-dichlorofluorescein diacetate (DCFDA) fluorescence. Cytosolic Ca^{2+} concentration ($[Ca^{2+}]_i$) was determined by Fura-2/AM fluorescence, SOCE from increase of $[Ca^{2+}]_i$ following re-addition of extracellular Ca^{2+} after store depletion with thapsigargin. Alizarin red S staining and calcium content assay were used to detect calcium deposition. ALP assay kit was used for the measurement of ALP activity.

Vasopressin (100 nM) obviously enhanced the expressions of ORAI1 and STIM1, as well as SOCE, which were dramatically attenuated by SGK1 inhibitor GSK-650394 (1 μM). ORAI1 blocker MRS1845 (10 μM) counteracted vasopressin-induced upregulation of SOCE. Vasopressin also significantly enhanced the transcript levels of *NHE1* and protein abundance of NHE1, an effect appreciably abolished by SGK1 inhibitor GSK-650394. Additional findings showed that vasopressin elevated ROS production in HAoSMCs, which was prevented by NHE1 inhibitor cariporide (10 μM). In turn, ROS scavenger N-acetyl-L-cysteine (NAC, 0.5 mM) downregulated vasopressin-stimulated NHE1 expressions in HAoSMCs. Vasopressin stimulated the upregulation of osteogenic transcription factors *CBFA1*, *MSX2*, *SOX9* and *ALPL*, as well as ALP activity and Ca^{2+} content, which were significantly blunted by SGK1 inhibitor GSK-650394, ORAI1 blocker MRS1845, NHE1 inhibitor cariporide or ROS scavenger NAC.

In summary, vasopressin stimulates at least partially via SGK1- SOCE and NHE1/ROS signaling, eventually leading to osteogenic signaling and vascular calcification.

6 Zusammenfassung

Gefäßverkalkung ist einer der Hauptrisikofaktoren für kardiovaskuläre Morbidität und Mortalität bei Patienten mit chronischer Nierenerkrankung (CKD). Gefäßverkalkung ist ein aktiver Prozess, der die Hochregulation osteogener Transkriptionsfaktoren wie des Core-binding factor α-1 (CBFA1), der msh-Homeobox 2 (MSX2), der SRY-Box 9 (SOX9) sowie der alkalischen Phosphatase (ALPL) umfasst. Obwohl ursprünglich angenommen wurde, dass Vasopressin dazu beiträgt, Wasserverluste zu verhindern, könnte es ein Risikofaktor für verschiedene Nierenerkrankungen sein, inklusive CKD. Die vorliegende Arbeit sollte die Wirkung von Vasopressin auf die osteogene Signalübertragung und Verkalkung, sowie die nachgeschalteten Mechanismen untersuchen.

In dieser Studie wurden glatte Muskelzellen der menschlichen Aorta (HAoSMCs) gewonnen kultiviert und in allen Experimenten in den Passagen 4 bis 10 verwendet. Die Transkriptniveaus wurden mittels qRT-PCR gemessen, Proteinmengen unter Verwendung von Immunoblotverfahren bestimmt, sowie die Entstehung reaktiver Sauerstoffspezies (ROS) mit 2', 7'-Dichlorfluorescindiacetat (DCFDA) -Fluoreszenz gemessen. Die zytosolische Ca^{2+}-Konzentration ($[Ca^{2+}]_i$) wurde durch Fura-2/AM-Fluoreszenz bestimmt und der speichergesteuerte Ca^{2+}-Eintritt wurde aus dem Anstieg von $[Ca^{2+}]_i$ nach erneuter Zugabe von extrazellulärem Ca^{2+} nach Speicherentleerung mit Thapsigargin ermittelt. Alizarinrot S-Färbung und Calciumgehaltstest wurden verwendet, um eine Calciumablagerung nachzuweisen. Ein ALP-Assay-Kit wurde zur Messung der ALP-Aktivität verwendet.

Vasopressin (100 nM) verstärkte die Expression von ORAI1 und STIM1 sowie den speichergesteuerten Ca^{2+}-Eintritt, der durch den SGK1-Inhibitor GSK-650394 (1 µM) dramatisch abgeschwächt wurde. Der ORAI1-Blocker MRS1845 (10 µM) wirkte der Vasopressin-induzierten Hochregulation des speichergesteuerten Ca^{2+}-Eintritts entgegen. Vasopressin erhöhte auch signifikant die Transkriptionsspiegel von *NHE1* und die Proteinmenge von NHE1, ein Effekt, der durch den SGK1-Inhibitor GSK-650394 nahezu aufgehoben wurde. Zusätzliche Befunde zeigten, dass Vasopressin die ROS-Produktion in HAoSMCs erhöhte, was durch den NHE1-Inhibitor Cariporid (10 µM) verhindert

wurde. Der ROS-Scavenger N-Acetyl-L-Cystein (NAC, 0.5 mM) verminderte wiederum die Vasopressin-stimulierte NHE1-Expression in HAoSMCs. Vasopressin stimulierte die Expression der osteogenen Transkriptionsfaktoren *CBFA1*, *MSX2*, *SOX9* und *ALPL* sowie die ALP-Aktivität und den Ca^{2+}-Gehalt, die durch den SGK1-Inhibitor GSK-650394, den ORAI1-Blocker MRS1845, den NHE1-Inhibitor Cariporid oder den ROS-Scavenger NAC signifikant abgeschwächt wurden.

Zusammenfassend lässt sich sagen, dass Vasopressin zumindest teilweise über SGK1 speichergesteuerten Ca^{2+}-Eintritt und den NHE1/ROS-Signalweg stimuliert, was schließlich zu osteogenen Signalen und Gefäßverkalkungen führt.

7 Bibliography

AGHARAZII, M., ST-LOUIS, R., GAUTIER-BASTIEN, A., UNG, R. V., MOKAS, S., LARIVIèRE, R. & RICHARD, D. E. 2015. Inflammatory cytokines and reactive oxygen species as mediators of chronic kidney disease-related vascular calcification. *Am J Hypertens,* 28**,** 746-55.

AKRAM, S., TEONG, H. F., FLIEGEL, L., PERVAIZ, S. & CLéMENT, M. V. 2006. Reactive oxygen species-mediated regulation of the Na+-H+ exchanger 1 gene expression connects intracellular redox status with cells' sensitivity to death triggers. *Cell Death Differ,* 13**,** 628-41.

ALBERS, H. E. 2015. Species, sex and individual differences in the vasotocin/vasopressin system: relationship to neurochemical signaling in the social behavior neural network. *Front Neuroendocrinol,* 36**,** 49-71.

ALESUTAN, I., MUSCULUS, K., CASTOR, T., ALZOUBI, K., VOELKL, J. & LANG, F. 2015. Inhibition of Phosphate-Induced Vascular Smooth Muscle Cell Osteo-/Chondrogenic Signaling and Calcification by Bafilomycin A1 and Methylamine. *Kidney Blood Press Res,* 40**,** 490-9.

AMBUDKAR, I. S., DE SOUZA, L. B. & ONG, H. L. 2017. TRPC1, Orai1, and STIM1 in SOCE: Friends in tight spaces. *Cell Calcium,* 63**,** 33-39.

ANTONI, F. A. 2017. Chapter 9 - Vasopressin as a Stress Hormone. *In:* FINK, G. (ed.) *Stress: Neuroendocrinology and Neurobiology.* San Diego: Academic Press.

AOYAGI, T., KOSHIMIZU, T. A. & TANOUE, A. 2009. Vasopressin regulation of blood pressure and volume: findings from V1a receptor-deficient mice. *Kidney Int,* 76**,** 1035-9.

ATTAPHITAYA, S., PARK, K. & MELVIN, J. E. 1999. Molecular cloning and functional expression of a rat Na+/H+ exchanger (NHE5) highly expressed in brain. *J Biol Chem,* 274**,** 4383-8.

BAARTSCHEER, A. 2006. Chronic inhibition of na(+)/h(+)-exchanger in the heart. *Curr Vasc Pharmacol,* 4**,** 23-9.

BERNA-ERRO, A., WOODARD, G. E. & ROSADO, J. A. 2012. Orais and STIMs: physiological mechanisms and disease. *J Cell Mol Med,* 16**,** 407-24.

BERRIDGE, M. J. & IRVINE, R. F. 1989. Inositol phosphates and cell signalling. *Nature,* 341**,** 197-205.

BIRNBAUMER, M. 2000. Vasopressin receptors. *Trends Endocrinol Metab,* 11**,** 406-10.

BLACHER, J., GUERIN, A. P., PANNIER, B., MARCHAIS, S. J. & LONDON, G. M. 2001. Arterial calcifications, arterial stiffness, and cardiovascular risk in end-stage renal disease. *Hypertension,* 38**,** 938-42.

BOBULESCU, I. A., DI SOLE, F. & MOE, O. W. 2005. Na+/H+ exchangers: physiology and link to hypertension and organ ischemia. *Curr Opin Nephrol Hypertens,* 14**,** 485-94.

BOEHMER, C., WILHELM, V., PALMADA, M., WALLISCH, S., HENKE, G., BRINKMEIER, H., COHEN, P., PIESKE, B. & LANG, F. 2003. Serum and glucocorticoid inducible kinases in the regulation of the cardiac sodium channel SCN5A. *Cardiovasc Res,* 57**,** 1079-84.

BORST, O., SCHMIDT, E. M., MüNZER, P., SCHöNBERGER, T., TOWHID, S. T., ELVERS, M., LEIBROCK, C., SCHMID, E., EYLENSTEIN, A., KUHL,

D., MAY, A. E., GAWAZ, M. & LANG, F. 2012. The serum- and glucocorticoid-inducible kinase 1 (SGK1) influences platelet calcium signaling and function by regulation of Orai1 expression in megakaryocytes. *Blood,* 119**,** 251-61.

BRANDMAN, O., LIOU, J., PARK, W. S. & MEYER, T. 2007. STIM2 is a feedback regulator that stabilizes basal cytosolic and endoplasmic reticulum Ca2+ levels. *Cell,* 131**,** 1327-39.

BRIET, M. & BURNS, K. D. 2012. Chronic kidney disease and vascular remodelling: molecular mechanisms and clinical implications. *Clin Sci (Lond),* 123**,** 399-416.

BRUEGGEMANN, L. I., MACKIE, A. R., MANI, B. K., CRIBBS, L. L. & BYRON, K. L. 2009. Differential effects of selective cyclooxygenase-2 inhibitors on vascular smooth muscle ion channels may account for differences in cardiovascular risk profiles. *Mol Pharmacol,* 76**,** 1053-61.

BYON, C. H., JAVED, A., DAI, Q., KAPPES, J. C., CLEMENS, T. L., DARLEY-USMAR, V. M., MCDONALD, J. M. & CHEN, Y. 2008. Oxidative stress induces vascular calcification through modulation of the osteogenic transcription factor Runx2 by AKT signaling. *J Biol Chem,* 283**,** 15319-27.

BYRON, K. L. 1996. Vasopressin stimulates Ca2+ spiking activity in A7r5 vascular smooth muscle cells via activation of phospholipase A2. *Circ Res,* 78**,** 813-20.

CAHALAN, M. D., ZHANG, S. L., YEROMIN, A. V., OHLSEN, K., ROOS, J. & STAUDERMAN, K. A. 2007. Molecular basis of the CRAC channel. *Cell Calcium,* 42**,** 133-44.

CANCELA, J. M., CHURCHILL, G. C. & GALIONE, A. 1999. Coordination of agonist-induced Ca2+-signalling patterns by NAADP in pancreatic acinar cells. *Nature,* 398**,** 74-6.

CANNATA-ANDIA, J. B., ROMAN-GARCIA, P. & HRUSKA, K. 2011. The connections between vascular calcification and bone health. *Nephrol Dial Transplant,* 26**,** 3429-36.

CHANG, J. F., CHOU, Y. S., WU, C. C., CHEN, P. C., KO, W. C., LIOU, J. C., HSIEH, C. Y., LIN, W. N., WEN, L. L., CHANG, S. W., TUNG, T. H. & WANG, T. M. 2020. A Joint Evaluation of Neurohormone Vasopressin-Neurophysin II-Copeptin and Aortic Arch Calcification on Mortality Risks in Hemodialysis Patients. *Front Med (Lausanne),* 7**,** 102.

CHATTERJEE, S., SCHMIDT, S., POULI, S., HONISCH, S., ALKAHTANI, S., STOURNARAS, C. & LANG, F. 2014. Membrane androgen receptor sensitive Na+/H+ exchanger activity in prostate cancer cells. *FEBS Lett,* 588**,** 1571-9.

CHEN, N. X., O'NEILL, K. D., CHEN, X., KIATTISUNTHORN, K., GATTONE, V. H. & MOE, S. M. 2011. Activation of arterial matrix metalloproteinases leads to vascular calcification in chronic kidney disease. *Am J Nephrol,* 34**,** 211-9.

CHILUKOTI, R. K., MOSTERTZ, J., BUKOWSKA, A., ADERKAST, C., FELIX, S. B., BUSCH, M., VöLKER, U., GOETTE, A., WOLKE, C., HOMUTH, G. & LENDECKEL, U. 2013. Effects of irbesartan on gene expression revealed by transcriptome analysis of left atrial tissue in a porcine model of acute rapid pacing in vivo. *Int J Cardiol,* 168**,** 2100-8.

CHOU, A. C., JU, Y. T. & PAN, C. Y. 2015. Calmodulin Interacts with the Sodium/Calcium Exchanger NCX1 to Regulate Activity. *PLoS One,* 10**,** e0138856.

COZZOLINO, M., CICERI, P., GALASSI, A., MANGANO, M., CARUGO, S., CAPELLI, I. & CIANCIOLO, G. 2019. The Key Role of Phosphate on Vascular Calcification. *Toxins (Basel),* 11.

CUZZO, B., PADALA, S. A. & LAPPIN, S. L. 2020. Physiology, Vasopressin. *StatPearls.* Treasure Island (FL): StatPearls Publishing

Copyright © 2020, StatPearls Publishing LLC.

CUZZO, B., PADALA, S. A. & LAPPIN, S. L. 2021. Physiology, Vasopressin. *StatPearls.* Treasure Island (FL): StatPearls Publishing

Copyright © 2021, StatPearls Publishing LLC.

DARMELLAH, A., BAETZ, D., PRUNIER, F., TAMAREILLE, S., RüCKER-MARTIN, C. & FEUVRAY, D. 2007. Enhanced activity of the myocardial Na+/H+ exchanger contributes to left ventricular hypertrophy in the Goto-Kakizaki rat model of type 2 diabetes: critical role of Akt. *Diabetologia,* 50**,** 1335-44.

DAVIES, A. G. 1972. Antidiuretic and growth hormones. *Br Med J,* 2**,** 282-4.

DELLA-MORTE, D., PASTORE, D., CAPUANI, B., PACIFICI, F. & LAURO, D. 2018. SGK-1 (Serum- and Glucocorticoid-Inducible Kinase-1). *In:* CHOI, S. (ed.) *Encyclopedia of Signaling Molecules.* Cham: Springer International Publishing.

DEMER, L. L. & TINTUT, Y. 2008. Vascular calcification: pathobiology of a multifaceted disease. *Circulation,* 117**,** 2938-48.

DERLER, I., JARDIN, I. & ROMANIN, C. 2016. Molecular mechanisms of STIM/Orai communication. *Am J Physiol Cell Physiol,* 310**,** C643-62.

DERLER, I., PLENK, P., FAHRNER, M., MUIK, M., JARDIN, I., SCHINDL, R., GRUBER, H. J., GROSCHNER, K. & ROMANIN, C. 2013. The extended transmembrane Orai1 N-terminal (ETON) region combines binding interface and gate for Orai1 activation by STIM1. *J Biol Chem,* 288**,** 29025-34.

DI GIGLIO, M. G., MUTTENTHALER, M., HARPSøE, K., LIUTKEVICIUTE, Z., KEOV, P., EDER, T., RATTEI, T., ARROWSMITH, S., WRAY, S., MAREK, A., ELBERT, T., ALEWOOD, P. F., GLORIAM, D. E. & GRUBER, C. W. 2017. Development of a human vasopressin V(1a)-receptor antagonist from an evolutionary-related insect neuropeptide. *Sci Rep,* 7**,** 41002.

DING, Y., WINTERS, A., DING, M., GRAHAM, S., AKOPOVA, I., MUALLEM, S., WANG, Y., HONG, J. H., GRYCZYNSKI, Z., YANG, S. H., BIRNBAUMER, L. & MA, R. 2011. Reactive oxygen species-mediated TRPC6 protein activation in vascular myocytes, a mechanism for vasoconstrictor-regulated vascular tone. *J Biol Chem,* 286**,** 31799-809.

DOBSA, L. & EDOZIEN, K. C. 2013. Copeptin and its potential role in diagnosis and prognosis of various diseases. *Biochem Med (Zagreb),* 23**,** 172-90.

DONG, H., JIANG, Y., TRIGGLE, C. R., LI, X. & LYTTON, J. 2006. Novel role for K+-dependent Na+/Ca2+ exchangers in regulation of cytoplasmic free Ca2+ and contractility in arterial smooth muscle. *Am J Physiol Heart Circ Physiol,* 291**,** H1226-35.

DORN, G. W., 2ND, OSWALD, K. J., MCCLUSKEY, T. S., KUHEL, D. G. & LIGGETT, S. B. 1997. Alpha 2A-adrenergic receptor stimulated calcium release is transduced by Gi-associated G(beta gamma)-mediated activation of phospholipase C. *Biochemistry,* 36**,** 6415-23.

DUPONT, G. & COMBETTES, L. 2016. Fine tuning of cytosolic Ca (2+) oscillations. *F1000Res,* 5.

DURHAM, A. L., SPEER, M. Y., SCATENA, M., GIACHELLI, C. M. & SHANAHAN, C. M. 2018. Role of smooth muscle cells in vascular calcification: implications in atherosclerosis and arterial stiffness. *Cardiovasc Res,* 114**,** 590-600.

ESSER, P. 2010. pH and pressure in closed tissue culture vessels. *Thermo Fisher Scientific Technical Bulletin-05*.

EYLENSTEIN, A., GEHRING, E. M., HEISE, N., SHUMILINA, E., SCHMIDT, S., SZTEYN, K., MüNZER, P., NURBAEVA, M. K., EICHENMüLLER, M., TYAN, L., REGEL, I., FöLLER, M., KUHL, D., SOBOLOFF, J., PENNER, R. & LANG, F. 2011. Stimulation of Ca2+-channel Orai1/STIM1 by serum- and glucocorticoid-inducible kinase 1 (SGK1). *Faseb j,* 25**,** 2012-21.

FADINI, G. P., PAULETTO, P., AVOGARO, A. & RATTAZZI, M. 2007. The good and the bad in the link between insulin resistance and vascular calcification. *Atherosclerosis,* 193**,** 241-4.

FAHRNER, M., DERLER, I., JARDIN, I. & ROMANIN, C. 2013. The STIM1/Orai signaling machinery. *Channels (Austin),* 7**,** 330-43.

FARACO, G., WIJASA, T. S., PARK, L., MOORE, J., ANRATHER, J. & IADECOLA, C. 2014. Water deprivation induces neurovascular and cognitive dysfunction through vasopressin-induced oxidative stress. *J Cereb Blood Flow Metab,* 34**,** 852-60.

FESKE, S., GWACK, Y., PRAKRIYA, M., SRIKANTH, S., PUPPEL, S. H., TANASA, B., HOGAN, P. G., LEWIS, R. S., DALY, M. & RAO, A. 2006. A mutation in Orai1 causes immune deficiency by abrogating CRAC channel function. *Nature,* 441**,** 179-85.

FLIEGEL, L. 2019. Structural and Functional Changes in the Na(+)/H(+) Exchanger Isoform 1, Induced by Erk1/2 Phosphorylation. *Int J Mol Sci,* 20.

FOLEY, R. N., PARFREY, P. S. & SARNAK, M. J. 1998. Clinical epidemiology of cardiovascular disease in chronic renal disease. *Am J Kidney Dis,* 32**,** S112-9.

GARCIARENA, C. D., CALDIZ, C. I., CORREA, M. V., SCHINELLA, G. R., MOSCA, S. M., CHIAPPE DE CINGOLANI, G. E., CINGOLANI, H. E. & ENNIS, I. L. 2008. Na+/H+ exchanger-1 inhibitors decrease myocardial superoxide production via direct mitochondrial action. *J Appl Physiol (1985),* 105**,** 1706-13.

GHASHGHAEINIA, M., KöBERLE, M., MROWIETZ, U. & BERNHARDT, I. 2019. Proliferating tumor cells mimick glucose metabolism of mature human erythrocytes. *Cell Cycle,* 18**,** 1316-1334.

GIACHELLI, C. M. 2004. Vascular calcification mechanisms. *J Am Soc Nephrol,* 15**,** 2959-64.

GOYAL, R. & JIALAL, I. 2021. Hyperphosphatemia. *StatPearls.* Treasure Island (FL): StatPearls Publishing Copyright © 2021, StatPearls Publishing LLC.

GRABMAYR, H., ROMANIN, C. & FAHRNER, M. 2020. STIM Proteins: An Ever-Expanding Family. *Int J Mol Sci,* 22.
GRUSZCZYNSKA-BIEGALA, J., POMORSKI, P., WISNIEWSKA, M. B. & KUZNICKI, J. 2011. Differential roles for STIM1 and STIM2 in store-operated calcium entry in rat neurons. *PLoS One,* 6**,** e19285.
GUDLUR, A. & HOGAN, P. G. 2017. The STIM-Orai Pathway: Orai, the Pore-Forming Subunit of the CRAC Channel. *Adv Exp Med Biol,* 993**,** 39-57.
HAARHAUS, M., BRANDENBURG, V., KALANTAR-ZADEH, K., STENVINKEL, P. & MAGNUSSON, P. 2017. Alkaline phosphatase: a novel treatment target for cardiovascular disease in CKD. *Nat Rev Nephrol,* 13**,** 429-442.
HACKAM, D. J., ROTSTEIN, O. D., ZHANG, W. J., DEMAUREX, N., WOODSIDE, M., TSAI, O. & GRINSTEIN, S. 1997. Regulation of phagosomal acidification. Differential targeting of Na+/H+ exchangers, Na+/K+-ATPases, and vacuolar-type H+-atpases. *J Biol Chem,* 272**,** 29810-20.
HAWKINS, C. L. 2018. Protein carbamylation: a key driver of vascular calcification during chronic kidney disease. *Kidney Int,* 94**,** 12-14.
HOLMAR, J., DE LA PUENTE-SECADES, S., FLOEGE, J., NOELS, H., JANKOWSKI, J. & ORTH-ALAMPOUR, S. 2020. Uremic Toxins Affecting Cardiovascular Calcification: A Systematic Review. *Cells,* 9.
HOU, X., PEDI, L., DIVER, M. M. & LONG, S. B. 2012. Crystal structure of the calcium release-activated calcium channel Orai. *Science,* 338**,** 1308-13.
HUANG, M., ZHENG, L., XU, H., TANG, D., LIN, L., ZHANG, J., LI, C., WANG, W., YUAN, Q., TAO, L. & YE, Z. 2020. Oxidative stress contributes to vascular calcification in patients with chronic kidney disease. *J Mol Cell Cardiol,* 138**,** 256-268.
HUMMERICH, W., KONRADS, A., ROESCH, R. & SOFRONIEW, M. 1983. Radioimmunoassay of arginine-vasopressin in human plasma: development and clinical application. *Klin Wochenschr,* 61**,** 203-8.
HWANG, S. Y., FOLEY, J., NUMAGA-TOMITA, T., PETRANKA, J. G., BIRD, G. S. & PUTNEY, J. W., JR. 2012. Deletion of Orai1 alters expression of multiple genes during osteoclast and osteoblast maturation. *Cell Calcium,* 52**,** 488-500.
HWANG, S. Y. & PUTNEY, J. W., JR. 2011. Calcium signaling in osteoclasts. *Biochim Biophys Acta,* 1813**,** 979-83.
IWAMOTO, T., KITA, S. & KATSURAGI, T. 2005. Salt-sensitive hypertension, Na+/Ca2+ exchanger, and vascular smooth muscle. *Trends Cardiovasc Med,* 15**,** 273-7.
IYEMERE, V. P., PROUDFOOT, D., WEISSBERG, P. L. & SHANAHAN, C. M. 2006. Vascular smooth muscle cell phenotypic plasticity and the regulation of vascular calcification. *J Intern Med,* 260**,** 192-210.
JEFFRIES, O., MCGAHON, M. K., BANKHEAD, P., LOZANO, M. M., SCHOLFIELD, C. N., CURTIS, T. M. & MCGEOWN, J. G. 2010. cAMP/PKA-dependent increases in Ca Sparks, oscillations and SR Ca stores in retinal arteriolar myocytes after exposure to vasopressin. *Invest Ophthalmol Vis Sci,* 51**,** 1591-8.
JONES, B. F., BOYLES, R. R., HWANG, S. Y., BIRD, G. S. & PUTNEY, J. W. 2008. Calcium influx mechanisms underlying calcium oscillations in rat hepatocytes. *Hepatology,* 48**,** 1273-81.

JONO, S., MCKEE, M. D., MURRY, C. E., SHIOI, A., NISHIZAWA, Y., MORI, K., MORII, H. & GIACHELLI, C. M. 2000. Phosphate regulation of vascular smooth muscle cell calcification. *Circ Res,* 87**,** E10-7.

KAPUSTIN, A. N., CHATROU, M. L., DROZDOV, I., ZHENG, Y., DAVIDSON, S. M., SOONG, D., FURMANIK, M., SANCHIS, P., DE ROSALES, R. T., ALVAREZ-HERNANDEZ, D., SHROFF, R., YIN, X., MULLER, K., SKEPPER, J. N., MAYR, M., REUTELINGSPERGER, C. P., CHESTER, A., BERTAZZO, S., SCHURGERS, L. J. & SHANAHAN, C. M. 2015. Vascular smooth muscle cell calcification is mediated by regulated exosome secretion. *Circ Res,* 116**,** 1312-23.

KARMAZYN, M., GAN, X. T., HUMPHREYS, R. A., YOSHIDA, H. & KUSUMOTO, K. 1999. The myocardial Na(+)-H(+) exchange: structure, regulation, and its role in heart disease. *Circ Res,* 85**,** 777-86.

KAWAMATA, H., NG, S. K., DIAZ, N., BURSTEIN, S., MOREL, L., OSGOOD, A., SIDER, B., HIGASHIMORI, H., HAYDON, P. G., MANFREDI, G. & YANG, Y. 2014. Abnormal intracellular calcium signaling and SNARE-dependent exocytosis contributes to SOD1G93A astrocyte-mediated toxicity in amyotrophic lateral sclerosis. *J Neurosci,* 34**,** 2331-48.

KHANANSHVILI, D. 2014. Sodium-calcium exchangers (NCX): molecular hallmarks underlying the tissue-specific and systemic functions. *Pflugers Arch,* 466**,** 43-60.

KLUG, N. R., CHECHNEVA, O. V., HUNG, B. Y. & O'DONNELL, M. E. 2021. High glucose-induced effects on Na(+)-K(+)-2Cl(-) cotransport and Na(+)/H(+) exchange of blood-brain barrier endothelial cells: involvement of SGK1, PKCβII, and SPAK/OSR1. *Am J Physiol Cell Physiol,* 320**,** C619-c634.

KOBAYASHI, T. & COHEN, P. 1999. Activation of serum- and glucocorticoid-regulated protein kinase by agonists that activate phosphatidylinositide 3-kinase is mediated by 3-phosphoinositide-dependent protein kinase-1 (PDK1) and PDK2. *Biochem J,* 339 (Pt 2)**,** 319-28.

KOLTAI, T. 2018. Chapter 5-The pH paradigm in cancer. The NHE-1 activity in cancer. Part I: How does NHE-1 work?

KORCHAK, H. M., DORSEY, L. B., LI, H., MACKIE, D. & KILPATRICK, L. E. 2007. Selective roles for alpha-PKC in positive signaling for O-(2) generation and calcium mobilization but not elastase release in differentiated HL60 cells. *Biochim Biophys Acta,* 1773**,** 440-9.

LANG, F., BöHMER, C., PALMADA, M., SEEBOHM, G., STRUTZ-SEEBOHM, N. & VALLON, V. 2006. (Patho)physiological significance of the serum- and glucocorticoid-inducible kinase isoforms. *Physiol Rev,* 86**,** 1151-78.

LANG, F., EYLENSTEIN, A. & SHUMILINA, E. 2012. Regulation of Orai1/STIM1 by the kinases SGK1 and AMPK. *Cell Calcium,* 52**,** 347-54.

LANG, F., GUELINCKX, I., LEMETAIS, G. & MELANDER, O. 2017. Two Liters a Day Keep the Doctor Away? Considerations on the Pathophysiology of Suboptimal Fluid Intake in the Common Population. *Kidney Blood Press Res,* 42**,** 483-494.

LANG, F., LEIBROCK, C., PELZL, L., GAWAZ, M., PIESKE, B., ALESUTAN, I. & VOELKL, J. 2018a. Therapeutic Interference With Vascular

Calcification-Lessons From Klotho-Hypomorphic Mice and Beyond. *Front Endocrinol (Lausanne),* 9**,** 207.
LANG, F., RITZ, E., ALESUTAN, I. & VOELKL, J. 2014a. Impact of aldosterone on osteoinductive signaling and vascular calcification. *Nephron Physiol,* 128**,** 40-5.
LANG, F., RITZ, E., VOELKL, J. & ALESUTAN, I. 2013. Vascular calcification--is aldosterone a culprit? *Nephrol Dial Transplant,* 28**,** 1080-4.
LANG, F. & STOURNARAS, C. 2013. Serum and glucocorticoid inducible kinase, metabolic syndrome, inflammation, and tumor growth. *Hormones (Athens),* 12**,** 160-71.
LANG, F., STOURNARAS, C. & ALESUTAN, I. 2014b. Regulation of transport across cell membranes by the serum- and glucocorticoid-inducible kinase SGK1. *Mol Membr Biol,* 31**,** 29-36.
LANG, F., STOURNARAS, C., ZACHAROPOULOU, N., VOELKL, J. & ALESUTAN, I. 2018b. Serum- and glucocorticoid-inducible kinase 1 and the response to cell stress. *Cell Stress,* 3**,** 1-8.
LAYCOCK, J. F. 2009. *Perspectives on vasopressin*, World Scientific.
LEE, H. C. 1997. Mechanisms of calcium signaling by cyclic ADP-ribose and NAADP. *Physiol Rev,* 77**,** 1133-64.
LEE, S. J., LEE, I. K. & JEON, J. H. 2020. Vascular Calcification-New Insights Into Its Mechanism. *Int J Mol Sci,* 21.
LI, J. D., BURTON, K. J., ZHANG, C., HU, S. B. & ZHOU, Q. Y. 2009. Vasopressin receptor V1a regulates circadian rhythms of locomotor activity and expression of clock-controlled genes in the suprachiasmatic nuclei. *Am J Physiol Regul Integr Comp Physiol,* 296**,** R824-30.
LI, Z., WU, J., ZHANG, X., OU, C., ZHONG, X., CHEN, Y., LU, L., LIU, H., LI, Y., LIU, X., WU, B., WANG, Y., YANG, P., YAN, J. & CHEN, M. 2019. CDC42 promotes vascular calcification in chronic kidney disease. *J Pathol,* 249**,** 461-471.
LIAKOPOULOS, V., ROUMELIOTIS, S., GORNY, X., DOUNOUSI, E. & MERTENS, P. R. 2017. Oxidative Stress in Hemodialysis Patients: A Review of the Literature. *Oxid Med Cell Longev,* 2017**,** 3081856.
LIBERMAN, M., PESARO, A. E., CARMO, L. S. & SERRANO, C. V., JR. 2013. Vascular calcification: pathophysiology and clinical implications. *Einstein (Sao Paulo),* 11**,** 376-82.
LIOU, J., FIVAZ, M., INOUE, T. & MEYER, T. 2007. Live-cell imaging reveals sequential oligomerization and local plasma membrane targeting of stromal interaction molecule 1 after Ca2+ store depletion. *Proc Natl Acad Sci U S A,* 104**,** 9301-6.
LISKOVA, V., HUDECOVA, S., LENCESOVA, L., IULIANO, F., SIROVA, M., ONDRIAS, K., PASTOREKOVA, S. & KRIZANOVA, O. 2019. Type 1 Sodium Calcium Exchanger Forms a Complex with Carbonic Anhydrase IX and Via Reverse Mode Activity Contributes to pH Control in Hypoxic Tumors. *Cancers (Basel),* 11.
LIU, L., SCHLESINGER, P. H., SLACK, N. M., FRIEDMAN, P. A. & BLAIR, H. C. 2011. High capacity Na+/H+ exchange activity in mineralizing osteoblasts. *J Cell Physiol,* 226**,** 1702-12.

LOLAIT, S. J., O'CARROLL, A. M., MCBRIDE, O. W., KONIG, M., MOREL, A. & BROWNSTEIN, M. J. 1992. Cloning and characterization of a vasopressin V2 receptor and possible link to nephrogenic diabetes insipidus. *Nature,* 357**,** 336-9.

LONDON, G. M., GUERIN, A. P., MARCHAIS, S. J., METIVIER, F., PANNIER, B. & ADDA, H. 2003. Arterial media calcification in end-stage renal disease: impact on all-cause and cardiovascular mortality. *Nephrol Dial Transplant,* 18**,** 1731-40.

LUIK, R. M., WANG, B., PRAKRIYA, M., WU, M. M. & LEWIS, R. S. 2008. Oligomerization of STIM1 couples ER calcium depletion to CRAC channel activation. *Nature,* 454**,** 538-42.

LUNZ, V., ROMANIN, C. & FRISCHAUF, I. 2019. STIM1 activation of Orai1. *Cell Calcium,* 77**,** 29-38.

MA, G., WEI, M., HE, L., LIU, C., WU, B., ZHANG, S. L., JING, J., LIANG, X., SENES, A., TAN, P., LI, S., SUN, A., BI, Y., ZHONG, L., SI, H., SHEN, Y., LI, M., LEE, M. S., ZHOU, W., WANG, J., WANG, Y. & ZHOU, Y. 2015. Inside-out Ca(2+) signalling prompted by STIM1 conformational switch. *Nat Commun,* 6**,** 7826.

MA, K., LIU, P., AL-MAGHOUT, T., SUKKAR, B., CAO, H., VOELKL, J., ALESUTAN, I., PIESKE, B. & LANG, F. 2019. Phosphate-induced ORAI1 expression and store-operated Ca(2+) entry in aortic smooth muscle cells. *J Mol Med (Berl),* 97**,** 1465-1475.

MACKIE, A. R. & BYRON, K. L. 2008. Cardiovascular KCNQ (Kv7) potassium channels: physiological regulators and new targets for therapeutic intervention. *Mol Pharmacol,* 74**,** 1171-9.

MALO, M. E. & FLIEGEL, L. 2006. Physiological role and regulation of the Na+/H+ exchanger. *Can J Physiol Pharmacol,* 84**,** 1081-95.

MARUYAMA, Y., OGURA, T., MIO, K., KATO, K., KANEKO, T., KIYONAKA, S., MORI, Y. & SATO, C. 2009. Tetrameric Orai1 is a teardrop-shaped molecule with a long, tapered cytoplasmic domain. *J Biol Chem,* 284**,** 13676-85.

MAVANI, G. P., DEVITA, M. V. & MICHELIS, M. F. 2015. A review of the nonpressor and nonantidiuretic actions of the hormone vasopressin. *Front Med (Lausanne),* 2**,** 19.

MAZZINI, M. J. & SCHULZE, P. C. 2006. Proatherogenic pathways leading to vascular calcification. *Eur J Radiol,* 57**,** 384-9.

MCNALLY, B. A., SOMASUNDARAM, A., JAIRAMAN, A., YAMASHITA, M. & PRAKRIYA, M. 2013. The C- and N-terminal STIM1 binding sites on Orai1 are required for both trapping and gating CRAC channels. *J Physiol,* 591**,** 2833-50.

MERCER, J. C., DEHAVEN, W. I., SMYTH, J. T., WEDEL, B., BOYLES, R. R., BIRD, G. S. & PUTNEY, J. W., JR. 2006. Large store-operated calcium selective currents due to co-expression of Orai1 or Orai2 with the intracellular calcium sensor, Stim1. *J Biol Chem,* 281**,** 24979-90.

MILBURN, C. C., DEAK, M., KELLY, S. M., PRICE, N. C., ALESSI, D. R. & VAN AALTEN, D. M. 2003. Binding of phosphatidylinositol 3,4,5-trisphosphate to the pleckstrin homology domain of protein kinase B induces a conformational change. *Biochem J,* 375**,** 531-8.

MITTAPALLI, G., ABGARYAN, L., BROWN, S. J., SALDANHA, S. A., VOLMAR, C. H., FERGUSON, J., ROBERTS, E., HODDER, P. & ROSEN, H. 2010. Optimization and characterization of an antagonist for vasopressin 1a (V1a) receptor. *Probe Reports from the NIH Molecular Libraries Program.* Bethesda (MD): National Center for Biotechnology Information (US).

MIZOBUCHI, M., TOWLER, D. & SLATOPOLSKY, E. 2009. Vascular calcification: the killer of patients with chronic kidney disease. *J Am Soc Nephrol,* 20**,** 1453-64.

MOCCIA, F., ZUCCOLO, E., SODA, T., TANZI, F., GUERRA, G., MAPELLI, L., LODOLA, F. & D'ANGELO, E. 2015. Stim and Orai proteins in neuronal Ca(2+) signaling and excitability. *Front Cell Neurosci,* 9**,** 153.

MOREL, A., O'CARROLL, A. M., BROWNSTEIN, M. J. & LOLAIT, S. J. 1992. Molecular cloning and expression of a rat V1a arginine vasopressin receptor. *Nature,* 356**,** 523-6.

MORGENTHALER, N. G., STRUCK, J., JOCHBERGER, S. & DüNSER, M. W. 2008. Copeptin: clinical use of a new biomarker. *Trends Endocrinol Metab,* 19**,** 43-9.

MUIK, M., FRISCHAUF, I., DERLER, I., FAHRNER, M., BERGSMANN, J., EDER, P., SCHINDL, R., HESCH, C., POLZINGER, B., FRITSCH, R., KAHR, H., MADL, J., GRUBER, H., GROSCHNER, K. & ROMANIN, C. 2008. Dynamic coupling of the putative coiled-coil domain of ORAI1 with STIM1 mediates ORAI1 channel activation. *J Biol Chem,* 283**,** 8014-22.

NAKAMURA, N., TANAKA, S., TEKO, Y., MITSUI, K. & KANAZAWA, H. 2005. Four Na+/H+ exchanger isoforms are distributed to Golgi and post-Golgi compartments and are involved in organelle pH regulation. *J Biol Chem,* 280**,** 1561-72.

NAVARRO-BORELLY, L., SOMASUNDARAM, A., YAMASHITA, M., REN, D., MILLER, R. J. & PRAKRIYA, M. 2008. STIM1-Orai1 interactions and Orai1 conformational changes revealed by live-cell FRET microscopy. *J Physiol,* 586**,** 5383-401.

NGUYEN, N. T., NGUYEN, T. T., DA LY, D., XIA, J. B., QI, X. F., LEE, I. K., CHA, S. K. & PARK, K. S. 2020. Oxidative stress by Ca(2+) overload is critical for phosphate-induced vascular calcification. *Am J Physiol Heart Circ Physiol,* 319**,** H1302-h1312.

NISHIWAKI-YASUDA, K., SUZUKI, A., KAKITA, A., SEKIGUCHI, S., ASANO, S., NISHII, K., NAGAO, S., OISO, Y. & ITOH, M. 2007. Vasopressin stimulates Na-dependent phosphate transport and calcification in rat aortic smooth muscle cells. *Endocr J,* 54**,** 103-12.

O'NEILL, W. C., LOMASHVILI, K. A., MALLUCHE, H. H., FAUGERE, M. C. & RISER, B. L. 2011. Treatment with pyrophosphate inhibits uremic vascular calcification. *Kidney Int,* 79**,** 512-7.

OH, Y. K. 2008. Vasopressin and vasopressin receptor antagonists. *Electrolyte Blood Press,* 6**,** 51-5.

ORLOWSKI, J. & GRINSTEIN, S. 2004. Diversity of the mammalian sodium/proton exchanger SLC9 gene family. *Pflugers Arch,* 447**,** 549-65.

ORLOWSKI, J., KANDASAMY, R. A. & SHULL, G. E. 1992. Molecular cloning of putative members of the Na/H exchanger gene family. cDNA cloning, deduced amino acid sequence, and mRNA tissue expression of the rat

Na/H exchanger NHE-1 and two structurally related proteins. *J Biol Chem,* 267**,** 9331-9.
PAI, A. S. & GIACHELLI, C. M. 2010. Matrix remodeling in vascular calcification associated with chronic kidney disease. *J Am Soc Nephrol,* 21**,** 1637-40.
PALOIAN, N. J. & GIACHELLI, C. M. 2014. A current understanding of vascular calcification in CKD. *Am J Physiol Renal Physiol,* 307**,** F891-900.
PALTY, R., STANLEY, C. & ISACOFF, E. Y. 2015. Critical role for Orai1 C-terminal domain and TM4 in CRAC channel gating. *Cell Res,* 25**,** 963-80.
PANI, B., BOLLIMUNTHA, S. & SINGH, B. B. 2012. The TR (i)P to Ca^{2+} signaling just got STIMy: an update on STIM1 activated TRPC channels. *Front Biosci (Landmark Ed),* 17**,** 805-23.
PARK, C. Y., HOOVER, P. J., MULLINS, F. M., BACHHAWAT, P., COVINGTON, E. D., RAUNSER, S., WALZ, T., GARCIA, K. C., DOLMETSCH, R. E. & LEWIS, R. S. 2009. STIM1 clusters and activates CRAC channels via direct binding of a cytosolic domain to Orai1. *Cell,* 136**,** 876-90.
PEARCE, L. R., KOMANDER, D. & ALESSI, D. R. 2010. The nuts and bolts of AGC protein kinases. *Nat Rev Mol Cell Biol,* 11**,** 9-22.
PEDERSEN, S. F. & COUNILLON, L. 2019. The SLC9A-C Mammalian Na(+)/H(+) Exchanger Family: Molecules, Mechanisms, and Physiology. *Physiol Rev,* 99**,** 2015-2113.
PELZL, L., SAHU, I., MA, K., HEINZMANN, D., BHUYAN, A. A. M., AL-MAGHOUT, T., SUKKAR, B., SHARMA, Y., MARINI, I., RIGONI, F., ARTUNC, F., CAO, H., GUTTI, R., VOELKL, J., PIESKE, B., GAWAZ, M., BAKCHOUL, T. & LANG, F. 2020. Beta-Glycerophosphate-Induced ORAI1 Expression and Store Operated Ca(2+) Entry in Megakaryocytes. *Sci Rep,* 10**,** 1728.
PENNA, A., DEMURO, A., YEROMIN, A. V., ZHANG, S. L., SAFRINA, O., PARKER, I. & CAHALAN, M. D. 2008. The CRAC channel consists of a tetramer formed by Stim-induced dimerization of Orai dimers. *Nature,* 456**,** 116-20.
PIRON, M. & VILLEREAL, M. L. 2013. Chronic exposure to stress hormones alters the subtype of store-operated channels expressed in H19-7 hippocampal neuronal cells. *J Cell Physiol,* 228**,** 1332-43.
PRASAD, V., LORENZ, J. N., MILLER, M. L., VAIRAMANI, K., NIEMAN, M. L., WANG, Y. & SHULL, G. E. 2013. Loss of NHE1 activity leads to reduced oxidative stress in heart and mitigates high-fat diet-induced myocardial stress. *J Mol Cell Cardiol,* 65**,** 33-42.
PROUDFOOT, D., SKEPPER, J. N., HEGYI, L., BENNETT, M. R., SHANAHAN, C. M. & WEISSBERG, P. L. 2000. Apoptosis regulates human vascular calcification in vitro: evidence for initiation of vascular calcification by apoptotic bodies. *Circ Res,* 87**,** 1055-62.
PROUDFOOT, D., SKEPPER, J. N., HEGYI, L., FARZANEH-FAR, A., SHANAHAN, C. M. & WEISSBERG, P. L. 2001. The role of apoptosis in the initiation of vascular calcification. *Z Kardiol,* 90 Suppl 3**,** 43-6.
RESHKIN, S. J., CARDONE, R. A. & HARGUINDEY, S. 2013. Na+-H+ exchanger, pH regulation and cancer. *Recent Pat Anticancer Drug Discov,* 8**,** 85-99.

ROSADO, J. A., DIEZ, R., SMANI, T. & JARDíN, I. 2015. STIM and Orai1 Variants in Store-Operated Calcium Entry. *Front Pharmacol,* 6**,** 325.
ROTHSTEIN, E. C., BYRON, K. L., REED, R. E., FLIEGEL, L. & LUCCHESI, P. A. 2002. H(2)O(2)-induced Ca(2+) overload in NRVM involves ERK1/2 MAP kinases: role for an NHE-1-dependent pathway. *Am J Physiol Heart Circ Physiol,* 283**,** H598-605.
SAGE, S. O. 1992. Three routes for receptor-mediated Ca2+ entry. *Curr Biol,* 2**,** 312-4.
SALLINGER, M., BERLANSKY, S. & FRISCHAUF, I. 2020. Orai channels: key players in Ca(2+) homeostasis. *Curr Opin Physiol,* 17**,** 42-49.
SCHLIEPER, G., SCHURGERS, L., BRANDENBURG, V., REUTELINGSPERGER, C. & FLOEGE, J. 2016. Vascular calcification in chronic kidney disease: an update. *Nephrol Dial Transplant,* 31**,** 31-9.
SCHMID, E., BHANDARU, M., NURBAEVA, M. K., YANG, W., SZTEYN, K., RUSSO, A., LEIBROCK, C., TYAN, L., PEARCE, D., SHUMILINA, E. & LANG, F. 2012. SGK3 regulates Ca(2+) entry and migration of dendritic cells. *Cell Physiol Biochem,* 30**,** 1423-35.
SCHMIDT, S., LIU, G., LIU, G., YANG, W., HONISCH, S., PANTELAKOS, S., STOURNARAS, C., HONIG, A. & LANG, F. 2014. Enhanced Orai1 and STIM1 expression as well as store operated Ca2+ entry in therapy resistant ovary carcinoma cells. *Oncotarget,* 5**,** 4799-810.
SEEBOHM, G., STRUTZ-SEEBOHM, N., URECHE, O. N., HENRION, U., BALTAEV, R., MACK, A. F., KORNIYCHUK, G., STEINKE, K., TAPKEN, D., PFEUFER, A., KääB, S., BUCCI, C., ATTALI, B., MEROT, J., TAVARE, J. M., HOPPE, U. C., SANGUINETTI, M. C. & LANG, F. 2008. Long QT syndrome-associated mutations in KCNQ1 and KCNE1 subunits disrupt normal endosomal recycling of IKs channels. *Circ Res,* 103**,** 1451-7.
SERRADEIL-LE GAL, C., HERBERT, J. M., DELISEE, C., SCHAEFFER, P., RAUFASTE, D., GARCIA, C., DOL, F., MARTY, E., MAFFRAND, J. P. & LE FUR, G. 1995. Effect of SR-49059, a vasopressin V1a antagonist, on human vascular smooth muscle cells. *Am J Physiol,* 268**,** H404-10.
SHAO, J. S., CAI, J. & TOWLER, D. A. 2006. Molecular mechanisms of vascular calcification: lessons learned from the aorta. *Arterioscler Thromb Vasc Biol,* 26**,** 1423-30.
SHAW, P. J. & FESKE, S. 2012. Regulation of lymphocyte function by ORAI and STIM proteins in infection and autoimmunity. *J Physiol,* 590**,** 4157-67.
SHI, X., GAO, J., LV, Q., CAI, H., WANG, F., YE, R. & LIU, X. 2020. Calcification in Atherosclerotic Plaque Vulnerability: Friend or Foe? *Front Physiol,* 11**,** 56.
SHIM, A. H., TIRADO-LEE, L. & PRAKRIYA, M. 2015. Structural and functional mechanisms of CRAC channel regulation. *J Mol Biol,* 427**,** 77-93.
SHUBA, Y. M. 2019. Ca(2+) channel-forming ORAI proteins: cancer foes or cancer allies? *Exp Oncol,* 41**,** 200-206.
SINGH, Y., ZHOU, Y., ZHANG, S., ABDELAZEEM, K. N. M., ELVIRA, B., SALKER, M. S. & LANG, F. 2017. Enhanced Reactive Oxygen Species Production, Acidic Cytosolic pH and Upregulated Na+/H+ Exchanger (NHE) in Dicer Deficient CD4+ T Cells. *Cell Physiol Biochem,* 42**,** 1377-1389.

SLEPKOV, E. R., RAINEY, J. K., SYKES, B. D. & FLIEGEL, L. 2007. Structural and functional analysis of the Na+/H+ exchanger. *Biochem J,* 401**,** 623-33.
SNABAITIS, A. K., HEARSE, D. J. & AVKIRAN, M. 2002. Regulation of sarcolemmal Na(+)/H(+) exchange by hydrogen peroxide in adult rat ventricular myocytes. *Cardiovasc Res,* 53**,** 470-80.
SPEER, M. Y. & GIACHELLI, C. M. 2004. Regulation of cardiovascular calcification. *Cardiovasc Pathol,* 13**,** 63-70.
STAINS, J. P., WEBER, J. A. & GAY, C. V. 2002. Expression of Na(+)/Ca(2+) exchanger isoforms (NCX1 and NCX3) and plasma membrane Ca(2+) ATPase during osteoblast differentiation. *J Cell Biochem,* 84**,** 625-35.
STATHOPULOS, P. B., LI, G. Y., PLEVIN, M. J., AMES, J. B. & IKURA, M. 2006. Stored Ca2+ depletion-induced oligomerization of stromal interaction molecule 1 (STIM1) via the EF-SAM region: An initiation mechanism for capacitive Ca2+ entry. *J Biol Chem,* 281**,** 35855-62.
STATHOPULOS, P. B., ZHENG, L., LI, G. Y., PLEVIN, M. J. & IKURA, M. 2008. Structural and mechanistic insights into STIM1-mediated initiation of store-operated calcium entry. *Cell,* 135**,** 110-22.
STEITZ, S. A., SPEER, M. Y., CURINGA, G., YANG, H. Y., HAYNES, P., AEBERSOLD, R., SCHINKE, T., KARSENTY, G. & GIACHELLI, C. M. 2001. Smooth muscle cell phenotypic transition associated with calcification: upregulation of Cbfa1 and downregulation of smooth muscle lineage markers. *Circ Res,* 89**,** 1147-54.
STRUCK, J., MORGENTHALER, N. G. & BERGMANN, A. 2005. Copeptin, a stable peptide derived from the vasopressin precursor, is elevated in serum of sepsis patients. *Peptides,* 26**,** 2500-4.
SUGIMOTO, T., SAITO, M., MOCHIZUKI, S., WATANABE, Y., HASHIMOTO, S. & KAWASHIMA, H. 1994. Molecular cloning and functional expression of a cDNA encoding the human V1b vasopressin receptor. *J Biol Chem,* 269**,** 27088-92.
SUN, H., ZHANG, F., XU, Y., SUN, S., WANG, H., DU, Q., GU, C., BLACK, S. M., HAN, Y. & TANG, H. 2019. Salusin-β Promotes Vascular Calcification via Nicotinamide Adenine Dinucleotide Phosphate/Reactive Oxygen Species-Mediated Klotho Downregulation. *Antioxid Redox Signal,* 31**,** 1352-1370.
TANOUE, A., ITO, S., HONDA, K., OSHIKAWA, S., KITAGAWA, Y., KOSHIMIZU, T. A., MORI, T. & TSUJIMOTO, G. 2004. The vasopressin V1b receptor critically regulates hypothalamic-pituitary-adrenal axis activity under both stress and resting conditions. *J Clin Invest,* 113**,** 302-9.
TóTH, A., BALOGH, E. & JENEY, V. 2020. Regulation of Vascular Calcification by Reactive Oxygen Species. *Antioxidants (Basel),* 9.
TOWLER, D. A., SHAO, J. S., CHENG, S. L., PINGSTERHAUS, J. M. & LOEWY, A. P. 2006. Osteogenic regulation of vascular calcification. *Ann N Y Acad Sci,* 1068**,** 327-33.
TRAN, T. D., YAO, S., HSU, W. H., GIMBLE, J. M., BUNNELL, B. A. & CHENG, H. 2015. Arginine vasopressin inhibits adipogenesis in human adipose-derived stem cells. *Mol Cell Endocrinol,* 406**,** 1-9.

TSAI, Y. M., JONES, F., MULLEN, P., PORTER, K. E., STEELE, D., PEERS, C. & GAMPER, N. 2020. Vascular Kv7 channels control intracellular Ca(2+) dynamics in smooth muscle. *Cell Calcium,* 92**,** 102283.

TüYSüZ, M. & DEDEMOĞLU, M. 2020. Vascular Calcifications.

VALLéS, P. G., BOCANEGRA, V., GIL LORENZO, A. & COSTANTINO, V. V. 2015. Physiological Functions and Regulation of the Na+/H+ Exchanger [NHE1] in Renal Tubule Epithelial Cells. *Kidney Blood Press Res,* 40**,** 452-66.

VAN BEUSECUM, J. P., BARBARO, N. R., MCDOWELL, Z., ADEN, L. A., XIAO, L., PANDEY, A. K., ITANI, H. A., HIMMEL, L. E., HARRISON, D. G. & KIRABO, A. 2019. High Salt Activates CD11c(+) Antigen-Presenting Cells via SGK (Serum Glucocorticoid Kinase) 1 to Promote Renal Inflammation and Salt-Sensitive Hypertension. *Hypertension,* 74**,** 555-563.

VAN KRUCHTEN, R., BRAUN, A., FEIJGE, M. A., KUIJPERS, M. J., RIVERA-GALDOS, R., KRAFT, P., STOLL, G., KLEINSCHNITZ, C., BEVERS, E. M., NIESWANDT, B. & HEEMSKERK, J. W. 2012. Antithrombotic potential of blockers of store-operated calcium channels in platelets. *Arterioscler Thromb Vasc Biol,* 32**,** 1717-23.

VOELKL, J., LANG, F., ECKARDT, K. U., AMANN, K., KURO, O. M., PASCH, A., PIESKE, B. & ALESUTAN, I. 2019. Signaling pathways involved in vascular smooth muscle cell calcification during hyperphosphatemia. *Cell Mol Life Sci,* 76**,** 2077-2091.

VOELKL, J., LIN, Y., ALESUTAN, I., AHMED, M. S., PASHAM, V., MIA, S., GU, S., FEGER, M., SAXENA, A., METZLER, B., KUHL, D., PICHLER, B. J. & LANG, F. 2012. Sgk1 sensitivity of Na(+)/H(+) exchanger activity and cardiac remodeling following pressure overload. *Basic Res Cardiol,* 107**,** 236.

VOELKL, J., LUONG, T. T., TUFFAHA, R., MUSCULUS, K., AUER, T., LIAN, X., DANIEL, C., ZICKLER, D., BOEHME, B., SACHERER, M., METZLER, B., KUHL, D., GOLLASCH, M., AMANN, K., MULLER, D. N., PIESKE, B., LANG, F. & ALESUTAN, I. 2018a. SGK1 induces vascular smooth muscle cell calcification through NF-kappaB signaling. *J Clin Invest,* 128**,** 3024-3040.

VOELKL, J., LUONG, T. T., TUFFAHA, R., MUSCULUS, K., AUER, T., LIAN, X., DANIEL, C., ZICKLER, D., BOEHME, B., SACHERER, M., METZLER, B., KUHL, D., GOLLASCH, M., AMANN, K., MüLLER, D. N., PIESKE, B., LANG, F. & ALESUTAN, I. 2018b. SGK1 induces vascular smooth muscle cell calcification through NF-κB signaling. *J Clin Invest,* 128**,** 3024-3040.

VOELKL, J., PASHAM, V., AHMED, M. S., WALKER, B., SZTEYN, K., KUHL, D., METZLER, B., ALESUTAN, I. & LANG, F. 2013. Sgk1-dependent stimulation of cardiac Na+/H+ exchanger Nhe1 by dexamethasone. *Cell Physiol Biochem,* 32**,** 25-38.

WANG, D., ZHANG, H., LANG, F. & YUN, C. C. 2007. Acute activation of NHE3 by dexamethasone correlates with activation of SGK1 and requires a functional glucocorticoid receptor. *Am J Physiol Cell Physiol,* 292**,** C396-404.

WANG, J., XU, C., ZHENG, Q., YANG, K., LAI, N., WANG, T., TANG, H. & LU, W. 2017. Orai1, 2, 3 and STIM1 promote store-operated calcium entry in pulmonary arterial smooth muscle cells. *Cell Death Discov,* 3**,** 17074.

WANG, Y., ZHANG, J., WIER, W. G., CHEN, L. & BLAUSTEIN, M. P. 2021. NO-induced vasodilation correlates directly with BP in smooth muscle-Na/Ca exchanger-1-engineered mice: elevated BP does not attenuate endothelial function. *Am J Physiol Heart Circ Physiol,* 320**,** H221-h237.

WEI, S., ROTHSTEIN, E. C., FLIEGEL, L., DELL'ITALIA, L. J. & LUCCHESI, P. A. 2001. Differential MAP kinase activation and Na(+)/H(+) exchanger phosphorylation by H(2)O(2) in rat cardiac myocytes. *Am J Physiol Cell Physiol,* 281**,** C1542-50.

WESTER, M., HELLER, A., GRUBER, M., MAIER, L. S., SCHACH, C. & WAGNER, S. 2019. Glucocorticoid stimulation increases cardiac contractility by SGK1-dependent SOCE-activation in rat cardiac myocytes. *PLoS One,* 14**,** e0222341.

WU, P., ZHENG, C., LIAO, M., WU, C., LU, K. & LIU, W. 2014. Bone turnover and vascular calcification. *J Nephrol Ther,* 4**,** 171.

XU, F., LIU, Y., ZHU, X., LI, S., SHI, X., LI, Z., AI, M., SUN, J., HOU, B., CAI, W., SUN, H., NI, L., ZHOU, Y. & QIU, L. 2019. Protective Effects and Mechanisms of Vaccarin on Vascular Endothelial Dysfunction in Diabetic Angiopathy. *Int J Mol Sci,* 20.

YAMASHITA, M., ING, C. E., YEUNG, P. S., MANESHI, M. M., POMèS, R. & PRAKRIYA, M. 2020. The basic residues in the Orai1 channel inner pore promote opening of the outer hydrophobic gate. *J Gen Physiol,* 152.

YANG, H., CURINGA, G. & GIACHELLI, C. M. 2004. Elevated extracellular calcium levels induce smooth muscle cell matrix mineralization in vitro. *Kidney Int,* 66**,** 2293-9.

YUN, C. C., CHEN, Y. & LANG, F. 2002. Glucocorticoid activation of Na(+)/H(+) exchanger isoform 3 revisited. The roles of SGK1 and NHERF2. *J Biol Chem,* 277**,** 7676-83.

ZHANG, L., WANG, X., CAO, H., CHEN, Y., CHEN, X., ZHAO, X., XU, F., WANG, Y., WOO, A. Y. & ZHU, W. 2016. Vasopressin V(1A) receptor mediates cell proliferation through GRK2-EGFR-ERK(1/2) pathway in A7r5 cells. *Eur J Pharmacol,* 792**,** 15-25.

ZHANG, Z., XU, Q., SONG, C., MI, B., ZHANG, H., KANG, H., LIU, H., SUN, Y., WANG, J., LEI, Z., GUAN, H. & LI, F. 2020. Serum- and Glucocorticoid-inducible Kinase 1 is Essential for Osteoclastogenesis and Promotes Breast Cancer Bone Metastasis. *Mol Cancer Ther,* 19**,** 650-660.

ZHENG, L., STATHOPULOS, P. B., SCHINDL, R., LI, G. Y., ROMANIN, C. & IKURA, M. 2011. Auto-inhibitory role of the EF-SAM domain of STIM proteins in store-operated calcium entry. *Proc Natl Acad Sci U S A,* 108**,** 1337-42.

ZHOU, K., ZHU, X., MA, K., LIU, J., NüRNBERG, B., GAWAZ, M. & LANG, F. 2021. Effect of MgCl2 and GdCl3 on ORAI1 Expression and Store-Operated Ca2+ Entry in Megakaryocytes. *International Journal of Molecular Sciences,* 22**,** 3292.

ZHU, X., MA, K., ZHOU, K., LIU, J., NüRNBERG, B. & LANG, F. 2021. Vasopressin-stimulated ORAI1 expression and store-operated Ca(2+) entry in aortic smooth muscle cells. *J Mol Med (Berl),* 99**,** 373-382.

ZHU, X., MA, K., ZHOU, K., VOELKL, J., ALESUTAN, I., LEIBROCK, C., NüRNBERG, B. & LANG, F. 2020. Reversal of phosphate-induced ORAI1 expression, store-operated Ca(2+) entry and osteogenic signaling by MgCl(2) in human aortic smooth muscle cells. *Biochem Biophys Res Commun,* 523**,** 18-24.

8 Declaration

This work was executed in the Department of Physiology and Department of Pharmacology, Experimental Therapy & Toxicology in the university of Tübingen under the supervision of Prof. Dr. Dr. h.c. Florian Lang and Prof. Dr. Dr. Bernd Nürnberg.

The conception of this work was proposed and designed by Prof. Dr. Dr. h.c. Florian Lang and Prof. Dr. Dr. Bernd Nürnberg. I performed all experiments and analyzed all data of this project. I declare that all data are derived from my own research, except for the references and figures cited. I hereby declare that this thesis entitled: “Influence of Vasopressin on Vascular Smooth Muscle Cell Calcification” is my original work and is entirely written by myself. This dissertation has not been submitted for any degree or diploma award from any other institute.

Parts of this thesis have been published:

Zhu X, Ma K, Zhou K, Liu J, Nürnberg B, Lang F. Vasopressin-stimulated ORAI1 Expression and Store-operated Ca^{2+} Entry in Aortic Smooth Muscle Cells. *J Mol Med (Berl)*. 2021, 99(3):373-382.

Parts of the results of this thesis are in preparation for submission:

Zhu X, Ma K, Zhou K, Pan X, Liu J, Nürnberg B, Alesutan I, Voelkl J, Lang F. Requirement of Na^+/H^+ exchanger NHE1 for vasopressin-induced osteogenic signaling and calcification in Human Aortic Smooth Muscle Cells.

9 Acknowledgements

I would like to express my deep gratitude for the tremendous opportunity to complete my dissertation in the Department of Physiology and Department of Pharmacology, Experimental Therapy & Toxicology, Eberhard-Karls-University of Tübingen, Germany.

I would like to thank all the people who helped me throughout my PhD study. First of all, I want to express my sincerest gratitude and deepest respect to my supervisors Prof. Dr. Dr. h.c. Florian Lang and Prof. Dr. Dr. Bernd Nürnberg. Without their constructive advice, consistent optimism, enlightening criticism, abundant freedom and patient guidance, I cannot conduct my PhD study and complete this thesis. In addition, I am very thankful to professors from the Doctoral Committee (Prof. Dr. Dr. h.c. Florian Lang, Prof. Dr. Dr. Bernd Nürnberg, Prof. Dr. Sandra Beer-hammer and Prof. Dr. Peter Ruth). Thank you for your patient guidance and valuable suggestions to my PhD project and thesis.

Secondly, I would like to appreciate the valuable help of all colleagues from the Institute of Physiology and Department of Pharmacology, Experimental Therapy & Toxicology. I am really grateful to my friends and colleagues Kuo Zhou, Ke Ma, Lina Schaefer, Xia Pan. During my experiment, their company, support, assistance and love inspired my passion for work and life. I am also thankful to Mehrdad Ghashghaeinia, Jibin Liu, Hang Cao, Peter Dreischer, Abdulla Al Mamun Bhuyan. Special thanks to Lejla Subasic, who provided plenty of help on the preparation of the manuscript and the orders.

I also would like to thank personnel from the Experimental medicine program coordination office, especially Dr. Inka Montero and Pia-Sarah Schmidt for their great assistance and help.

I must express my gratitude to my besties Lina, Franziska and Kuo. We always had a wonderful, enjoyable and sweet time every Saturday. We always shared diverse cultures and cuisines together. Besides, my roommates Li Huang, Junru Jiang and Thi Thu Trang Phan have helped me a lot in daily life.

Particularly, I want to acknowledge my motherland and the China Scholarship Council (CSC) for their financial support, which makes my dream study abroad come true.

Last but not least, my heartfelt thanks to my dear family. During the long study period, my family always took care of my growth. Special thanks to my parents and my partner Lin for tolerating my willfulness and supporting my decision over the years. No matter what difficulties I encounter, you always stood by my side. Thank you for your kindness in raising me and thank you for being your daughter.